



THE HONG KONG  
POLYTECHNIC UNIVERSITY

香港理工大學

Pao Yue-kong Library

包玉剛圖書館

---

## Copyright Undertaking

This thesis is protected by copyright, with all rights reserved.

**By reading and using the thesis, the reader understands and agrees to the following terms:**

1. The reader will abide by the rules and legal ordinances governing copyright regarding the use of the thesis.
2. The reader will use the thesis for the purpose of research or private study only and not for distribution or further reproduction or any other purpose.
3. The reader agrees to indemnify and hold the University harmless from and against any loss, damage, cost, liability or expenses arising from copyright infringement or unauthorized usage.

### IMPORTANT

If you have reasons to believe that any materials in this thesis are deemed not suitable to be distributed in this form, or a copyright owner having difficulty with the material being included in our database, please contact [lbsys@polyu.edu.hk](mailto:lbsys@polyu.edu.hk) providing details. The Library will look into your claim and consider taking remedial action upon receipt of the written requests.

**SELECTIVE OXIDATION OF  
UNACTIVATED C-H BONDS BY  
SUPRAMOLECULAR CONTROL**

**YAT-SING FUNG**

**M.Phil**

**The Hong Kong Polytechnic University**

**2011**

**The Hong Kong Polytechnic University**

**Department of Applied Biology and Chemical Technology**

**Selective Oxidation of Unactivated C-H Bonds by  
Supramolecular Control**

By

**Yat-Sing FUNG**

A Thesis Submitted in Partial Fulfillment of the Requirements  
for the Degree of Master of Philosophy

August, 2011

## **CERTIFICATE OF ORIGINALITY**

I hereby declare that this thesis entitled “**SELECTIVE OXIDATION OF UNACTIVATED C-H BONDS BY SUPRAMOLECULAR CONTROL**” is my own work within the period of September, 2009 to August, 2011 and that, to the best of my knowledge and belief, it reproduces no material previously published or written, nor material that has been accepted for the award of any other degree or diploma, except where due acknowledgement has been made in the text.

---

Yat-Sing FUNG

## Abstract

The objective of this project is to develop efficient methods for selective C-H bond oxidation by supramolecular control. This work focuses to (1) develop an efficient protocol for C-H bond oxidation by dioxiranes generated *in situ*, (2) study the effect of cyclodextrins on site-selective C-H bond oxidation of aliphatic esters containing multiple tertiary C-H bonds, and (3) investigate the effect of cyclodextrins on selective C-H bond oxidation of hydrocarbon mixtures.

Using adamantane as substrate, the reaction conditions for C-H bond oxidation by dioxiranes generated *in situ* was optimized. The optimized C-H bond oxidation reaction was carried out by stirring 0.1 mmol of adamantane and 0.1 mmol of 1,1,1-trifluoroacetone in a mixture of water (1 mL) and acetonitrile (1.5 mL) at 25 °C, followed by three additions of 0.5 mmol of Oxone and 1.55 mmol of NaHCO<sub>3</sub> at 0 h, 2 h and 4 h. On the basis of <sup>1</sup>H NMR analysis of the crude reaction mixture, the ratio of adamantane to 1-adamantanol to 1,3-adamantandiol was found to be 7 : 50 : 43.

Site-selective oxidation of unactivated tertiary C-H bonds on aliphatic esters was achieved by supramolecular approach using cyclodextrins. Using 3,7-dimethyl octyl benzoate as the substrate, the reaction was performed by stirring 0.2 mmol of substrate, 0.2 mmol of 1,1,1-trifluoroacetone, and 0.22

mmol of  $\beta$ -cyclodextrin in water at 25 °C, followed by eight additions of 0.5 mmol of Oxone and 1.55 mmol of NaHCO<sub>3</sub> at 0 h, 1 h, 2 h, 3 h, 4 h, 5 h, 6 h and 7 h. 3,7-Dimethyl octyl benzoate was oxidized to 7-hydroxy-3,7-dimethyl octyl benzoate and 3-hydroxy-3,7-dimethyl octyl benzoate with 71% total yield based on 40% conversion (no reaction occurred without  $\beta$ -cyclodextrin). The product ratio of 7-hydroxy-3,7-dimethyl octyl benzoate to 3-hydroxy-3,7-dimethyl octyl benzoate was found to be 20 : 1, as determined by <sup>1</sup>H NMR analysis of the crude reaction mixture. This product ratio (20 : 1) was almost three-fold higher than the product ratio (7 : 1) given by the reaction carried out in a mixture of water and acetonitrile without  $\beta$ -cyclodextrin. By <sup>1</sup>H NMR titration experiments, 3,7-dimethyl octyl benzoate was found to form inclusion complex with  $\beta$ -cyclodextrin in water with an 1 : 1 stoichiometry. The product ratio varied from 14 : 1 to 5 : 1 when the benzoate moiety of the ester was changed to 4-*tert*-butylbenzoate, pivalate and acetate. By 2D ROESY <sup>1</sup>H NMR analysis, the difference in the product ratios could be attributed to the different binding geometries of the substrates to  $\beta$ -cyclodextrin.

$\beta$ -Cyclodextrin was found to achieve selective C-H oxidation of hydrocarbon mixtures in water. In the presence of  $\beta$ -cyclodextrin, the dioxirane-based oxidation of cumene was more favored to ethylbenzene with a

product ratio of cumyl alcohol : acetophenone = 8 : 1 while the reaction conducted in the absence of  $\beta$ -cyclodextrin gave cumyl alcohol and acetophenone in a ratio of 2 : 1.

## **Acknowledgements**

I appreciate to my supervisor, Dr. Man-Kin Wong for offering me a chance to study on dioxirane-based C-H bond oxidation and supramolecular chemistry. I would like to express my deepest gratitude to his invaluable advice, supervision and guidance throughout my study, in both experimental work and writing up of this thesis.

I am grateful to my group members, Ms. Ka-Yan Karen Kung, Ms. Gai-Li Li and Mr. King-Chi Leung for sharing of their research experience with me.

I would like to thank all academic and technical staffs of the Department of Applied Biology and Chemical Technology for their technical support, especially thank Dr. Siu-Cheong Yan for his guidance in NMR analysis, Dr. Pui-Kin So for recording MS spectra, and Mr. Koon-Hung Wan for his guidance in GC analysis.

Last but not the least, I would like to express my deepest gratitude to my parents and my sister for their love, care, support and patience.



# Table of Contents

---

<b>Certificate of Originality</b>	i
<b>Abstract</b>	ii
<b>Acknowledgements</b>	v
<b>Table of Contents</b>	vi
<b>List of Figures</b>	x
<b>List of Tables</b>	xiii
<b>List of Schemes</b>	xv
<b>Abbreviations</b>	xvii
<b>Chapter 1 Introduction</b>	1
1.1 Introduction	1
1.2 Current Methods for C-H Bond Oxidation	3
1.2.1 Electronic Effect	3
1.2.2 Steric Effect	6
1.2.3 Substrate-Directing Effect	8
1.3 Dioxiranes	10
1.4 Cyclodextrins	16
1.4.1 Driving Force of Inclusion Complex Formation between Organic Guests and CD Hosts	18
1.4.2 Evidence of Inclusion Complex Formation	19
1.4.3 Selectivity of Guest for Inclusion Complex Formation with CDs	20

1.4.4	Measurement of the Stoichiometry and Stability of Inclusion Complexes	21
1.4.5	Studies on the Binding Geometry of CD Inclusion Complexes by 2D ROESY	24
1.5	Current Challenges of C-H Bond Activation	26
1.6	The Objectives and Achievements of the Thesis	28
1.7	References	31
<b>Chapter 2</b>	<b>Optimization of Reaction Conditions for C-H Bond Oxidation by Dioxiranes Generated <i>in situ</i></b>	<b>38</b>
2.1	Introduction	38
2.2	Optimization of Experimental Parameters for <i>in situ</i> C-H Bond Oxidation of Adamantane	39
2.2.1	Effect of Reaction Temperature	41
2.2.2	Choice of Base	42
2.2.3	Study on the Amount of Oxone and Base	45
2.2.4	Effect of Loading of 1,1,1-Trifluoroacetone	48
2.3	Ketone Screening	50
2.4	Optimized Reaction Conditions for <i>in situ</i> C-H bond Oxidation of Adamantane	53
2.5	Conclusion	53
2.6	Experimental Section	54
2.6.1	General Procedures for Adamantane Oxidation	54
2.6.2	<sup>1</sup> H NMR Spectra of Adamantane Oxidation	55
2.7	References	67

<b>Chapter 3</b>	<b>Site-Selective C-H Bond Oxidation through</b>	<b>70</b>
	<b>Supramolecular Control by Cyclodextrins</b>	
3.1	Introduction	70
3.2	Design of Substrates	75
3.3	Optimization of Reaction Conditions for Site-Selective C-H Bond Oxidation	76
3.4	Effect of $\beta$ -CD on Site-Selectivity of C-H Bond Oxidation of <b>3.1a</b>	80
3.5	$^1\text{H}$ NMR Titration for Binding of <b>3.1a</b> to $\beta$ -CD	85
3.6	Effect of Loading of $\beta$ -CD on the Yield and Site-Selectivity of C-H Bond Oxidation of <b>3.1a</b>	88
3.7	Effect of Different Substituents on the Site-Selectivity of C-H Bond Oxidation of 3,7-Dimethyl Octyl Ester in the Presence of $\beta$ -CD	91
3.8	Studies of the Binding Geometry between 3,7-Dimethyl Octyl Esters and $\beta$ -CD through 2D ROESY Experiments	95
3.9	The Effect of Different Binding Geometries of the Substituents on the Site-Selective C-H Bond Oxidation of 3,7-Dimethyl Octyl Esters	101
3.10	Effect of Different CDs on the Site-Selective C-H Bond Oxidation	104
3.11	Conclusion	106
3.12	Experimental Section	107
	3.12.1 Experimental Procedure	107
	3.12.2 Characterization Data of 3,7-Dimethyl Octyl Esters <b>3.1b</b> , <b>3.2b</b> , and <b>3.2b'</b>	116
	3.12.3 $^1\text{H}$ NMR Spectra of Site-selective C-H Bond Oxidation of Aliphatic Esters with Two Tertiary C-H Bonds	119
3.13	References	131

<b>Chapter 4</b>	<b>Selective C-H Bond Oxidation of Hydrocarbon Mixtures</b>	<b>134</b>
	<b>by Supramolecular Approach</b>	
4.1	Introduction	134
4.2	Effect of $\beta$ -CD on the Oxidation of Cumene	136
4.3	Effect of $\beta$ -CD on the Oxidation of Ethyl Benzene	138
4.4	Effect of $\beta$ -CD on the Selective Oxidation of a Hydrocarbon Mixture	143
4.5	Conclusion	146
4.6	Experimental Section	147
4.6.1	Experimental Procedures	147
4.6.2	Calibration Curve of GC Analysis	149
4.6.3	Chromatogram of C-H Bond Oxidation of Aromatic Substrates	151
4.7	References	159

---

## Table of Figures

---

Figure 1.1	Two commonly used dioxiranes for organic oxidation	11
Figure 1.2	Three commonly used cyclodextrins	16
Figure 1.3	General structure of cyclodextrins	17
Figure 1.4	Schematic diagram of inclusion complex formation	18
Figure 1.5	100 MHz $^1\text{H}$ NMR spectra of a mixture of <i>p</i> -hydroxybenzoic acid and $\beta$ -CD in a ratio of (A) 0, (B) 0.19, (C) 0.40, (D) 0.77, (E) 1.16, (F) 3.09 in $\text{D}_2\text{O}$	20
Figure 1.6	2D ROESY spectrum of inclusion complex of ethyl dodecanoate and $\text{TM}\alpha$ -CD	25
Figure 1.7	Possible binding geometry of ethyl dodecanoate in the cavity of $\text{TM}\alpha$ -CD based on a 2 : 1 ratio of $\text{TM}\alpha$ -CD to ethyl dodecanoate	25
Figure 1.8	Schematic diagrams for selective C-H bond oxidation by supramolecular approach	27
Figure 2.1	Partial $^1\text{H}$ NMR spectrum of crude reaction mixture of adamantane oxidation	40
Figure 2.2	Effect of different amounts of Oxone and $\text{NaHCO}_3$	46
Figure 3.1	Cyclodextrin-attached manganese porphyrin catalyst	71
Figure 3.2	Structure of 3,7-dimethyl octyl ester	75
Figure 3.3	Partial $^1\text{H}$ NMR spectrum of the crude reaction mixture of oxidation of <b>3.1a</b>	77
Figure 3.4	LCMS (ESI+) spectra of $\beta$ -CD in dioxirane-based	81

	oxidation of <b>3.1a</b>	
Figure 3.5	Positions of protons located in $\beta$ -cyclodextrin	85
Figure 3.6	Partial $^1\text{H}$ NMR spectra of a mixture of <b>3.1a</b> and $\beta$ -CD in $\text{D}_2\text{O}$ (signals of $\beta$ -CD)	86
Figure 3.7	$^1\text{H}$ NMR titration curve for <b>3.1a</b> and $\beta$ -CD	87
Figure 3.8	Model compounds of 3,7-dimethyl octyl ester for 2D ROESY experiments	95
Figure 3.9	Partial contour plot of 600 MHz 2D ROESY spectrum for binding of <b>3.3a</b> to $\beta$ -CD in $\text{D}_2\text{O}$	97
Figure 3.10	Proposed binding geometry for the inclusion of <b>3.3a</b> and $\beta$ -CD	97
Figure 3.11a	Partial contour plot of 600 MHz 2D ROESY spectrum for binding of <b>3.3b</b> ( <i>tert</i> -butyl moiety) to $\beta$ -CD in $\text{D}_2\text{O}$	98
Figure 3.11b	Partial contour plot of 600 MHz 2D ROESY spectrum for binding of <b>3.3b</b> (phenyl ring moiety) to $\beta$ -CD in $\text{D}_2\text{O}$	99
Figure 3.12	Proposed binding geometry for the inclusion of <b>3.3b</b> and $\beta$ -CD	99
Figure 3.13	Partial contour plot of 600 MHz 2D ROESY spectrum for binding of <b>3.3c</b> to $\beta$ -CD in $\text{D}_2\text{O}$	100
Figure 3.14	Proposed binding geometry for the inclusion of <b>3.3c</b> and $\beta$ -CD	101
Figure 3.15	Schematic diagrams for site selective C-H bond oxidation of <b>3.1a-c</b>	102
Figure 3.16	Scott's plot of $^1\text{H}$ NMR titration of <b>3.1a</b> and $\beta$ -CD	113
Figure 3.17	Scott's plot of $^1\text{H}$ NMR titration of <b>3.1b</b> and $\beta$ -CD	114

Figure 3.18	Scott's plot of $^1\text{H}$ NMR titration of <b>3.1c</b> and $\beta$ -CD	115
Figure 4.1	(a) No C-H bond oxidation occurs in water in the absence of $\beta$ -CD. (b) C-H bond oxidation occurs in water in the presence of $\beta$ -CD.	134
Figure 4.2	GC-FID chromatograph of the crude product mixture of dioxirane-based cumene oxidation in the presence of $\beta$ -CD	137

---

## Table of Tables

---

Table 1.1	Basic properties of $\alpha$ -, $\beta$ -, and $\gamma$ -cyclodextrins	17
Table 2.1	Adamantane oxidation at different temperature	42
Table 2.2	Adamantane oxidation conducted with different bases	43
Table 2.3	Adamantane oxidation with different amounts of Oxone and NaHCO <sub>3</sub>	45
Table 2.4	Effect of loading of 1,1,1-trifluoroacetone on adamantane oxidation	49
Table 2.5	Catalytic activities of ketones towards adamantane oxidation	51
Table 3.1	Oxidation of <b>3.1a</b> with different loading of Oxone and NaHCO <sub>3</sub>	79
Table 3.2	Oxidation of 3,7-dimethyl octyl benzenoate	82
Table 3.3	Oxidation of <b>3.1a</b> with different amounts of $\beta$ -CD	90
Table 3.4	Effect of different substituents and $\alpha$ -, $\beta$ - and $\gamma$ - CDs on the site-selectivity of oxidation of 3,7-dimethyl octyl ester	92
Table 3.5	Amount of <b>3.1a-c</b> , $\beta$ -CD, and D <sub>2</sub> O for <sup>1</sup> H NMR titration	108
Table 3.6	$\Delta\delta_{\text{obs}}$ of H3 of $\beta$ -CD in <sup>1</sup> H NMR titration of <b>3.1a</b> and $\beta$ -CD	109
Table 3.7	$\Delta\delta_{\text{obs}}$ of H3 of $\beta$ -CD in <sup>1</sup> H NMR titration of <b>3.1b</b> and $\beta$ -CD	110
Table 3.8	$\Delta\delta_{\text{obs}}$ of H3 of $\beta$ -CD in <sup>1</sup> H NMR titration of <b>3.1c</b> and $\beta$ -CD	111
Table 3.9	Data of Scott's plot of <sup>1</sup> H NMR titration of <b>3.1a</b> and $\beta$ -CD	113
Table 3.10	Data of Scott's plot of <sup>1</sup> H NMR titration of <b>3.1b</b> and $\beta$ -CD	114
Table 3.11	Data of Scott's plot of <sup>1</sup> H NMR titration of <b>3.1c</b> and $\beta$ -CD	115
Table 4.1	Oxidation of cumene	136



Table 4.2	Oxidation of ethyl benzene	140
Table 4.3	Effect of $\beta$ -CD on selective C-H bond oxidation of hydrocarbon mixtures	144

---

## Table of Schemes

---

Scheme 1.1	Catalytic C-H bond oxidation of aliphatic ester by H <sub>2</sub> O <sub>2</sub> with iron-based catalyst reported by White	4
Scheme 1.2	C-H bond oxidation of aliphatic ester catalyzed by PFP-substituted benzoxathiazine	6
Scheme 1.3	Catalytic C-H bond oxidation of 1-menthyl acetate	7
Scheme 1.4	Directed bromination of C-H bond reported by Baran	8
Scheme 1.5	Directed regioselective C-H bond oxidation by dioxirane generated <i>in situ</i>	9
Scheme 1.6	Generation of dioxiranes from ketones	10
Scheme 1.7	Dioxirane-based C-H bond oxidation in total synthesis of 4-epiajanol	12
Scheme 1.8	Asymmetric epoxidation of <i>trans</i> -stilbene catalyzed by chiral ketone	13
Scheme 1.9	Asymmetric epoxidation of <i>trans</i> -stilbene catalyzed by fructose-derived ketone	14
Scheme 1.10	Enantioselective epoxidation catalyzed by arabinose-derived ketone	15
Scheme 2.1	Generation of dioxirane by reaction of Oxone and ketone	39
Scheme 2.2	Dioxirane-based adamantane oxidation	40
Scheme 2.3	Dioxirane-based adamantane oxidation in biphasic system	47
Scheme 3.1	Regioselective C-H bond oxidation by cyclodextrin-attached catalyst	72

Scheme 3.2	Stereoselective epoxidation with cyclodextrin-ketoester catalyst	73
Scheme 3.3	Oxidation of 3,7-dimethyl octyl ester	75
Scheme 3.4	Dioxirane-based oxidation of 3,7-dimethyl octyl benzenoate	76

---

## Abbreviations

---

OAc	Acetate group
OBz	Benzenoate group
EtO	Ethoxyl group
Ph	Phenyl group
R, R'	Generalized alkyl group
AcOH	Acetic acid
CD	Cyclodextrin
DMAP	4-Dimethylaminopyridine
DCM	Dichloromethane
EtOAc	Ethyl acetate
$\delta$	Chemical shift
s	Singlet
d	Doublet
t	Triplet
q	Quartet
m	Multiplet
m/z	Mass-to-charge ratio
ee	Enantiomeric excess
TLC	Thin layer chromatography
NMR	Nuclear magnetic resonance spectroscopy
ROESY	Rotating frame overhauser effect spectroscopy
LCMS	Liquid chromatography mass spectrometry
HRMS	High resolution mass spectroscopy

---

---

ESI	Electrospray ionization
NOE	Nuclear overhauser effect
FID	Flame ionization detector
r.t.	Room temperature
h	Hour
Conv.	Conversion
R <sub>f</sub>	Retention factor
Equiv.	Equivalent
calcd.	Calculated

---

# Chapter 1

## Introduction

### 1.1 Introduction

Organic synthesis is of fundamental importance in everyday life. Drugs for preventing or curing diseases, pesticides, insecticides, dyes, cosmetics, polymers and fabrics, the manufacture of them all involves organic synthesis. The goal of organic synthesis is to produce desirable products from readily available starting materials and reagents in the most efficient way. During the planning of synthetic scheme, the number of steps is an important issue needed to be considered. It affects the feasibility and practicality in organic synthesis, involves the input of materials and manpower, and determines the amount of byproducts and wastes to be handled.

Functional group transformation is a major means in traditional organic synthesis. To obtain desirable products, numerous steps are usually required, which is not step-economical.<sup>1</sup> Moreover, over-dependence on existing synthetic strategies and methods for functional group transformation severely limits the diversity of synthetic targets. To broaden the scope of organic synthesis with reduction of steps, development of new synthetic approaches is of urgent need.

In general, C-H bonds are not regarded as functional groups in organic synthesis. This is attributed to the intrinsic properties of C-H bonds. Based on Pauling's scale,<sup>2</sup> the electronegativity difference of carbon (2.5) and hydrogen (2.1) atoms is 0.4. Due to this small electronegativity difference, the dipole moment of the C-H bonds is rather small, and the C-H bonds are regarded as nonpolar. Due to this nonpolar property, C-H bonds are not reactive towards electrophilic and nucleophilic attack. Besides, the average bond energy of a C-H single bond is about 101 kcal/mol,<sup>3</sup> and the energy requirements for both homo- and heterolytic cleavage are significantly high. In addition, the large HOMO-LUMO gap, extremely high pKa value, low electron affinity and high ionization energy contribute to the difficulties for C-H bond activation.<sup>4</sup> Based on the properties mentioned above, C-H bonds are not easy to be activated by ordinary redox or acid-base reactions.

After decades' effort on understanding the basis of C-H bond activation, different approaches for C-H bond activation have been developed.<sup>5</sup> By selective activation of C-H bonds, functional groups can be strategically incorporated at the desired positions of hydrocarbons, providing an efficient way for the synthesis of structurally diverse organic molecules.

## 1.2 Current Methods for C-H Bond Oxidation

C-H bonds are ubiquitous in organic molecules. Selective oxidation of unactivated C-H bonds remains a great challenge in contemporary organic synthesis. In general, the selectivity of C-H bond oxidation is mainly governed by electronic,<sup>6</sup> steric,<sup>7</sup> and substrate-based directing<sup>8</sup> factors.

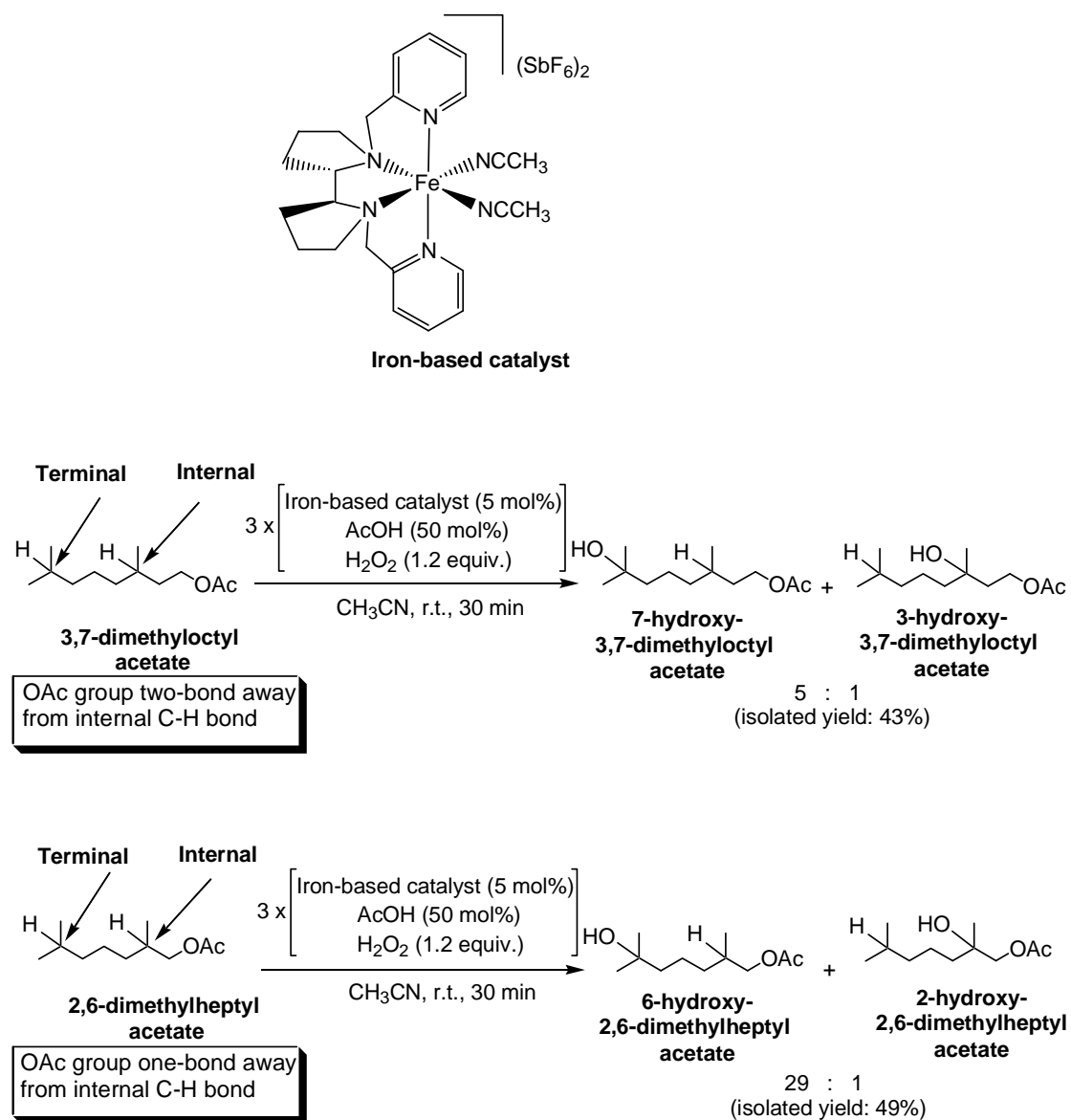
### 1.2.1 Electronic Effect

Based on electronic effect, C-H bonds proximal to electron-donating groups are more reactive toward electrophilic oxidation, whereas C-H bonds proximal to electron-withdrawing groups are less reactive toward electrophilic oxidation.

White and co-workers<sup>6b</sup> utilized synthetic iron-based catalysts to perform oxidation of 3,7-dimethyloctyl acetate (Scheme 1.1). The reaction was carried out by stirring the substrate in CH<sub>3</sub>CN at room temperature, followed by three additions of 5 mol% of catalyst, 50 mol% of AcOH and 1.2 equivalent of H<sub>2</sub>O<sub>2</sub>. The reaction gave 7-hydroxy-3,7-dimethyloctyl acetate and 3-hydroxy-3,7-dimethyloctyl acetate in 43% total isolated yield. The product ratio of 7-hydroxy-3,7-dimethyloctyl acetate to 3-hydroxy-3,7-dimethyloctyl acetate was 5 : 1. Proposed by White, the preferred hydroxylation of the terminal C-H bond would be due to the electronic deactivation of the internal C-H bond



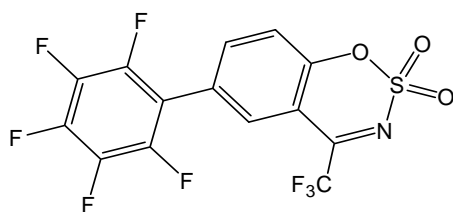
by electron-withdrawing groups towards oxidation.



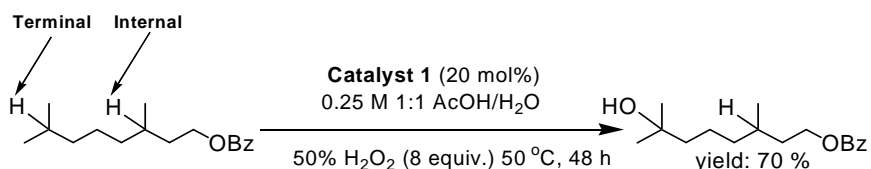
**Scheme 1.1** Catalytic C-H bond oxidation of aliphatic ester by H<sub>2</sub>O<sub>2</sub> with iron-based catalyst reported by White.

Using the same catalyst and reaction conditions, 2,6-dimethyl heptyl acetate was oxidized to 6-hydroxy-2,6-dimethyl heptyl acetate and 2-hydroxy-2,6-dimethyl heptyl acetate in 49% total isolated yield with a product ratio of 29 : 1. The site selectivity of C-H bond oxidation of 2,6-dimethyl heptyl acetate was higher than that of 3,7-dimethyloctyl acetate. It is likely because the electron-withdrawing effect given by the acetate group one-bond away from the internal C-H bond in 2,6-dimethyl heptyl acetate is stronger than that given by the acetate group two-bond away from the internal C-H bond in 3,7-dimethyloctyl acetate.

Du Bois and co-workers<sup>6d</sup> used pentafluorophenyl (PFP)-substituted benzoxathiazine as catalyst to carry out oxaziridine-based C-H bond oxidation of 3,7-dimethyloctyl benzoate. The reaction was performed by stirring a mixture of the substrate, 20 mol% of benzoxathiazine catalyst, 8 equivalent of 50% H<sub>2</sub>O<sub>2</sub> in 0.25 M 1 : 1 AcOH/H<sub>2</sub>O at 50 °C for 48 h. The reaction gave 7-hydroxy-3,7-dimethyloctyl benzoate in 70% yield (Scheme 1.2). As indicated in the paper by Du Bois, the catalyst was sensitive to the electronic property of the C-H bond, leading to the exclusive oxidation of the tertiary C-H bond most distant from the electron-withdrawing OBz group.



**Catalyst 1, PFP-substituted benzoxathiazine**

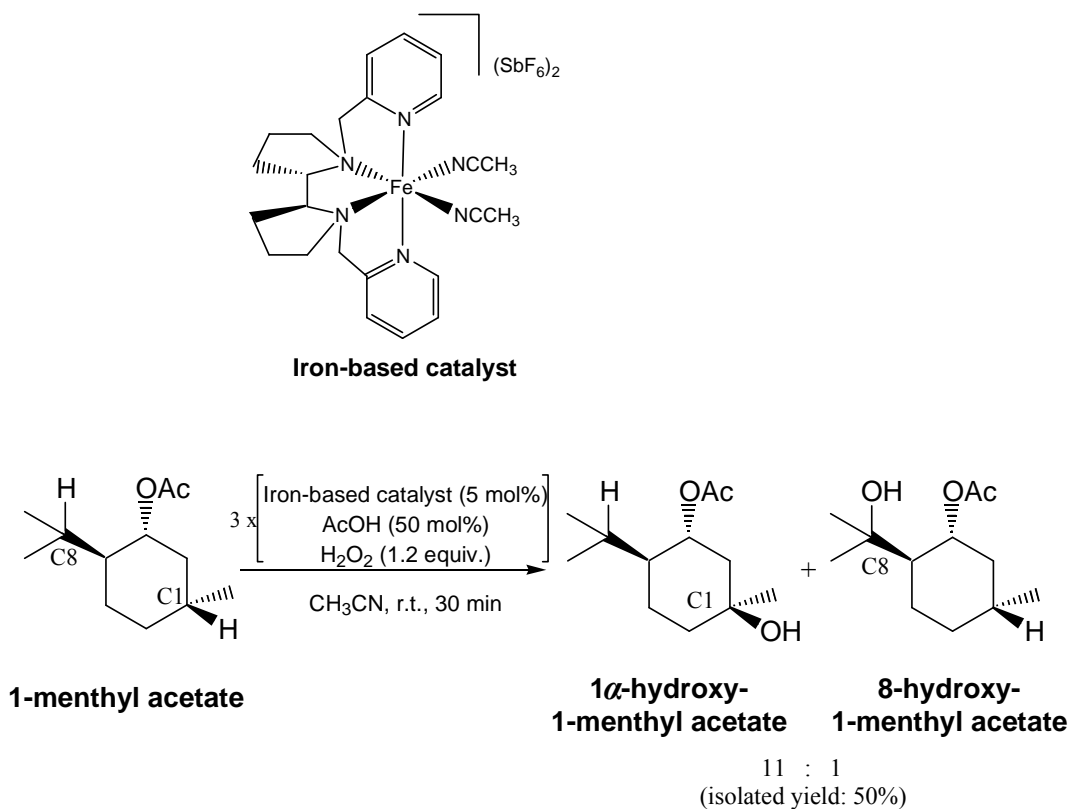


**Scheme 1.2** C-H bond oxidation of aliphatic ester catalyzed by PFP-substituted benzoxathiazine.

### 1.2.2 Steric Effect

White and co-workers<sup>6b</sup> used the synthetic iron-based catalyst mentioned above to conduct oxidation of 1-menthyl acetate (Scheme 1.3). The reaction was carried out by stirring the substrate in CH<sub>3</sub>CN at room temperature, followed by three additions of 5 mol% of catalyst, 50 mol% of AcOH and 1.2 equivalent of H<sub>2</sub>O<sub>2</sub> at room temperature. 1 $\alpha$ -Hydroxy-1-menthyl acetate and 8-hydroxy-1-menthyl acetate were produced in 50% total yield with the product ratio of 11 : 1, respectively. Indicated in the paper by White, the electron density of the two tertiary C-H bonds of C-1 and C-8 are similar, and the levels of oxidation at these sites are expected to be comparable. Reported by White, the unfavorable steric environment of C-8 induced by the acetate group makes the

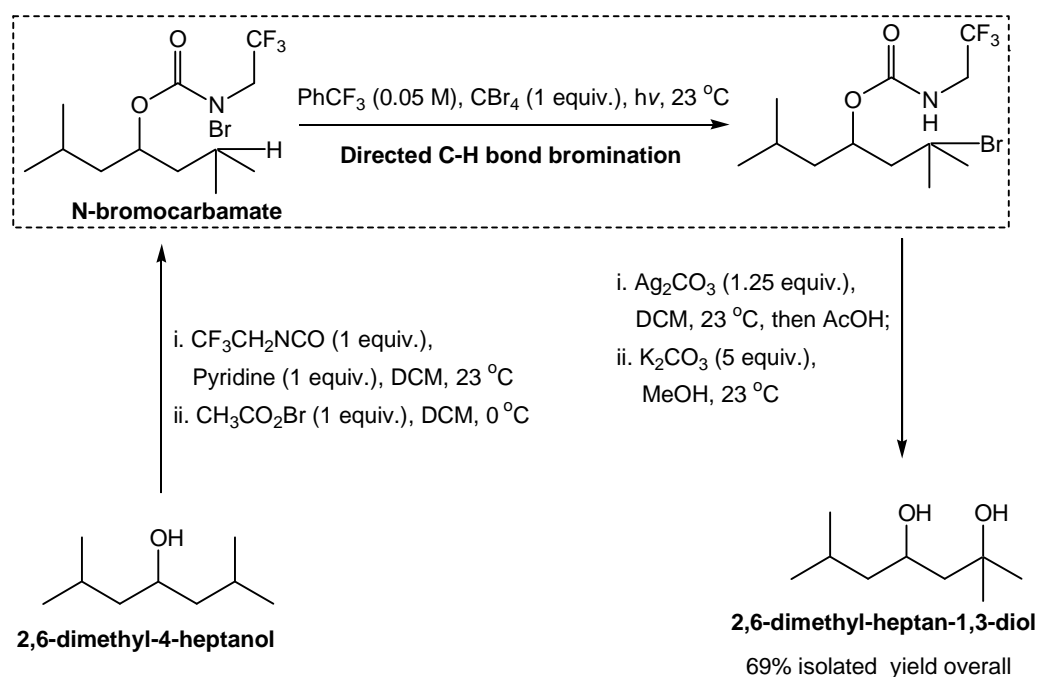
C-H bond oxidation at C-8 less accessible. As a result, the C-H bond at C-1 is preferentially oxidized. Therefore, 1 $\alpha$ -hydroxy-1-menthyl acetate is the major product while 8-hydroxy-1-menthyl acetate is the minor product.



**Scheme 1.3** Catalytic C-H bond oxidation of 1-menthyl acetate.

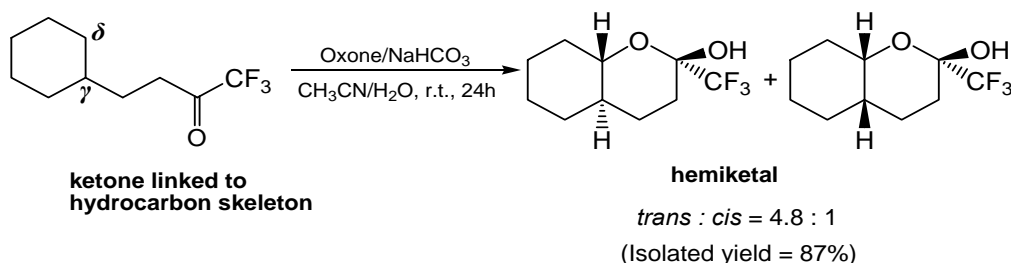
### 1.2.3 Substrate-Directing Effect

Apart from electronic and steric effects, selective C-H bond activation can be achieved by substrate-directing effect.<sup>8a</sup> According to a paper on 1,3-diol synthesis reported by Baran, a N-bromocarbamate moiety is directed to the terminal tertiary C-H bond for C-H bond bromination (Scheme 1.4). The reaction was carried out by adding trifluorotoluene (0.05 M) and 1 equivalent of tetrabromomethane into a solution of N-bromocarbamate, followed by irradiating the reaction mixture by a UV lamp until TLC showed that N-bromocarbamate was completely consumed. The terminal tertiary C-H bond was found to be brominated.



**Scheme 1.4** Directed bromination of C-H bond reported by Baran.

Yang and co-workers<sup>8b,c,d</sup> reported a novel method for regioselective intramolecular oxidation of unactivated C-H bonds at the  $\delta$  site of ketones based on substrate-based directing effect. 5-Cyclohexyl-1,1,1-trifluoropentan-2-one was used as substrate (Scheme 1.5). The reaction was performed by stirring 0.01 M solution of the substrate in a 1.5 : 1 mixture of CH<sub>3</sub>CN and aqueous Na<sub>2</sub>EDTA solution ( $4 \times 10^{-4}$  M) with 5 equivalent of Oxone and 15.5 equivalent of NaHCO<sub>3</sub> at room temperature for 24 h. The reaction gave hemiketal as the product in 87% isolated yield. The secondary C-H bond at the  $\delta$  site was selectively oxidized by *in situ* generated dioxirane although the tertiary C-H bond was present. As indicated in this article, the unusual regioselectivity ( $\delta$ -selectivity) suggests that the nature of this oxidation is nonradical. Proposed by Yang, the mechanism of hemiketal formation is that a  $\delta$ -hydroxyl ketone generated by the oxidation of  $\delta$  C-H bond forms hemiketal by cyclization.

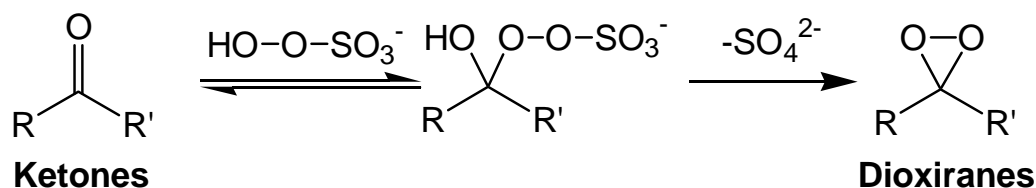


**Scheme 1.5** Directed Regioselective C-H bond oxidation by dioxirane generated *in situ*.

### 1.3 Dioxiranes

Conventionally, C-H bond oxidation is achieved by using oxidants containing transition metals, such as chromium and manganese. The waste generated from reaction with transition metals is toxic and harmful to the environment. Given the environmental problem caused by transition metals, the organic oxidants, such as dioxiranes are good alternative for green organic oxidation.<sup>9</sup> In this project, dioxiranes were used as the oxidant for C-H bond oxidation.

Dioxiranes are three-membered ring peroxides. They can be generated by the reaction of ketones and Oxone (a mix salt of 2KHSO<sub>5</sub>, KHSO<sub>4</sub> and K<sub>2</sub>SO<sub>4</sub>)<sup>10</sup> and have been widely used in heteroatom oxidation, epoxidation, and C-H bond oxidation. Dioxiranes can be used in isolated form or generated *in situ*.



**Scheme 1.6** Generation of dioxiranes from ketones.

In 1986, Murray and co-workers gave the first example of C-H bond oxidation of a variety of hydrocarbons using dimethyldioxirane as oxidant.<sup>12</sup>

They have successfully utilized a solution of dimethyldioxirane in acetone (25 mL, 0.025 M) to oxidize adamantane (2.35 mmol) to 1-adamantanol in 87% yield with 2-adamantanone in 2.6% yield in 18 h at 22 °C. This reaction demonstrated the notable efficiency of dioxiranes as oxidant for C-H bond oxidation.

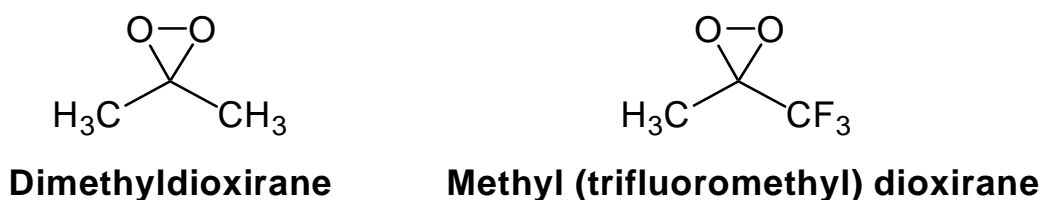


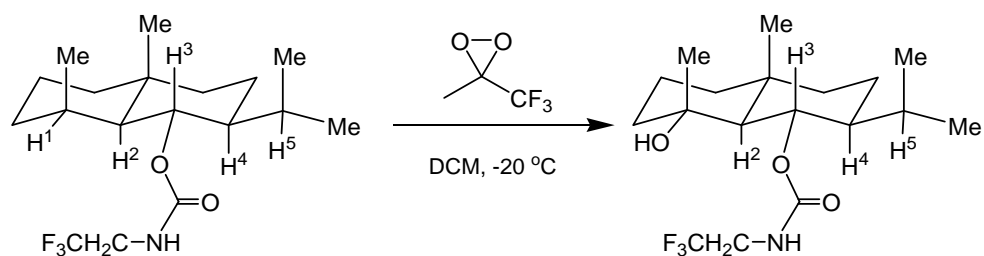
**Figure 1.1** Two commonly used dioxiranes for organic oxidation.

In 1989, Curci and co-workers studied C-H bond oxidation of a variety of hydrocarbons by methyl (trifluoromethyl) dioxirane.<sup>13a</sup> The C-H bond oxidation by methyl (trifluoromethyl) dioxirane was carried out by mixing the dioxirane in TFP (0.7 mL, 0.63 M) with 0.08 M hydrocarbon in 7 mL of dichloromethane at -20 °C. With adamantane as substrate, the reaction gave 1-adamantanol in 94% yield, 1,3-admantandiol in 5% yield and 2-adamantanone in 1% yield within 1 minute. Compared with the adamantane oxidation by dimethyldioxirane (87% yield of 1-adamantanol in 18 h), methyl (trifluoromethyl) dioxirane is much more efficient.



Owing to the high efficiency of methyl (trifluoromethyl) dioxirane in C-H bond oxidation as demonstrated by Curci, it has been applied in modification of a variety of natural products, such as steroids,<sup>15</sup> and also applied in total synthesis.

For instant, Baran utilized methyl (trifluoromethyl) dioxirane to carry out C-H bond oxidation of dihydrojunenol as a key step in the total synthesis of 4-epiajanol.<sup>16</sup> The reaction was carried out by portion-wise addition of 1 equivalent of methyl (trifluoromethyl) dioxirane into the solution of substrate in DCM over 30 min, then stirring for additional 30 min, the reaction was performed at -20 °C. The reaction gave the oxidized product with 82% yield.

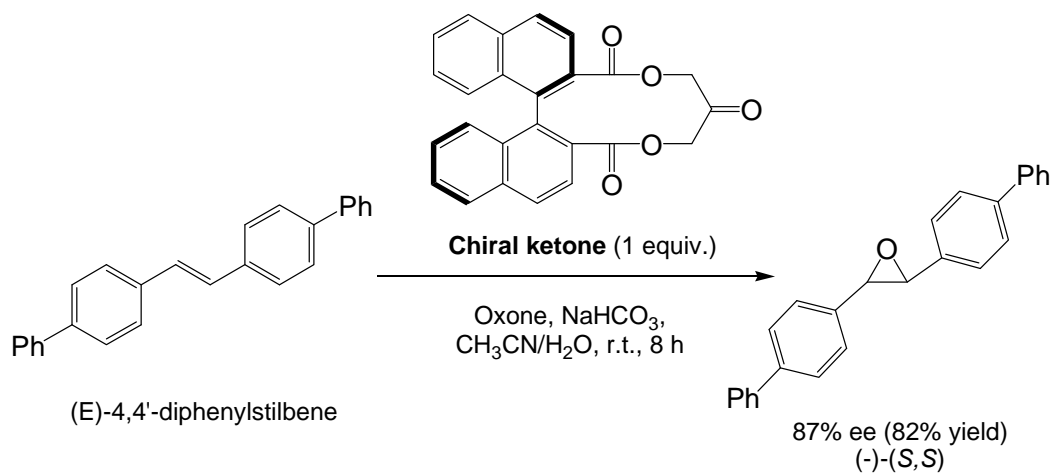


**Scheme 1.7** Dioxirane-based C-H bond oxidation in total synthesis of 4-epiajanol.

Methyl (trifluoromethyl) dioxirane is usually used in isolated form due to its high efficiency of oxidation. However, distillation is involved in the isolation of dioxiranes which is cumbersome. Moreover, the requirement of low boiling point

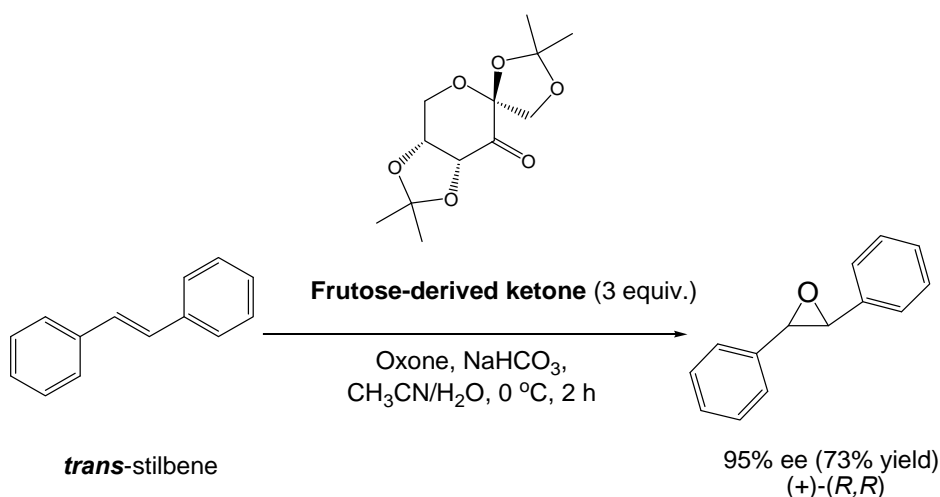
and low molecular weight severely limits the variety of dioxiranes to be used.

To solve this problem, Yang and co-workers performed dioxirane-based epoxidation by dioxiranes generated *in situ* in a solvent mixture of H<sub>2</sub>O and CH<sub>3</sub>CN.<sup>17</sup> Using the H<sub>2</sub>O-CH<sub>3</sub>CN solvent system, Yang and co-workers have developed a series of chiral binaphthalene ketones as catalysts for asymmetric epoxidation.<sup>18d</sup> As shown in Scheme 1.8, with (*E*)-4,4'-diphenylstilbene as substrate, the reaction was carried out by stirring 0.1 mmol of substrate and 0.1 mmol of chiral ketone, 0.5 mmol of Oxone and 1.55 mmol of NaHCO<sub>3</sub> in a mixture of H<sub>2</sub>O and CH<sub>3</sub>CN at room temperature for 8 h. The stilbene substrate was converted to corresponding epoxide in 82 % yield with 87 % ee.



**Scheme 1.8** Asymmetric epoxidation of *trans*-stilbene catalyzed by chiral ketone.

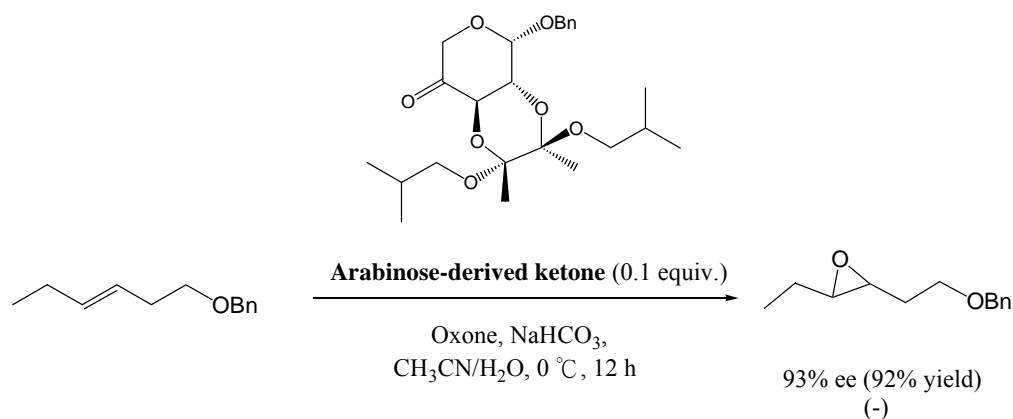
Then, Shi used fructose-derived ketones as catalyst for epoxidation with high enantioselectivity using H<sub>2</sub>O-CH<sub>3</sub>CN as co-solvent system.<sup>18c</sup> As shown in Scheme 1.9, the reaction was performed by stirring 1 equivalent of *trans*-stilbene with 3 equivalent of fructose-derived ketone catalyst, 5 equivalent of Oxone and 15.5 equivalent of NaHCO<sub>3</sub> in a mixture of H<sub>2</sub>O and CH<sub>3</sub>CN at 0 °C for 2 h. *trans*-stilbene was converted to corresponding epoxide in 73 % yield with 95 % ee.



**Scheme 1.9** Asymmetric epoxidation of *trans*-stilbene catalyzed by fructose-derived ketone.

Shing and co-workers<sup>19</sup> have also developed arabinose-derived ketone catalysts for enantioselective epoxidation conducted in H<sub>2</sub>O-CH<sub>3</sub>CN solvent system. In the paper by Shing, the epoxidation was carried out with 0.1 mmol of

substrate, 0.01 mmol of arabinose-derived ketone catalyst, 1 mmol of Oxone and 3.1 mmol of NaHCO<sub>3</sub> in a mixture of H<sub>2</sub>O and CH<sub>3</sub>CN (H<sub>2</sub>O : CH<sub>3</sub>CN = 1 : 5 v/v) at 0 °C for 12 h. The reaction gave the epoxide in 92% yield with 93% ee.



**Scheme 1.10** Enantioselective epoxidation catalyzed by arabinose-derived ketone.

For C-H bond oxidation, Yang and co-workers<sup>8b,c,d</sup> performed the regioselective intramolecular C-H oxidation of hydrocarbon chain linked with ketone moiety in a mixture of H<sub>2</sub>O and CH<sub>3</sub>CN. The ketone moiety was converted to dioxirane and oxidized the secondary C-H bond at the  $\delta$  position of the dioxirane. Details of the reaction are illustrated in the earlier part of this chapter.

## 1.4 Cyclodextrins

Cyclodextrins (CDs)<sup>20</sup> are cyclic supramolecular compounds comprising of glucopyranose units. The three major members are  $\alpha$ -,  $\beta$ -, and  $\gamma$ -CDs consisting of six, seven and eight glucopyranose units, respectively. The structures of  $\alpha$ -,  $\beta$ -, and  $\gamma$ -CDs are shown in Figure 1.2.

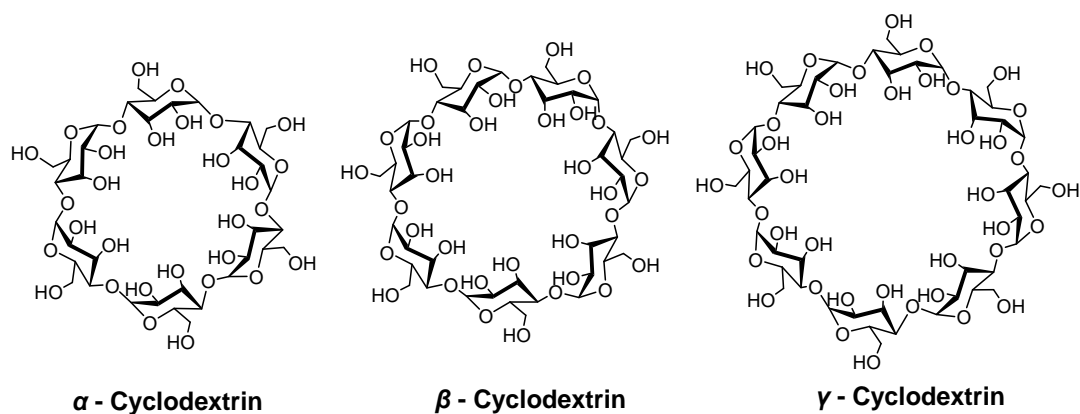


**Figure 1.2** Three commonly used cyclodextrins.

CDs appear as bucket structures (Figure 1.3) with primary hydroxyl groups at the rim of the narrower entrance (called primary face) and secondary hydroxyl groups at the rim of the wider entrance (called secondary face). Within a  $\beta$ -CD molecule, the C-2 hydroxyl group of the glucopyranoside units can form hydrogen bonds with the C-3 hydroxyl group of neighbor glucopyranoside units. The belt-like hydrogen bond system provides rigidity to the structure of  $\beta$ -CD. This leads to the especially low solubility of  $\beta$ -CD among the three major types

of CDs. For  $\alpha$ -CD, as the hydrogen bond system is not completed due to distortion occurs at one of the glucopyranose units, only four effective hydrogen bonds can be formed, instead of six. The structure of  $\gamma$ -CD is non-coplanar and more flexible, hence the solubility of  $\gamma$ -CD is the highest among the three major CDs. The basic properties of  $\alpha$ -,  $\beta$ -, and  $\gamma$ -CDs are summarized in Table 1.1.

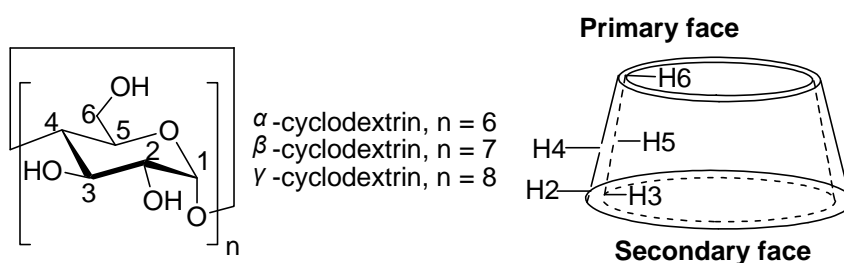


**Figure 1.3** General structure of cyclodextrins.

**Table 1.1** Basic properties of  $\alpha$ -,  $\beta$ -, and  $\gamma$ -cyclodextrins

Properties	$\alpha$ -CD	$\beta$ -CD	$\gamma$ -CD
Number of glucopyranose units	6	7	8
Molecular weight	972	1135	1297
Solubility in water at room temperature (g/L)	145	18.5	23.2
Cavity diameter (pm)	470-530	600-650	750-830
Approximate volume of cavity ( $10^6 \text{ pm}^3$ )	174	262	427

### 1.4.1 Driving Force of Inclusion Complex Formation between Organic Guests and CD Hosts

Cyclodextrins (CDs) are water-soluble with hydrophobic cavity (Figure 1.3).

When the cavity of CD binds with molecule, it is called inclusion complex. The compounds bound in the cavity of CD are mainly hydrophobic organic compounds. In aqueous medium, the apolar-polar interaction between the organic compound and the surrounding water molecules and that between the hydrophobic cavity of CD and water molecules inside the CD cavity are energetically unfavorable. The driving force for the inclusion complex formation mainly come from the substitution of these energetically unfavorable interactions by the energetically favorable apolar-apolar interaction between organic molecule and the CD cavity.<sup>20a</sup> This leads to the replacement of water molecules in the CD cavity by organic molecule (Figure 1.4).

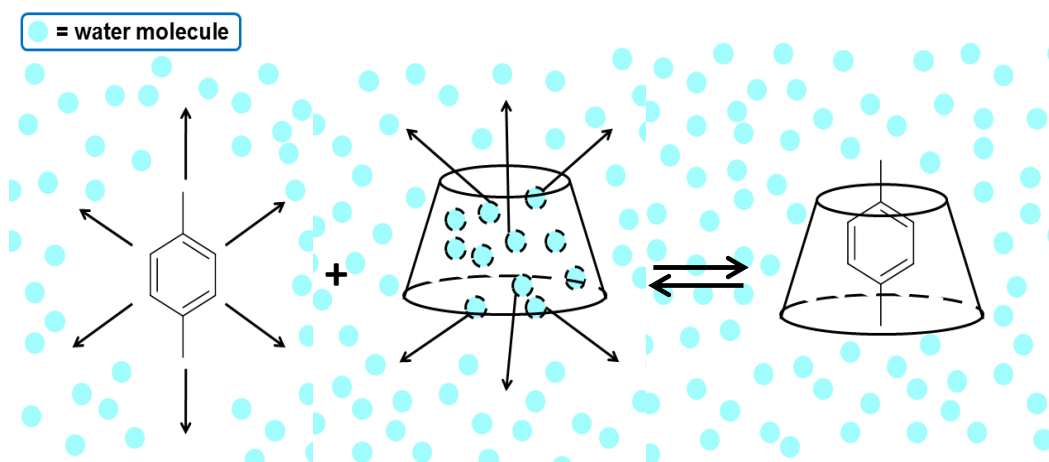


**Figure 1.4** Schematic diagram of inclusion complex formation.

### 1.4.2 Evidence of Inclusion Complex Formation

Although absorption and fluorescence spectroscopies show the presence of interaction between organic guests and CDs, they cannot provide evidence for the formation of inclusion complexes. Beside the X-ray analysis of crystalline complexes directly,<sup>21</sup> the formation of inclusion complexes between the guests and CDs can be supported by NMR spectroscopy.<sup>22</sup>

Demarco and Thakkar are the pioneers in studying the inclusion complex of CD in solution through <sup>1</sup>H NMR spectroscopy.<sup>23</sup> They found that with increasing amount of *p*-hydroxybenzoic acid in a solution of  $\beta$ -CD in D<sub>2</sub>O, the signals of H-3 and H-5 of  $\beta$ -CD shifted upfield progressively (refer to Figure 1.5). This reflects that the guest was included in the cavity of  $\beta$ -CD and interacted with the protons H-3 and H-5 inside the CD cavity. In addition, they pointed out that the exchange rate between the free  $\beta$ -CD and  $\beta$ -CD complex is fast on the time scale of NMR, as averaged signals of free  $\beta$ -CD and  $\beta$ -CD complex were obtained, instead of separated signals of free  $\beta$ -CD and  $\beta$ -CD complex.



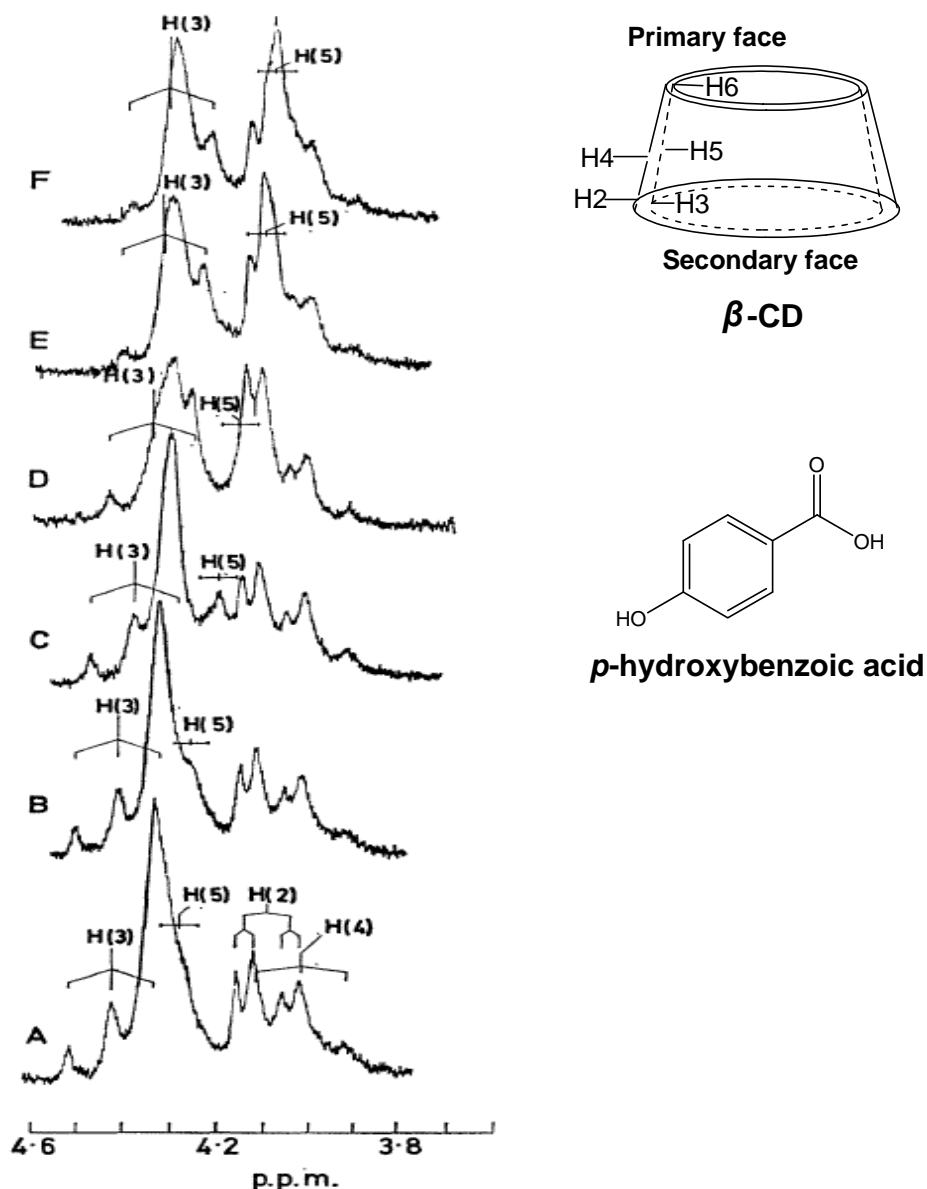


**Figure 1.5** 100 MHz  $^1\text{H}$  NMR spectra of a mixture of *p*-hydroxybenzoic acid and  $\beta$ -CD in a ratio of (A) 0, (B) 0.19, (C) 0.40, (D) 0.77, (E) 1.16, (F) 3.09 in  $\text{D}_2\text{O}$ .

### 1.4.3 Selectivity of Guest for Inclusion Complex Formation with CDs

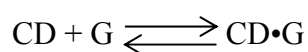
CDs have different selectivity with various guests and form inclusion complexes with different stability. The guests with higher preference to bind to CD will give more stable inclusion complex.

In general, the stability of inclusion complexes increases with the chain length of both aliphatic and cyclic alkane guests.<sup>20a</sup> The inclusion complexes with cyclic alkane guests are more stable than that with aliphatic alkanes. By increasing the rigidity of the guests, the stability of the inclusion complexes would be enhanced.

Specifically, the inclusion complexes of aliphatic hydrocarbons with  $\alpha$ -CD are more stable than that with  $\beta$ -CD.<sup>24</sup>  $\beta$ -CD forms extra stable inclusion complexes with cyclic hydrocarbons than  $\alpha$ -CD and  $\gamma$ -CD. The inclusion complexes of  $\beta$ -CD with aromatic guests are remarkably more stable than the inclusion complexes of  $\alpha$ -CD and  $\gamma$ -CD.<sup>25</sup>

#### **1.4.4 Measurement of the Stoichiometry and Stability of Inclusion Complexes**

The guest is not held in the CD cavity permanently, and the binding between the guest and CD is in equilibrium indeed. The binding constant ( $K_c$ ) is an important parameter of inclusion complexes, especially when CD is used as controlled release agents for pharmaceutical purposes in drug delivery.



$$K_c = \frac{[CD \cdot G]}{[CD][G]}$$

To assess the binding constant of inclusion complexes, the stoichiometric ratio of CDs to guests (or guests to CDs) must be found out. As proven by Demarco and Thakkar, the guest interacts with the protons inside the cavity of CD during the formation of inclusion complexes, leading to the upfield shift of the  $^1\text{H}$  NMR signals of H-3 and H-5. By conducting  $^1\text{H}$  NMR titration, the stoichiometric ratio of CD to guest can be found. By plotting the change of the chemical shift of the H-3 or H-5 of CD against the ratio of the guest to CD, the stoichiometric ratio can be determined at the turning point.

After determination of stoichiometry of the inclusion complexes, the binding constant can be found by specific data treatment of the data obtained in  $^1\text{H}$  NMR titration and stoichiometry.<sup>26</sup> For 1 : 1 stoichiometry, the mathematical expression of the observed chemical shift is shown as equation (1).

$$\delta = f_{10}\delta_H + f_{11}\delta_{GH} \quad (1)$$

Where  $\delta$  is observed chemical shift,  $\delta_H$  is chemical shift of free CD,  $\delta_{GH}$  is chemical shift of complexed CD,  $f_{10}$  is fraction of free CD,  $f_{11}$  is fraction of complexed CD.

As  $f_{10} + f_{11} = 1$ , after rewriting equation (1), it gives:

$$\delta = f_{11}[(\delta)_{GH} - \delta_H] + \delta_H \quad (2)$$

Expressing  $f_{11}$  as:

$$f_{11} = \frac{K_c[G]}{1 + K_c[G]} \quad (3)$$

And expressing the change of chemical shift as:

$$\Delta = \delta - \delta_H \quad (4)$$

Let  $\Delta = f_{11}\Delta_{11}$  which represents the change of chemical shift at the end point of titration. Combining equation (2), (3) and (4), it gives:

$$\Delta = \frac{\Delta_{11}K_c[G]}{1 + K_c[G]} \quad (5)$$

After rewriting equation (5), an equation of double reciprocal plot (6) (or called Benesi-Hildebrand equation) can be obtained:

$$\frac{1}{\Delta} = \frac{1}{\Delta_{11}K_c[G]} + \frac{1}{\Delta_{11}} \quad (6)$$

The binding constant can be found by plotting the titration data following equation (6). The drawback of Benesi-Hildebrand equation is that the equation only valid when observing the signal of guest (or CD) in excess of CD (or guest).

Alternatively, the Scott's plot (shown as equation (7)) can be used to determine the binding constant for a 1:1 ratio of guest to CD.<sup>27</sup>

$$\frac{[S]}{\Delta} = \frac{[S]}{\Delta_{11}} + \frac{\Delta_{11}}{K_c} \quad (7)$$

For the inclusion complexes which the ratio of guest to CD is not 1:1, the binding constant is determined by curve fitting methods which are well documented in literature.<sup>22b</sup>

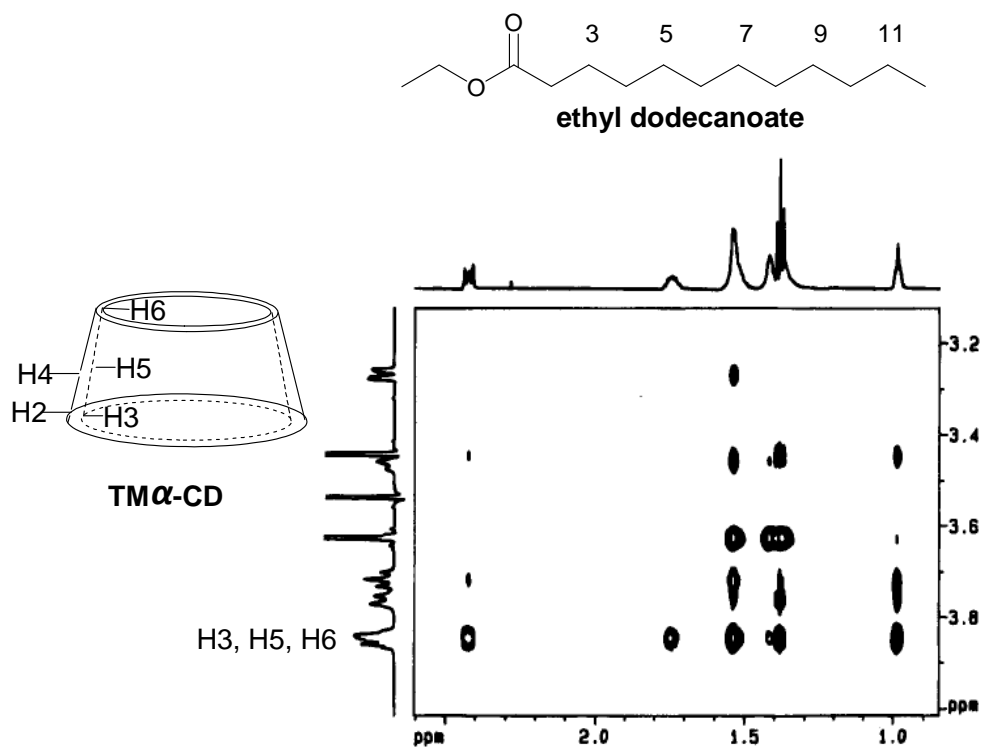
### 1.4.5 Studies on the Binding Geometry of CD Inclusion Complexes by 2D

#### ROESY

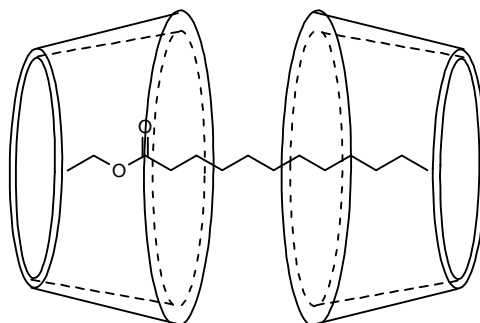
The binding geometry of the guest in the cavity of CD affects the binding constant of the inclusion complexes and also the reaction based on the inclusion complexes between the guest and CD. The binding geometry of the guest of the inclusion complexes is usually studied by 2D  $^1\text{H}$  ROESY experiment.<sup>22a</sup> In 2D ROESY of CD inclusion complexes, NOE correlation signal between the protons of the guest and the protons of CD can be observed when the distance of the protons is shorter than 4 Å through space. If NOE correlation signals between H-3, H-5 and H-6 of CD and the protons of the guest are observed, the guest is likely included in the cavity of CD. The intensity of NOE correlation signal increases when the protons are more proximal to each other.

Figure 1.6 shows the 2D ROESY spectrum of inclusion complex of ethyl dodecanoate and tri-O-methyl- $\alpha$ -CD (TM $\alpha$ -CD) reported by Botsi.<sup>27</sup> As indicated in this article, the EtO moiety and the protons of C-3, 11, and 12 of ethyl dodecanoate show NOE interactions with H-3 of TM $\alpha$ -CD; all protons of ethyl dodecanoate have NOE interaction with H-5 of TM $\alpha$ -CD; the protons of C-12 and EtO moiety of ethyl dodecanoate have NOE interactions with H-6 of TM $\alpha$ -CD. Based on a 2 : 1 stoichiometry of TM $\alpha$ -CD and ethyl dodecanoate and

the results of 2D ROESY, Botsi proposed the possible binding geometry ethyl dodecanoate in the cavity of TM $\alpha$ -CD as shown Figure 1.7.



**Figure 1.6** 2D ROESY spectrum of inclusion complex of ethyl dodecanoate and TM $\alpha$ -CD.



**Figure 1.7** Possible binding geometry of ethyl dodecanoate in the cavity of TM $\alpha$ -CD based on a 2 : 1 ratio of TM $\alpha$ -CD to ethyl dodecanoate.

## 1.5 Current Challenges of C-H Bond Activation

Selective C-H bond oxidation is a great challenge in organic synthesis. Over the decades, chemists spend lots of efforts on the design of catalysts for selective C-H bond oxidation based on electronic, steric and substrate-based directing factors. However, these approaches are significantly limited by the inherent structures of the substrates. Thus, it is of high demand to develop new strategies for selective C-H bond oxidation to cater for a wide diversity of substrates.

Supramolecular host-guest chemistry provides a promising means to achieve selectivity in a wide diversity of organic reactions. In general, the supramolecular hosts function in two ways for selectivity enhancement of organic reactions (Figure 1.8, using cyclodextrins as a model). One way is by positioning the target site of the substrates close to the active reaction centre and hence allows the reaction centre preferentially to react with the target site in close proximity.

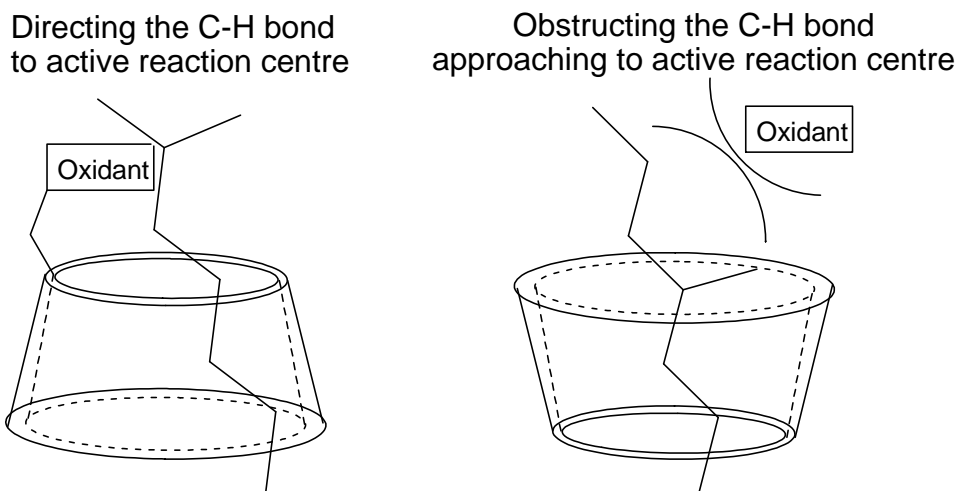


**Figure 1.8** Schematic diagrams for selective C-H bond oxidation by supramolecular approach.

Another way is by obstructing the approach of the undesirable site of the substrates to the active reaction centre through increasing the steric hindrance around the undesirable site. In this regard, the probability of reaction at the desirable site would be enhanced.

For C-H bond activation by supramolecular approach, the selectivity enhanced by directing the target site of the substrates to the reaction centre has been widely investigated.<sup>28</sup> However, selective C-H bond activation by obstructing the approach of undesirable C-H bonds to the reaction centre remains unexplored.<sup>29</sup>



## 1.6 The Objectives and Achievements of the Thesis

The objective of this project is to develop efficient methods for selective C-H bond oxidation by supramolecular approach. Cyclodextrins were chosen as the supramolecular host, and dioxiranes generated *in situ* were used as the oxidant. The selectivity of the C-H bond oxidation was achieved by obstructing the approach of dioxiranes to the C-H bond bound in the hydrophobic cavity of cyclodextrins. As a result, the unbound C-H bonds would be preferentially oxidized.

This work focuses on (1) the development of an efficient protocol for C-H bond oxidation by dioxiranes generated *in situ*, (2) the investigation of the effect of cyclodextrins on site-selective C-H bond oxidation of aliphatic esters containing multiple tertiary C-H bonds, and (3) the investigation of the effect of cyclodextrins on selective C-H bond oxidation of hydrocarbon mixtures.

In Chapter two, the reaction conditions of C-H bond oxidation were optimized. Using adamantane as a substrate, the C-H bond oxidation using dioxiranes generated *in situ* was performed at room temperature (25 °C); NaHCO<sub>3</sub> was used to maintain neutral pH for the reaction. It was found that multiple additions of Oxone and NaHCO<sub>3</sub> would increase the conversion of the C-H bond oxidation. By examining of a variety of ketones towards adamantane

oxidation, 1,1,1-trifluoroacetone was found to exhibit the highest activity towards C-H bond oxidation.

In Chapter 3, the effects of cyclodextrins on the site-selective C-H bond oxidation by dioxiranes generated *in situ* were studied. 3,7-Dimethyloctyl benzoate was used as a substrate with two tertiary C-H bonds. In the presence of  $\beta$ -CD, 3,7-dimethyloctyl benzoate was oxidized to 7-hydroxy-3,7-dimethyloctyl benzoate and 3-hydroxy-3,7-dimethyloctyl benzoate in H<sub>2</sub>O. The ratio of 7-hydroxy-3,7-dimethyloctyl benzoate to 3-hydroxy-3,7-dimethyloctyl benzoate was found to be 20 : 1. This ratio was higher than that given by the reaction performed in a mixture of H<sub>2</sub>O and CH<sub>3</sub>CN without  $\beta$ -CD. The formation of inclusion complex between the substrate and  $\beta$ -CD was supported by <sup>1</sup>H NMR titration. When the benzoate moiety of the substrate was changed to 4-*t*-butylbenzoate, pivalate and acetate, the product ratio varied from 14 : 1 to 5 : 1. By 2D ROESY <sup>1</sup>H NMR analysis, the change in the product ratios could be attributed to the different binding geometries of the substrates to  $\beta$ -CD.

Apart from site selectivity, in Chapter 4, selective C-H bond oxidation of hydrocarbon mixtures was achieved by supramolecular approach using  $\beta$ -CD. With addition of  $\beta$ -CD, preferential oxidation of cumene was observed in the dioxirane-based oxidation of a mixture of cumene and ethyl benzene. The

product ratio of cumyl alcohol to acetophenone was found to be 8 : 1 while the reaction performed in the absence of  $\beta$ -CD gave cumyl alcohol and ethyl benzene in a ratio of 2 : 1.

## 1.7 References

- (1) Newhouse, T.; Baran, P. S. and Hoffmann, R. W. *Chem. Soc. Rev.*, **2009**, *38*, 3010–3021.
- (2) (a) Pauling, L. *J. Am. Chem. Soc.*, **1932**, *54*, 3570–3582. (b) Pauling, L. *Nature of the Chemical Bond*, Cornell University Press (1960).
- (3) Blanksby, S. J. and Ellison, G. B. *Acc. Chem. Res.* **2003**, *36*, 255-263.
- (4) Schwarz, H. *Angew. Chem. Int. Ed.* **2011**, *50*, (Article first published online: 8 JUN 2011)
- (5) For the reviews and examples on C-H bond functionalization, see: (a) Shilov, A. E. and Shul'pin, G. B. *Activation and Catalytic Reactions of Saturated Hydrocarbons in the Presence of Metal Complexes*, Kluwer Academic Publishers, 2000. (b) Goldberg, K. I. and Goldman, A. S. *Activation and Functionalization of C-H Bonds*, Oxford University Press, 2004. (c) Shilov, A. E. and Shul'pin, G. B. *Chem. Rev.* **1997**, *97*, 2879. (d) Dyker, G. *Angew. Chem., Int. Ed.* **1999**, *38*, 1698. (e) Labinger, J. A.; Bercaw, J. E. *Nature* **2002**, *417*, 507. (f) Dyker, G. *Handbook of C-H Transformations: Applications in Organic Synthesis*, Weinheim: Wiley-VCH, 2005. (g) Kakiuchi, F.; Chatani, N. *Adv. Syn. Catal.* **2003**, *345*, 1077. (h) Dick, A. R.; Sanford, M. S. *Tetrahedron* **2006**, *62*, 2439. (i) Godula, K.; Sames, D. *Science* **2006**, *312*, 67.

(j) Mas-Ballesté, R.; Que, L. Jr. *Science* **2006**, *312*, 1885 (k) Davies, H. M. L. *Angew. Chem., Int. Ed.* **2006**, *45*, 6422. (l) Herrerías, C. I.; Yao, X.; Li, Z.; Li, C. J. *Chem. Rev.* **2007**, *107*, 2546. (m) Chan, Y. W.; Chan, K. S. *Organometallics* **2008**, *27*, 4625–4635 (n) Que, Jr, L.; Tolman, W. B. *Nature* **2008**, *455*, 333. (o) Choi, K. S.; Chiu, vvvvP. F.; Chan, K. S. *Organometallics* **2010**, *29*, 624–629 (p) Shul' pin, G. B. *Org. Biomol. Chem.* **2010**, *8*, 4217–4228. (q) Newhouse, T.; Baran, P. S. *Angew. Chem. Int. Ed.* **2011**, *50*, 3362–3374.

(6) Examples for selective C-H bond activation by electronic effect, see: (a) Brodsk, B. H. and Du Bois, J. *J. Am. Chem. Soc.* **2005**, *127*, 15391-15393. (b) Chen, M. S. and White, M. C. *Science*, **2007**, *318*, 783–787. (c) Desai, L. V.; Stowers, K. J. and Sanford, M. S. *J. Am. Chem. Soc.*, **2008**, *130*, 13285–13293. (d) Litvinas, N. D.; Brodsky, B. H. and Du Bois, J. *Angew. Chem. Int. Ed.* **2009**, *48*, 4513-4516. (e) Do, H. Q. and Daugulis, O. *Chem. Commun.*, **2009**, 6433–6435. (f) Gomez, L.; Bosch, I.G.; Company, A.; Buchholz, J. B.; Polo, A.; Sala, X.; Ribas, X. and Costas, M. *Angew. Chem. Int. Ed.* **2009**, *48*, 5720-5723.

(7) Examples for selective C-H bond activation by steric factor, see: (a) Y. Asakawa, R. Matsuda, M. Tori, T. Hashimoto, *Phytochemistry*. **1988**, *27*,

3861 (b) Gomez, L.; Bosch, I. G.; Company, A.; Buchholz, J. B.; Polo, A.; Sala, X.; Ribas, X. and Costas, M. *Angew. Chem. Int. Ed.* **2009**, *48*, 5720-5723 (d) Li, L.; Brennessel, W. W. and Jones, W. D. *Organometallics*, **2009**, *28*, 3492–3500. And also the reference 5b.

(8) Examples for selective C-H bond activation by substrate-based directing factor, see: (a) Chen, K.; Richer, J. M.; and Baran P. S. *J. Am. Chem. Soc.* **2008**, *130*, 7247-7249 (b) Yang, D.; Wong, M. K.; Wang, X. C. and Tang, Y. *J. Am. Chem. Soc.* **1998**, *120*, 6611-6612. (c) Wong, M. K.; Chung, N. W.; He, L. and Yang, D. *J. Am. Chem. Soc.* **2003**, *125*, 158-162. (d) Wong, M. K.; Chung, N. W.; He, L.; Wang, X. C.; Yan, Z.; Tang, Y. C. and Yang, D. *J. Org. Chem.* **2003**, *68*, 6321-6328.

(9) For reviews on dioxiranes, see: (a) Adam, W.; Curci, R.; Edwards, J. O. *Acc. Chem. Res.* **1989**, *22*, 205. (b) Murray, R. W. *Chem. Rev.* **1989**, *89*, 1187. (c) Adam, W.; Hadjiarapoglou, L. *Top. Curr. Chem.* **1993**, *164*, 45. (d) Denmark, S. E.; Wu, Z. *Synlett* **1999**, 847. (e) Adam, W.; Saha-Möller, C. R.; Zhao, C.-G. *Org. React.* **2002**, *61*, 219. (f) Shi, Y. *Acc. Chem. Res.* **2004**, *37*, 488. (g) Yang, D. *Acc. Chem. Res.* **2004**, *37*, 497. (h) Adam, W.; Zhao, C.-G.; Jakka, K. *Org. React.* **2007**, *69*, 1. (i) Wong, O. A.; Shi, Y. *Chem. Rev.* **2008**, *108*, 3958.

(10) Edwards, J. O.; Pater, R. H.; Curci, R. and DiFuria, F. *Photochem.*

*Photobiol.* **1979**, *30*, 63.

(11) For dioxirane-based C-H bond oxidation, see: (a) Curci, R.; D'Accolti, L.;

Fusco, C. *Acc. Chem. Res.* **2006**, *39*, 1.

(12) Murray, R. W.; Jeyaraman, R.; Mohan, L. *J. Am. Chem. Soc.* **1986**, *108*,

2470.

(13) Dioxirane-mediated oxidation of C-H bonds by Curci and co-workers, see:

(a) Mello, R.; Fiorentino, M.; Fusco, C.; Curci, R. *J. Am. Chem. Soc.* **1989**,

*111*, 6749. (b) Kuck, D.; Schuster, A.; Fusco, C.; Fiorentino, M.; Curci, R. *J.*

*Am. Chem. Soc.* **1994**, *116*, 2375. (c) Curci, R.; Detomaso, A.; Prencipe, T.;

Carpenter, G. B. *J. Am. Chem. Soc.* **1994**, *116*, 8112. (d) Curci, R.; Detomaso,

A.; Lattanzio, M. E.; Carpenter, G. B. *J. Am. Chem. Soc.* **1996**, *118*, 11089. (e)

D'Accolti, L.; Fusco, C.; Lucchini, V.; Carpenter, G. B.; Curci, R. *J. Org.*

*Chem.* **2001**, *66*, 9063. (f) D'Accolti, L.; Fiorentino, M.; Fusco, C.; Capitelli,

F.; Curci, R. *Tetrahedron Lett.* **2007**, *48*, 3575. (g) D'Accolti, L.; Fusco, C.;

Lampignano, G.; Capitelli, F.; Curci, R. *Tetrahedron Lett.* **2008**, *49*, 5614.

(14) Dioxirane-mediated oxidation of C-H bonds by Asensio and co-workers, see:

(a) Asensio, G.; Nunez, M. E. G.; Bernardini, C. B.; Mello, R.; Adam, W. *J.*

*Am. Chem. Soc.* **1993**, *115*, 7250. (b) Nunez, M. E. G.; Royo, J.; Castellano,

G.; Andreu, C.; Boix, C.; Mello, R.; Asensio, G. *Org. Lett.* **2000**, *2*, 831. (c)

- Nunez, M. E. G.; Castellano, G.; Andreu, C.; Royo, J.; Bagueña, M.; Mello, R.; Asensio, G. *J. Am. Chem. Soc.* **2001**, *123*, 7487. (d) González-Núñez, M. E.; Royo, J.; Mello, R.; Bagueña, M.; Martínez Ferrer, J.; Ramírez de Arellano, C.; Asensio, G.; Surya Prakash, G. K. *J. Org. Chem.* **2005**, *70*, 7919.
- (e) Mello, R.; Royo, J.; Andreu, C.; Bagueña-Añó, M.; Asensio, G.; González-Núñez, M. E. *Eur. J. Org. Chem.* **2008**, 455.
- (15) Bovicelli, P.; Lupattelli, P. and Mincione, E. *J. Org. Chem.* **1992**, *57*, 2182-2184.
- (16) Chen, K. and Baran, P. S. *Nature* **2009**, *459*, 824-828.
- (17) The first example of organic oxidation by dioxirane generated *in situ*: Yang, D.; Wong, M. K. and Yip, Y. C. *J. Org. Chem.* **1996**, *60*, 3887-3889.
- (18) Reviews for asymmetric epoxidation by chiral ketone catalyst, see: (a) Denmark, S. E.; Wu, Z. *Synlett* **1999**, 847. (b) Frohn, M.; Shi, Y. *Synthesis* **2000**, 1979. (c) Shi, Y. *Acc. Chem. Res.* **2004**, *37*, 488. (d) Yang, D. *Acc. Chem. Res.* **2004**, *37*, 497.
- (19) For enantioselective epoxidation by catalyst developed by Shing, see: (a) Shing, T. K. M.; Leung, G. Y. C.; Yeung, K. W. *Tetrahedron Lett.* **2003**, *44*, 9225. (b) Shing, T. K. M.; Luk, T.; Lee, C. M. *Tetrahedron* **2006**, *62*, 6621. (c) Shing, T. K. M.; Leung, G. Y. C.; Luk, T. *J. Org. Chem.* **2005**, *70*,



7279-7289.

- (20) For the introduction of cyclodextrins, see: (a) Szejtli, J.; Osa, T. Cyclodextrins. In *Comprehensive Supramolecular Chemistry*; Lehn, J.-M., Atwood, J. L., Davies, J. E. D., MacNicol, D. D., Vogtle, F., Eds.; Pergamon: New York, 1996; Vol. 3. (b) Szejtli, J. *Cyclodextrin Technology*; Kluwer Academic Publishers, 1988. (c) Connors, K. A. *Chem. Rev.* **1997**, *97*, 1325-1357. (d) Breslow, R. and Dong, S. D. *Chem. Rev.* **1998**, *98*, 1997-2011 (e) Szejtli, J. *Chem. Rev.* **1998**, *98*, 1743-1753. (f) Takahashi, K. *Chem. Rev.* **1998**, *98*, 2013-2033. (g) Szejtli, J. *Pure Appl. Chem.*, **2004**, *76*, 1825–1845.
- (21) Some early examples for X-ray study of cyclodextrin inclusion complex: (a) Hamilton, J. A.; Steinrauf, L. K. and Van Etten, R. L. *Acta. Cryst.*, **1968**, *324*, 1660. (b) James, W. J. and French, D. *Proc. Iowa Acad. Sci.*, **1952**, *59*, 197. (c) Dietrich, H. V. and Cramer, F. *Chem. Bsr.*, **1954**, *87*, 806.
- (22) For the review of <sup>1</sup>H NMR analysis of cyclodextrin inclusion complex, see: (a) Schneider, H. J.; Hacket, F. and Rüdiger, V. *Chem. Rev.* **1998**, *98*, 1755-1785. (b) Fielding, L. *Tetrahedron* **2000**, *56*, 6151-6170.
- (23) Demarco, P. V.; Thakkar, A. L. *J. Chem. Soc., Chem. Commun.* **1970**, *2*.
- (24) Wishnia, A. and Lappi, S.J. *J. Mol. Biol.* **1974**, *82*, 77.
- (25) Sanemasa, I.; Akamine, Y. *Bull. Chem. Soc. Jpn.* **1987**, *60*, 2059.

- (26) Connors, K. A. *Binding Constants*, Wiley: New York, 1987
- (27) Botsi, A.; Yannakopoulou, K.; Perly, B. and Hadjoudis, E. *J. Org. Chem.* **1995**, *60*, 4017-4023.
- (28) For directing target site of substrate to reaction centre by supramolecular approach, see: (a) Sanders, J. K. M. In *Supramolecular Science: Where It Is and Where It Is Going*; Ungaro, R., Dalcanale, E., Eds.; Kluwer: Netherlands, 1999 (b) Lehn, J.-M. *Supramolecular Chemistry: Concepts and Perspectives*; VCH: Weinheim, 1995. (c) Murakami, Y.; Kikuchi, J.-I.; Hisaeda, Y.; Hayashida, O. *Chem. Rev.* **1996**, *96*, 721. (d) Shingaki, T.; Miura, K.; Higuchi, T.; Hirobe, M.; Nagano, T. *Chem. Commun.* **1997**, Motherwell, W. B.; Bingham, M. J.; Six, J. *Tetrahedron* **2001**, *57*, 4663. (e) Feiters, M. C.; Rowan, A. E.; Nolte, R. J. M. *Chem. Soc. Rev.* **2000**, *29*, 375. (f) Sham, K. C.; Yeung, H. L.; Yiu, S. M.; Lau, T. C.; Kwong, H. L. *Dalton Trans.*, **2010**, *39*, 9469–9471.
- (29) Oiwka, K.; Furuya, K. *Ekmchintica Acta* **1992**, *37*, 1135-1141.

## Chapter 2

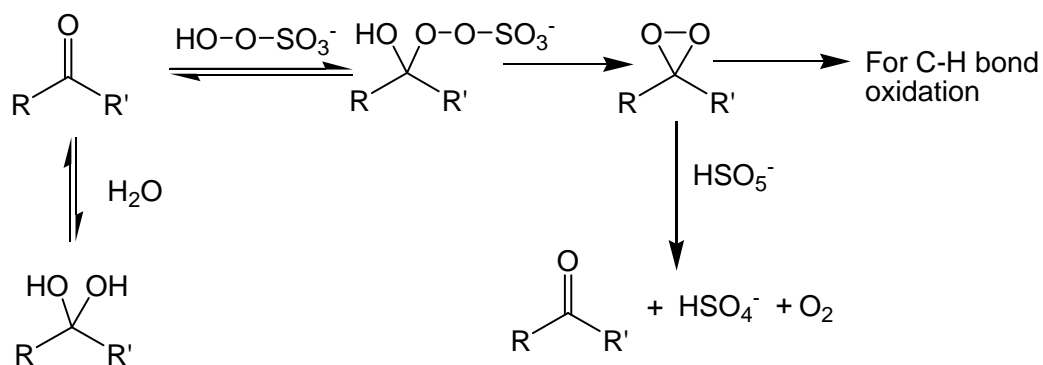
### Optimization of Reaction Conditions for C-H Bond Oxidation by Dioxiranes Generated *in situ*

#### 2.1 Introduction

Dioxiranes are powerful oxidants for C-H bond oxidation.<sup>1-5</sup> They can be generated from ketones and Oxone, followed by isolation through vacuum distillation at subambient temperatures in a gentle stream of inert gas and be collected at -60 to -75 °C.<sup>2a</sup> However, the tedious procedures and special experimental setup required for isolation of dioxiranes severely limit the variety of dioxiranes for C-H bond oxidation. Only ketone precursors with high volatility and low molecular weight can be employed. This hinders the systematic investigations on the structure-activity relationship of dioxirane-based C-H bond oxidation. Besides, the isolated dioxiranes are extremely unstable in the presence of trace metal and impurities and under the exposure of light, demanding strictly controlled storage conditions for isolated dioxiranes.<sup>2a</sup>

*In situ* generation of dioxiranes<sup>6</sup> provides a more convenient alternative way of using dioxiranes for oxidation. However, it is less efficient for C-H oxidation as compared to the isolated dioxiranes, probably due to the *in situ* decomposition

of dioxiranes by peroxy anion  $\text{HSO}_5^-$  (Scheme 2.1).<sup>7,8</sup> To maintain a high level of dioxirane concentration and hence a higher C-H oxidation efficiency, we have conducted optimization of reaction conditions.



**Scheme 2.1** Generation of dioxiranes by reaction of Oxone and ketones.

## 2.2 Optimization of Experimental Parameters for *in situ* C-H Bond

### Oxidation of Adamantane

At the outset, C-H bond oxidation was carried out using the reaction conditions reported in Yang's article.<sup>9</sup> Adamantane was used as a substrate, and the reaction was conducted by stirring adamantane (0.1 mmol), 1,1,1-trifluoroacetone (0.1 mmol), Oxone (0.5 mmol) and  $\text{NaHCO}_3$  (1.55 mmol) in a mixture of  $\text{H}_2\text{O}$  (1 mL) and  $\text{CH}_3\text{CN}$  (1.5 mL) at 25 °C for 2 h. The products were separated by flash column chromatography and analyzed by  $^1\text{H}$  NMR, it was found that adamantane was oxidized to 1-adamantanol and 1,3-adamantandiol (Scheme 2.2).



The reaction parameters affecting the oxidation rate of adamantane were studied, including reaction temperature, choice of base, amount of Oxone, base, and 1,1,1-trifluoroacetone used.

### **2.2.1 Effect of Reaction Temperature**

The effect of reaction temperature on adamantane oxidation was examined. The conversion of adamantane was very low (13%) when the reaction was carried out at 0 °C (Table 2, entry 1). When the adamantane oxidation was conducted at 25 °C, the conversion of adamantane was as follows (52%) (Entry 2). However, the conversion of adamantane decreased (33%) when the reaction was performed at 40 °C (Entry 3). Probably, the higher reaction temperature at 40 °C would increase the rate of decomposition of Oxone, leading to the decrease in the conversion. Thus, reaction temperature at 25 °C was chosen for subsequent studies.

**Table 2.1** Adamantane oxidation at different temperature <sup>a</sup>

Entry	Temperature (°C)	adamantane : 1-adamantanol :	
		1,3-adamantandiol <sup>b</sup>	
1	0	87 : 13 : 0	13
2	25	48 : 47 : 5	52
3	40	60 : 33 : 7	40

<sup>a</sup> Unless otherwise indicated, reactions were carried out by stirring 0.1 mmol of adamantane and 0.1 mmol of 1,1,1-trifluoroacetone in a mixture of 1 mL of H<sub>2</sub>O and 1.5 mL of CH<sub>3</sub>CN, followed by addition of 0.5 mmol of Oxone and 1.55 mmol of NaHCO<sub>3</sub>.

<sup>b</sup> Determined by <sup>1</sup>H NMR analysis of the crude reaction mixture.

### 2.2.2 Choice of Base

The oxidation by dioxiranes generated *in situ* is usually conducted at neutral pH. Under acidic conditions, referring to Scheme 2.1, HSO<sub>5</sub><sup>-</sup> anion is protonated, and dioxiranes could not be generated by nucleophilic addition of HSO<sub>5</sub><sup>-</sup> efficiently. On the contrary, Oxone decomposition would become too fast under basic conditions.<sup>10</sup> In this section, the effect of various bases on adamantane oxidation was investigated.

**Table 2.2** Adamantane oxidation conducted with different bases. <sup>a</sup>

Entry	Base	pH	adamantane : 1-adamantanol :		Conv. (%)
			1,3-adamantandiol <sup>b</sup>		
1	NaHCO <sub>3</sub>	6.9	48	47 : 5	52
2	CaCO <sub>3</sub>	6.4	44	41 : 15	56
3	Na <sub>2</sub> CO <sub>3</sub>	9.0	98	2 : 0	2
4	K <sub>2</sub> CO <sub>3</sub>	8.7	97	3 : 0	3
5	CS <sub>2</sub> CO <sub>3</sub>	9.1	100	0 : 0	0

<sup>a</sup> Unless otherwise indicated, reactions were carried out by stirring 0.1 mmol of adamantane and 0.1 mmol of 1,1,1-trifluoroacetone in a mixture of 1 mL of H<sub>2</sub>O and 1.5 mL of CH<sub>3</sub>CN at room temperature, followed by addition of 0.5 mmol of Oxone and 1.55 mmol of base. <sup>b</sup> Determined by <sup>1</sup>H NMR analysis of the crude reaction mixture.

Oxone is a mix salt of 2KHSO<sub>5</sub>, KHSO<sub>4</sub> and K<sub>2</sub>SO<sub>4</sub> containing three acidic protons. To provide neutral reaction conditions, the ratio of Oxone to the monobasic NaHCO<sub>3</sub> was designed to be 1 : 3.1. Based on this ratio, the reaction conditions were neutral (pH = 6.9) when NaHCO<sub>3</sub> was used as a base, determined by pH meter. The adamantane oxidation performed with Oxone and NaHCO<sub>3</sub> in a ratio of 1 : 3.1 gave 52% conversion. Apart from NaHCO<sub>3</sub>, CaCO<sub>3</sub> could also provide neutral reaction conditions (pH = 6.4) for adamantane



oxidation. The reaction conducted with  $\text{CaCO}_3$  (entry 2) gave the conversion of adamantane (56%) similar to that using  $\text{NaHCO}_3$  as the base. The stronger base could not benefit the dioxirane-based adamantane oxidation and only gave a trace amount of conversion. The reaction performed with  $\text{Na}_2\text{CO}_3$  (entry 3) only gave 2% conversion, and the reaction performed with  $\text{K}_2\text{CO}_3$  (entry 4) gave only 3% conversion. No conversion was observed when the reaction was conducted with  $\text{Cs}_2\text{CO}_3$  (entry 5). The pH of the reaction systems conducted with  $\text{Na}_2\text{CO}_3$ ,  $\text{K}_2\text{CO}_3$  and  $\text{Cs}_2\text{CO}_3$  were 9.0, 8.7 and 9.1. This revealed that the dioxirane-based adamantane oxidation needs to be conducted in neutral reaction conditions, but not basic conditions.

### 2.2.3 Study on the Amount of Oxone and Base

**Table 2.3** Adamantane oxidation with different amounts of Oxone and NaHCO<sub>3</sub><sup>a</sup>

Entry	Oxone (mmol)	NaHCO <sub>3</sub> (mmol)	Time	adamantane :	
				1-adamantanol :	Conv. (%)
				1,3-adamantandiol <sup>b</sup>	
1	0.5	1.55	2 h	48 : 47 : 5	52
2	0.5×2	1.55×2	4 h	24 : 67 : 9	76
3	0.5×3	1.55×3	6 h	7 : 49 : 44	93
4	0.5×4	1.55×4	8 h	16 : 59 : 25	84
5	0.25×8	0.775×8	8 h	12 : 54 : 34	88

<sup>a</sup> Unless otherwise indicated, reactions were carried out by stirring 0.1 mmol of adamantane and 0.1 mmol of 1,1,1-trifluoroacetone in a mixture of 1 mL of H<sub>2</sub>O and 1.5 mL of CH<sub>3</sub>CN at room temperature with different additions of 0.5 mmol of Oxone and 1.55 mmol of NaHCO<sub>3</sub>. <sup>b</sup> Determined by <sup>1</sup>H NMR analysis of the crude reaction mixture.

The effect of amount of Oxone and base used was studied. The conversion of adamantane increased when the loading of Oxone and NaHCO<sub>3</sub> increased. With one addition of 0.5 mmol of Oxone and 1.55 mmol of NaHCO<sub>3</sub> at 0 h, the

conversion of adamantane was 52% after 2 h stirring. The reaction carried out with two additions of 0.5 mmol of Oxone and 1.55 mmol of NaHCO<sub>3</sub> at 0 h and 2 h gave the 76% conversion over 4 h; while the reaction conducted with three additions of Oxone and NaHCO<sub>3</sub> at 0 h, 2 h and 4 h gave 93% conversion (total reaction time: 6 h).

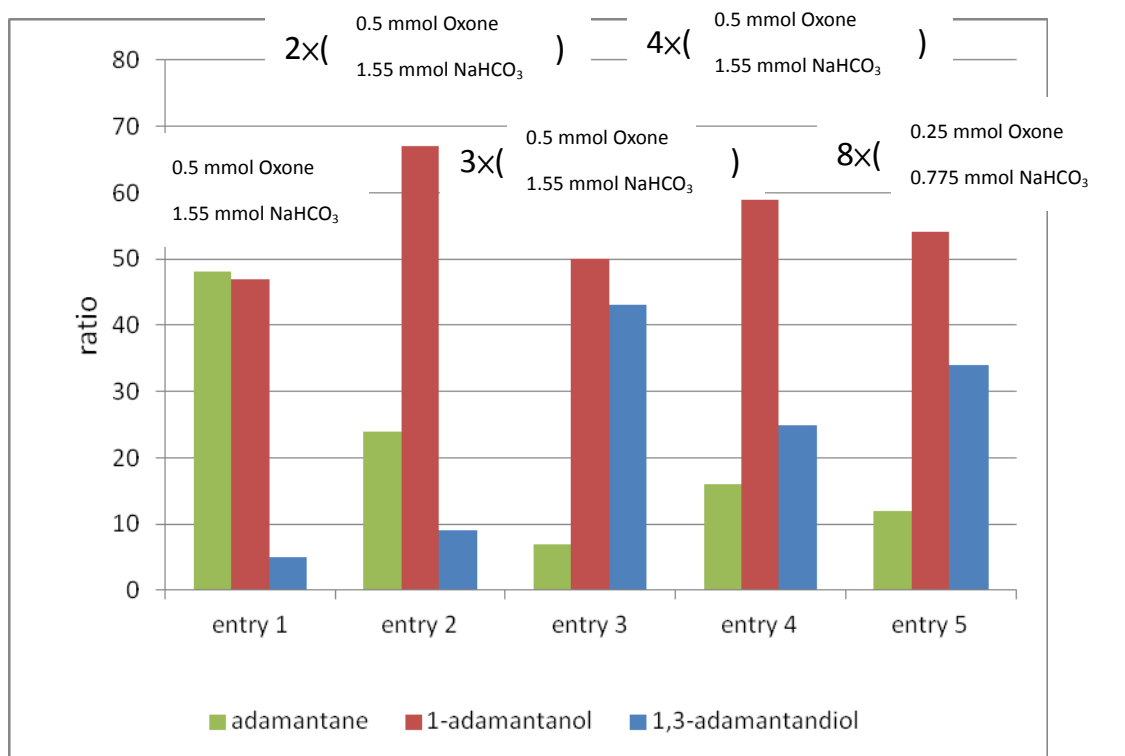
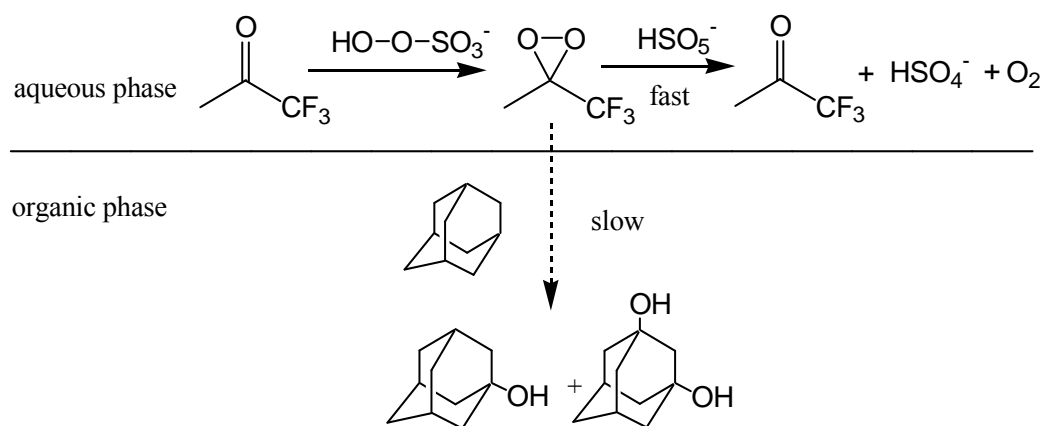


**Figure 2.2** Effect of different amounts of Oxone and NaHCO<sub>3</sub>

However, the conversion of adamantane did not increase with four additions of Oxone and NaHCO<sub>3</sub> at 0 h, 2 h, 4 h and 6 h (entry 4) (84%, total reaction time: 8 h). This would be due to the excessive formation of Na<sub>2</sub>SO<sub>4</sub> by the reaction of

Oxone and  $\text{NaHCO}_3$ . The  $\text{Na}_2\text{SO}_4$  absorbed  $\text{H}_2\text{O}$  and hence reduced the amount of water available for dissolution of Oxone and  $\text{NaHCO}_3$ , leading to reduced efficiency for dioxirane generation. Besides, the high ionic strength induced by a large amount of  $\text{Na}_2\text{SO}_4$  would lead to biphasic separation of  $\text{H}_2\text{O}$  and  $\text{CH}_3\text{CN}$ . In such a biphasic system, the good solubility of 1,1,1-trifluoroacetone in aqueous phase facilitates the generation of dioxiranes. However, owing to the high concentration of Oxone in the aqueous phase, the decomposition of dioxiranes by peroxy anion  $\text{HSO}_5^-$  may also be faster. As a result, only a small amount of dioxiranes would go back to the organic phase for oxidation. Thus, the rate of adamantane oxidation was low.



**Scheme 2.3** Dioxirane-based adamantane oxidation in biphasic system

When the reaction was performed with 8 additions of 0.5 mmol of Oxone and 1.55 mmol of  $\text{NaHCO}_3$  at 0 h, 1 h, 2 h, 3 h, 4 h, 5 h, 6 h and 7 h (entry 5), the

conversion of adamantane was slightly higher (88%), compared to that given by the reaction carried out with four additions of Oxone and NaHCO<sub>3</sub> at 0 h, 2 h, 4 h and 6 h (entry 4) (84%). This would be due to less decomposition of dioxiranes by excess amount of Oxone.

#### **2.2.4 Effect of Loading of 1,1,1-Trifluoroacetone**

The effect of 1,1,1-trifluoroacetone loading was examined. The oxidation of adamantane was initially performed by using 1 equivalent of 1,1,1-trifluoroacetone (Table 2.4, entry 2). The reaction gave 93% conversion of adamantane. Decreasing 1,1,1-trifluoroacetone loading to 0.5 equivalent (entry 3), the conversion of adamantane remained 49%; when the reaction was conducted with 0.1 equivalent of 1,1,1-trifluoroacetone (entry 4), 36% conversion of adamantane could still be obtained.

**Table 2.4** Effect of loading of 1,1,1-trifluoroacetone on adamantane oxidation <sup>a</sup>

Entry	Loading of	adamantane : 1-adamantanol :	Conv. (%)
	1,1,1-trifluoroacetone	1,3-adamantane <sup>b</sup>	
1	2 equiv.	23 : 52 : 25	77
2	1 equiv.	7 : 50 : 43	93
3	0.5 equiv.	51 : 38 : 11	49
4	0.1 equiv.	64 : 31 : 5	46

<sup>a</sup> Unless otherwise indicated, reactions were carried out by stirring 0.1 mmol of adamantane and different amount of 1,1,1-trifluoroacetone in a mixture of 1 mL of H<sub>2</sub>O and 1.5 mL of CH<sub>3</sub>CN at room temperature with 3 additions of 0.5 mmol of Oxone and 1.55 mmol of NaHCO<sub>3</sub> at 0 h, 2 h and 4 h (total reaction time: 6 h). <sup>b</sup> Determined by <sup>1</sup>H NMR analysis of the crude reaction mixture.

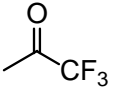
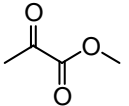
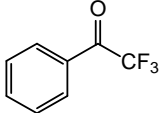
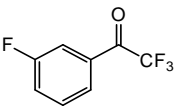
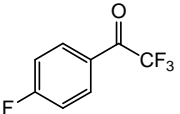
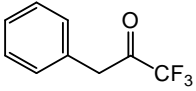
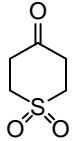
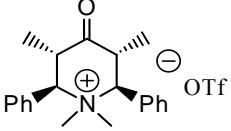
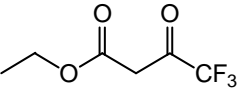
However, the reaction conducted with 2 equivalents of 1,1,1-trifluoroacetone (entry 1) did not give higher adamantane conversion (77%) compared with that conducted with 1 equivalent of 1,1,1-trifluoroacetone (93%). This would be due to the more significant decomposition of Oxone by excess ketone, leading to the low conversion of adamantane.

### 2.3 Ketone Screening

Using the newly developed protocol of adamantane oxidation by dioxiranes generated *in situ*, an extended scope of ketones towards adamantane oxidation could be examined. This is not possible to be achieved by using isolated dioxiranes. The results are summarized in Table 2.5.

The adamantane oxidation conducted with 1,1,1-trifluoroacetone gave the highest conversion of adamantane (entry 1) (93%). This could be attributed to the strong electron-withdrawing trifluoromethyl group. According to literature reports, incorporation of electron-withdrawing groups adjacent to the dioxirane functionality could enhance its activity in oxidation.<sup>10,11</sup>

**Table 2.5** Catalytic activities of ketones towards adamantane oxidation <sup>a</sup>

Entry	Ketone	adamantane : 1-adamantanol : 1,3-adamantane <sup>b</sup>	Conv. (%)
1		7 : 50 : 43	93
2		14 : 71 : 15	86
3		43 : 52 : 5	57
4		24 : 66 : 10	76
5		52 : 43 : 5	48
6		61 : 35 : 4	39
7		22 : 61 : 17	78
8		60 : 40 : 0	40
9		100 : 0 : 0	0

<sup>a</sup> Unless otherwise indicated, reactions were carried out by stirring 0.1 mmol of adamantane, 0.1 mmol of ketone in a mixture of 1.5 mL CH<sub>3</sub>CN & 1 mL H<sub>2</sub>O at room temperature with 3 additions of 0.5 mmol of Oxone and 1.55 mmol of NaHCO<sub>3</sub> at 0 h, 2 h and 4 h (total reaction time: 6 h). <sup>b</sup> Determined by <sup>1</sup>H NMR analysis of the crude reaction mixture.



The activity of methyl pyruvate (entry 2) towards nucleophilic addition would be attributed to the electron withdrawing ability of ester group, it gave 86% conversion of adamantane, the electron-withdrawing property of the  $\alpha$ -ester adjacent to the dioxirane leads to the high activity of adamantane oxidation. Ketones in entries 3 to 6 are with trifluoromethyl group as 1,1,1-trifluoroacetone, but the reaction conducted with ketones in entries 3 to 6 gave lower conversion of adamantane. This would be due to the electron-donating property and unfavorable steric effect of the phenyl ring.

Interestingly, the cyclic ketones in entries 7<sup>12</sup> and 8<sup>13</sup> also gave moderate to good conversion of adamantane. The activity of ketone in entry 7 would be attributed to the dipole-dipole interaction of sulfone to the carbonyl group, and the activity of ketone in entry 8 was attributed to the through-space charge-dipole interaction of ammonium cation to the carbonyl group, called 'Field effect'.<sup>6c</sup>

The reaction conducted with ethyl 4,4,4-trifluoroacetoacetate (entry 9) gave no conversion; this would be attributed to the formation of enol from the ketone moiety.

## 2.4 Optimized Reaction Conditions for *in situ* C-H bond Oxidation of Adamantane

On the basis of the studies of the reaction parameters above, a general protocol for C-H bond oxidation was developed as follows:

To a reaction mixture of adamantane (0.1 mmol) in a mixture of H<sub>2</sub>O (1 mL) and CH<sub>3</sub>CN (1.5 mL), 0.1 mmol of 1,1,1-trifluoroacetone was added, followed by three additions of 0.5 mmol of Oxone and 1.55 mmol of NaHCO<sub>3</sub> at 0 h, 2 h, and 4 h. After 6 h, 4 mL of H<sub>2</sub>O was added and the resulting mixture was extracted with ethyl acetate (3×10 mL). The combined organic extract was dried over anhydrous Na<sub>2</sub>SO<sub>4</sub>. The organic solvent was evaporated under reduced pressure. The crude reaction mixture was then dissolved in CDCl<sub>3</sub> and analyzed by <sup>1</sup>H NMR.

### 2.4 Conclusion

In summary, the effects of reaction temperature, type of bases, amount of Oxone and base, and loading of ketones on adamantane oxidation were studied. The adamantane oxidation using dioxiranes generated *in situ* is conducted at room temperature (25 °C); NaHCO<sub>3</sub> is a suitable base to maintain neutral pH for adamantane oxidation; the multiple additions of Oxone and NaHCO<sub>3</sub> increase the

conversion of C-H bond oxidation. Besides, the conversion of C-H bond oxidation can be improved by increasing the loading of ketone. Using the protocol of adamantane oxidation by dioxiranes generated *in situ*, a wide variety of ketones towards adamantane oxidation was examined. The results showed that 1,1,1-trifluoroacetone exhibits the highest activity towards adamantane oxidation.

## **2.5 Experimental Section**

### **2.5.1 General Procedures for Adamantane Oxidation**

To a solution of 0.1 mmol of adamantane in a mixture of 1 mL of H<sub>2</sub>O and 1.5 mL of CH<sub>3</sub>CN, 0.1 mmol of 1,1,1-trifluoroacetone was added. The reaction mixture was being stirred, followed by three additions of 0.5 mmol of Oxone and 1.55 mmol of NaHCO<sub>3</sub> at 0 h, 2 h and 4 h. After stirring for 6 h, 4 mL of H<sub>2</sub>O was added, and the resulting mixture was extracted with ethyl acetate (3 × 10 mL). The combined organic extract was dried by anhydrous Na<sub>2</sub>SO<sub>4</sub>, and the organic solvent was evaporated under reduced pressure. The residue was then dissolved in CDCl<sub>3</sub> and analyzed by <sup>1</sup>H NMR.

## 2.5.2 $^1\text{H}$ NMR Spectra of Adamantane Oxidation

Table 2.1, entry 1 (Table 2.2, entry 1; Table 2.3, entry 1)

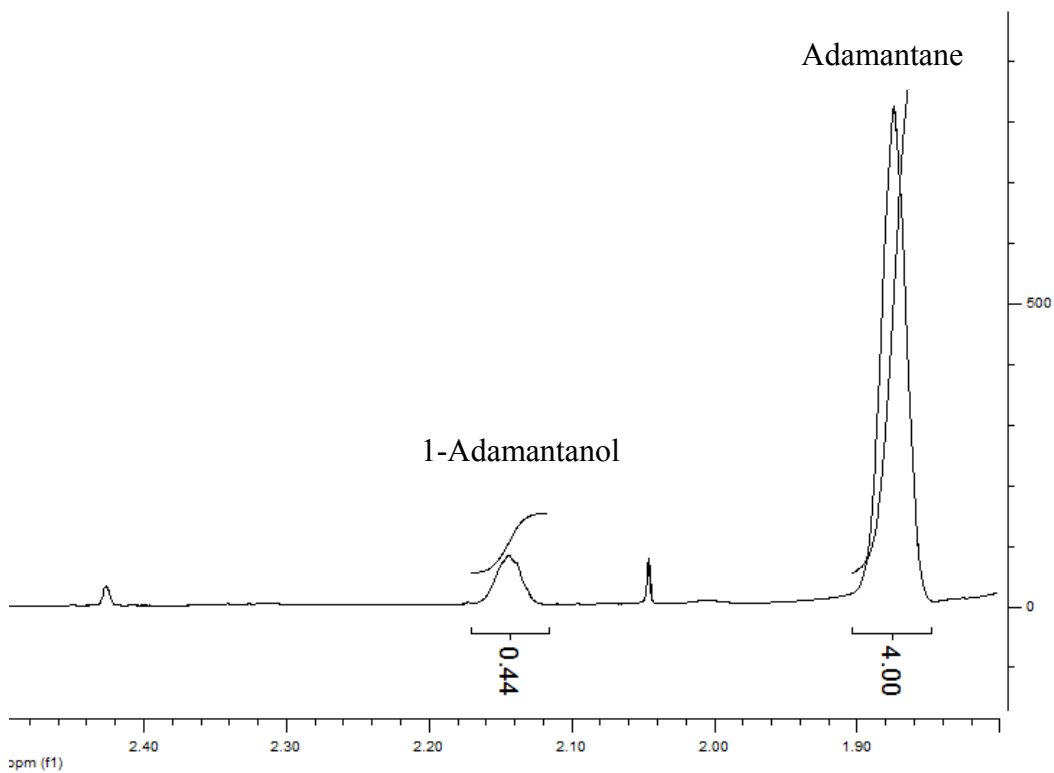


Table 2.1, entry 2

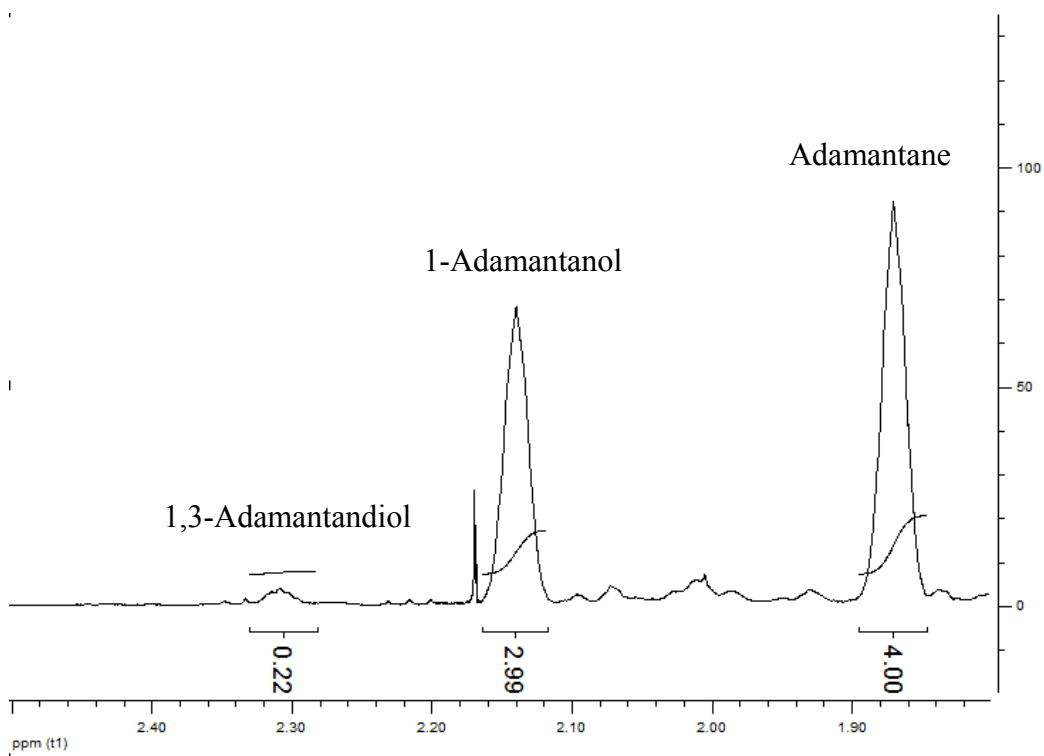


Table 2.1, entry 3

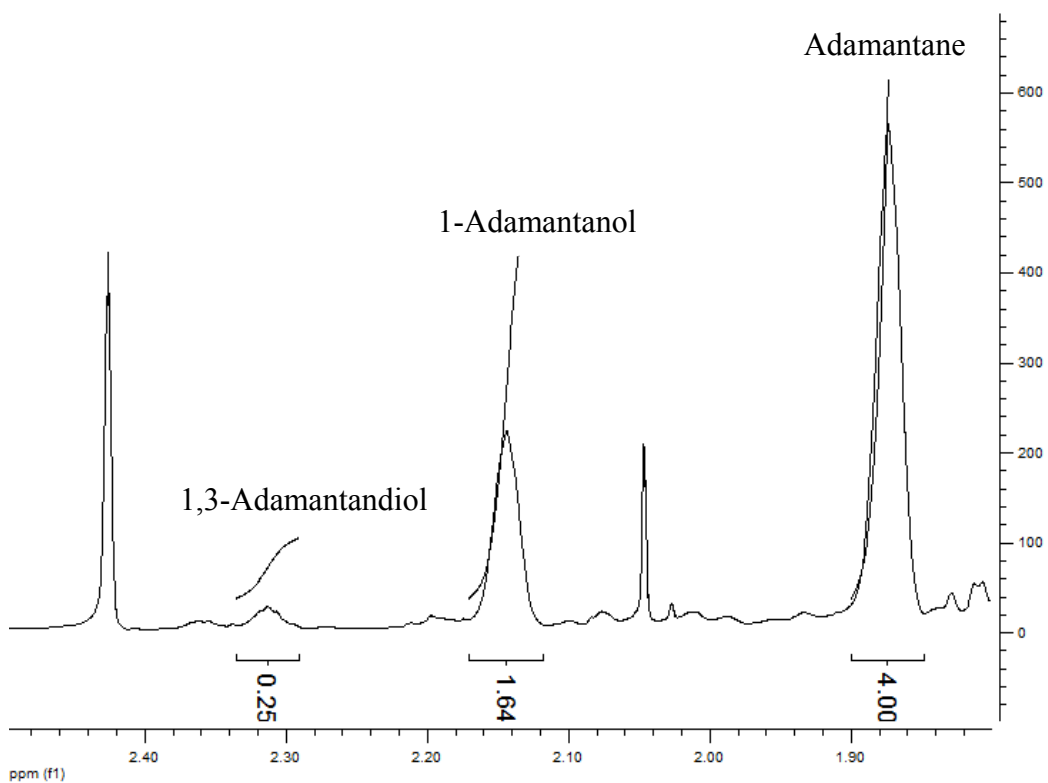


Table 2.2, entry 2

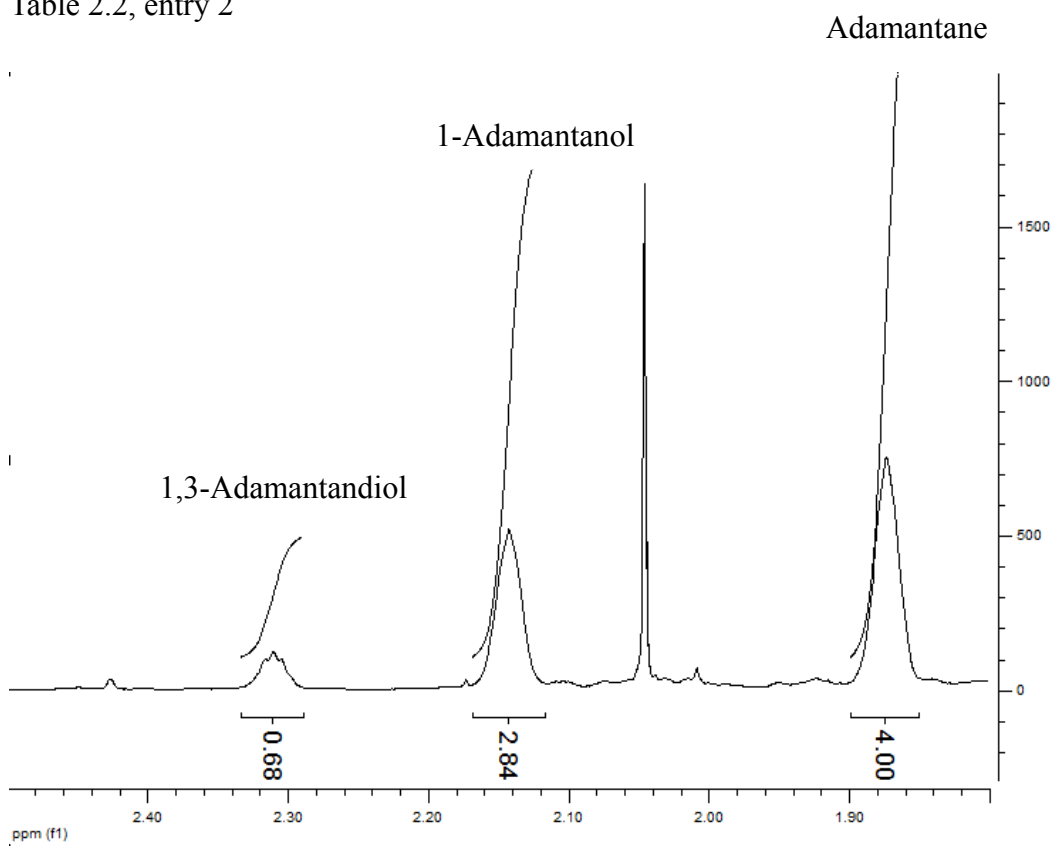


Table 2.2, entry 3

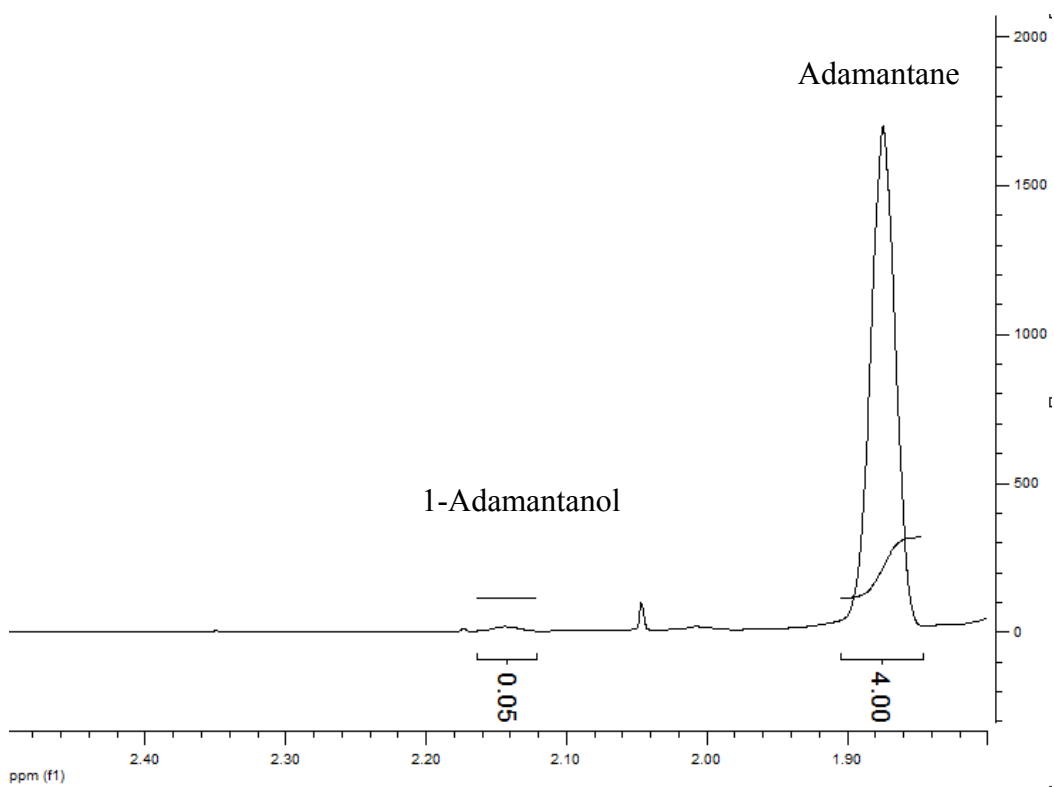


Table 2.2, entry 4

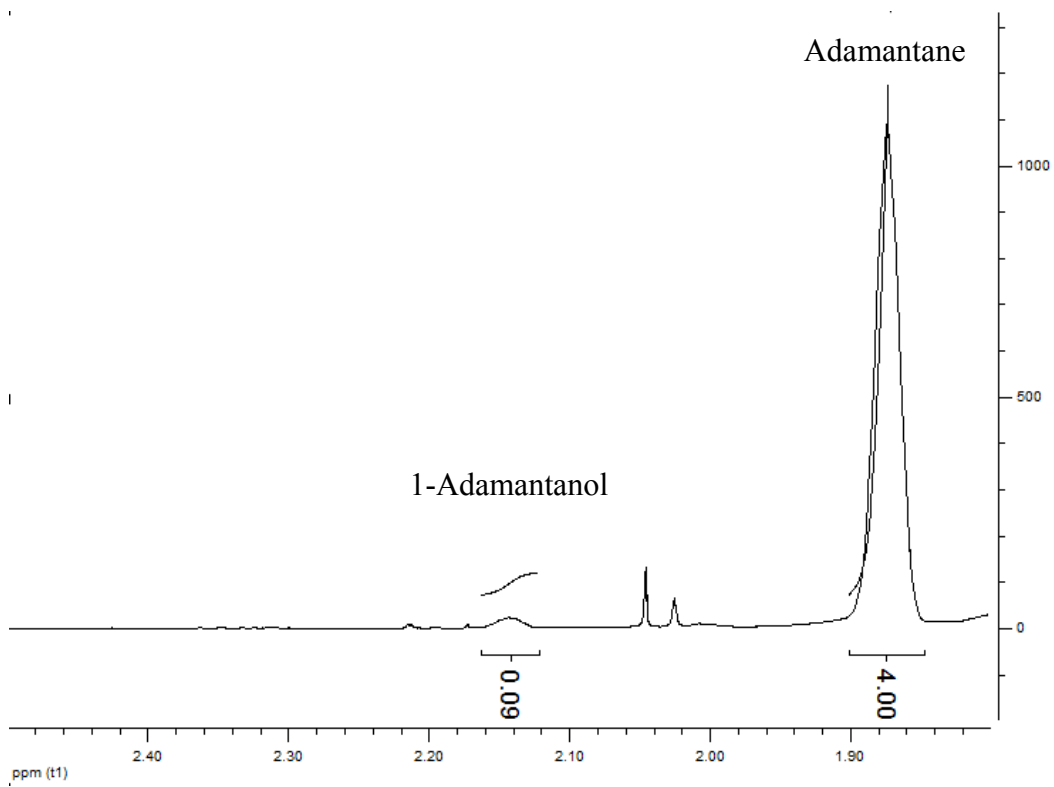


Table 2.2, entry 5

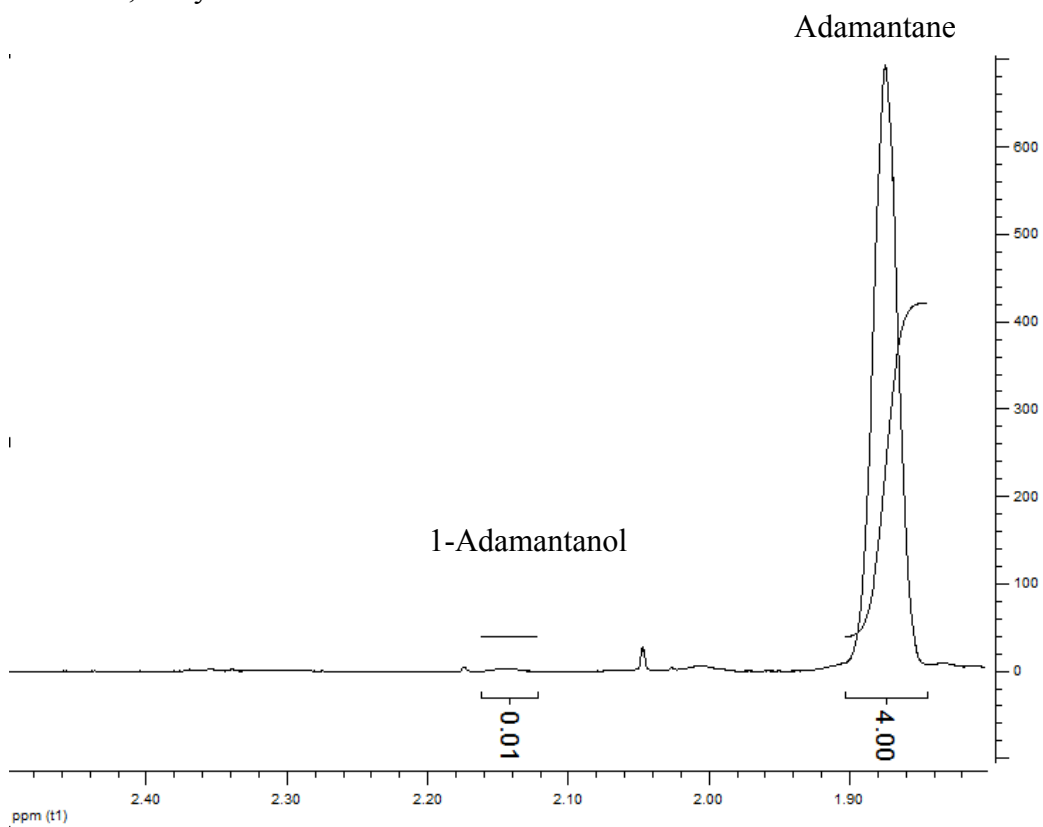


Table 2.3, entry 2

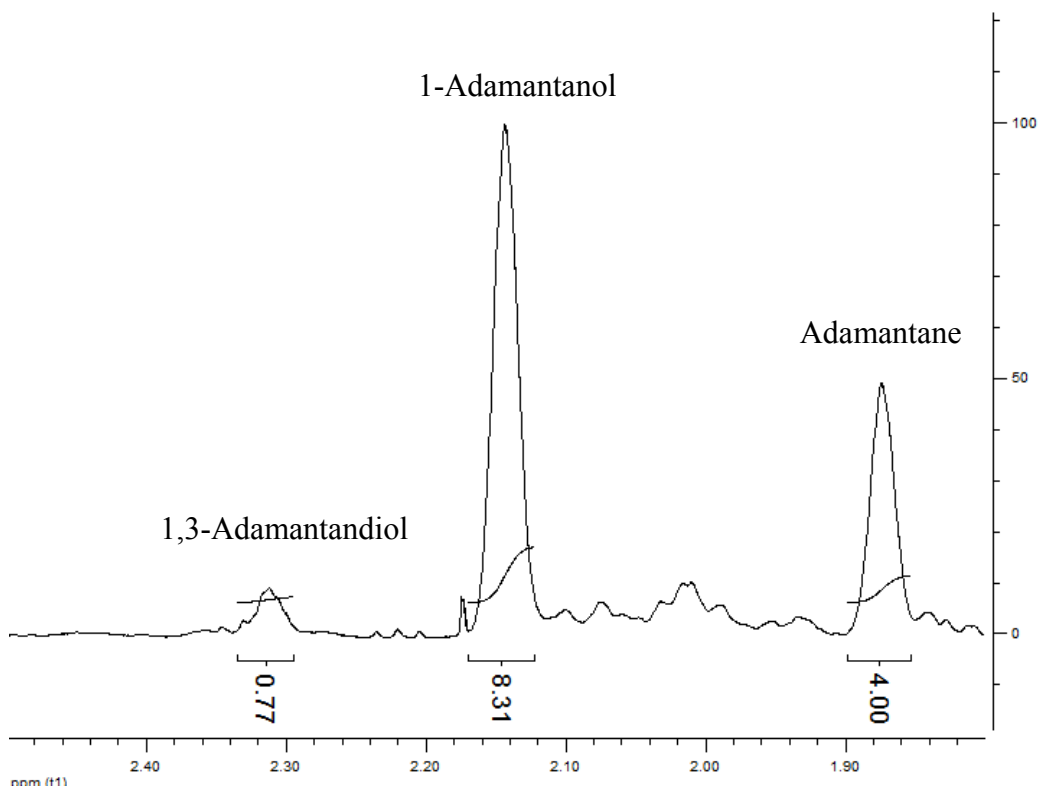


Table 2.3, entry 3 (Table 2.4, entry 2; Table 2.5, entry 1)

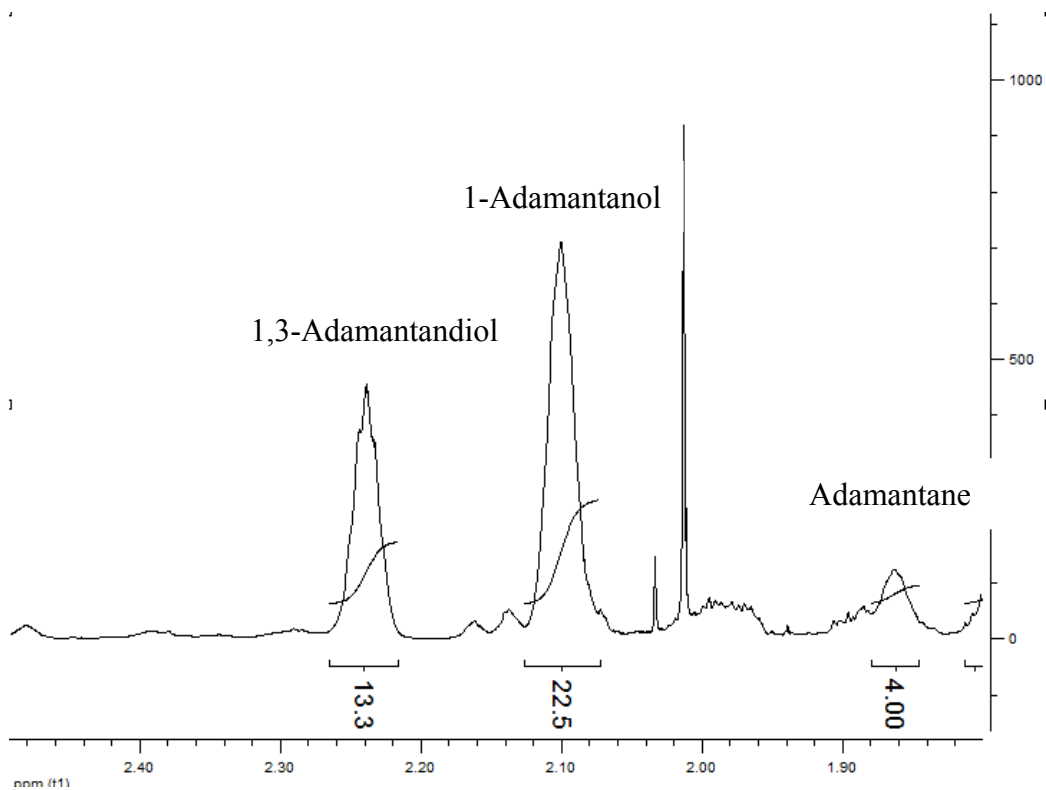


Table 2.3, entry 4

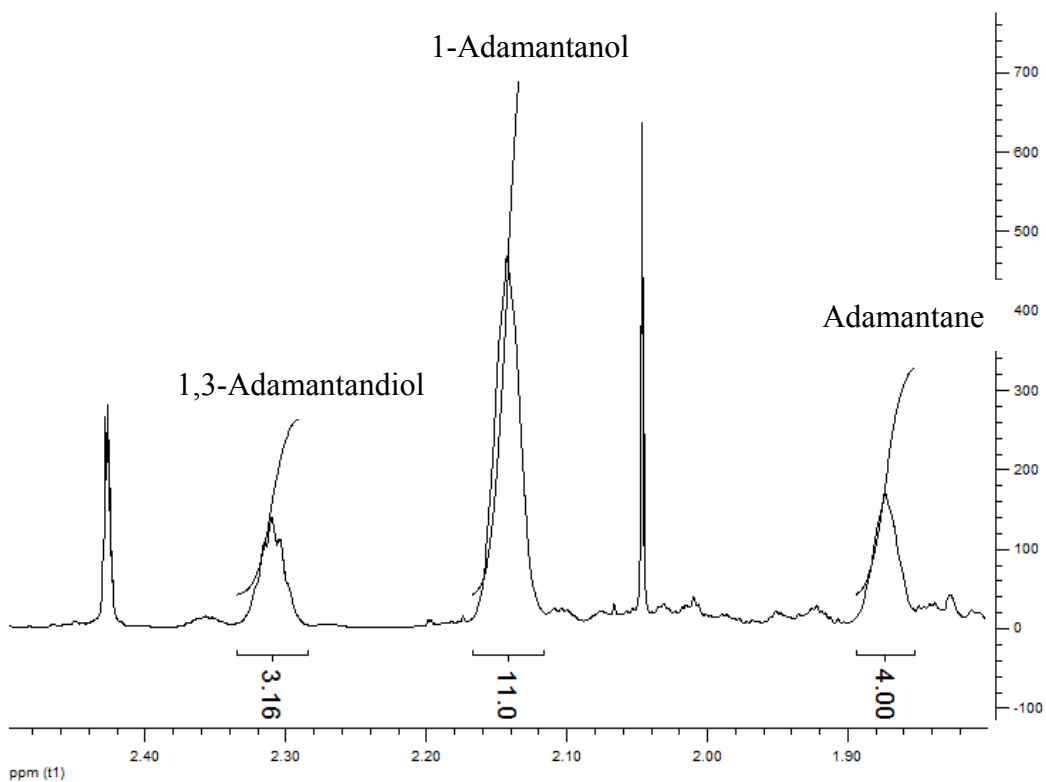




Table 2.3, entry 5

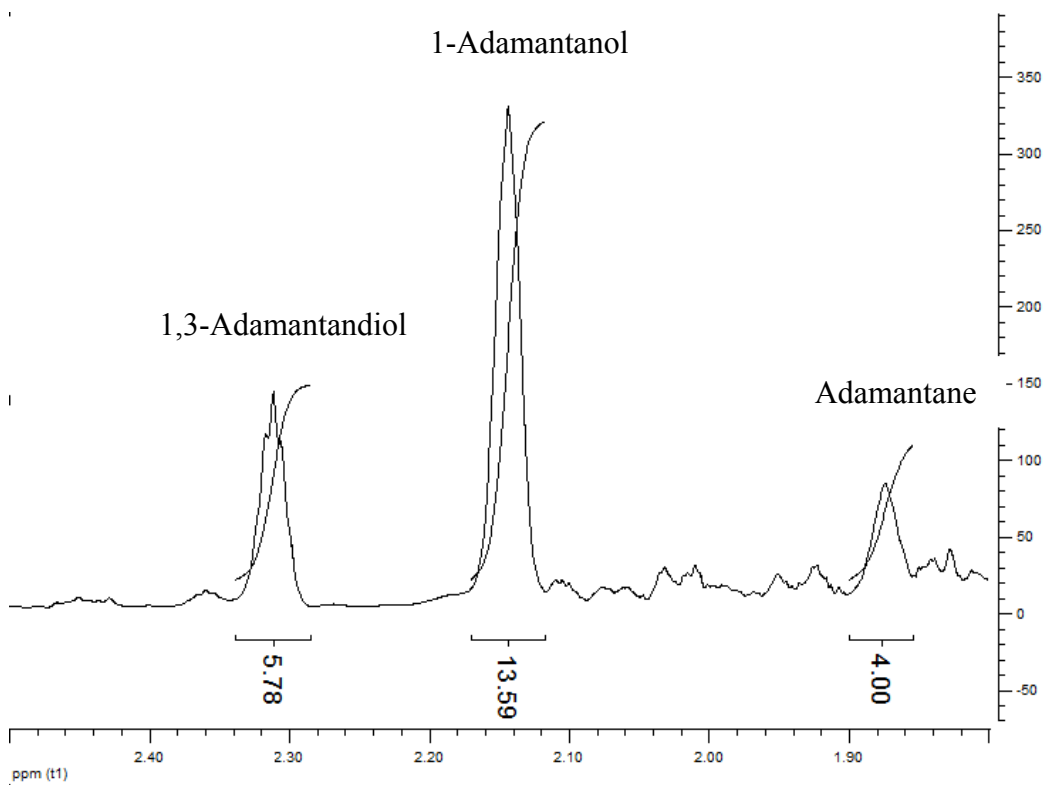


Table 2.4, entry 1

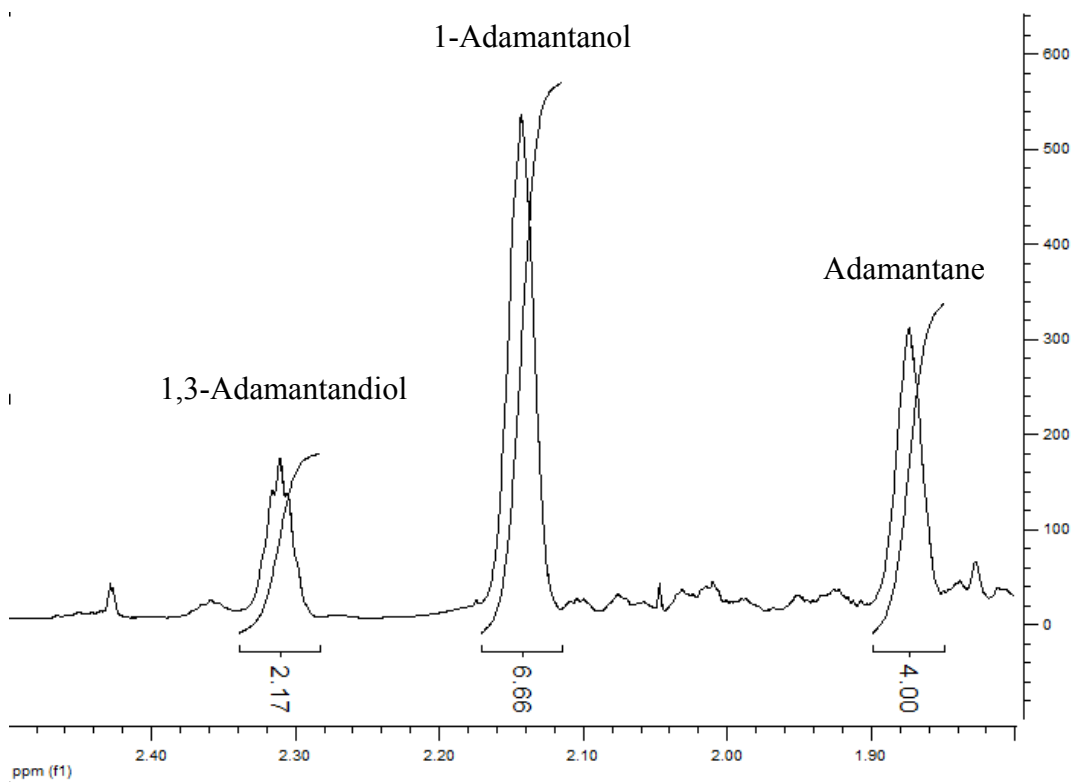


Table 2.4, entry 3

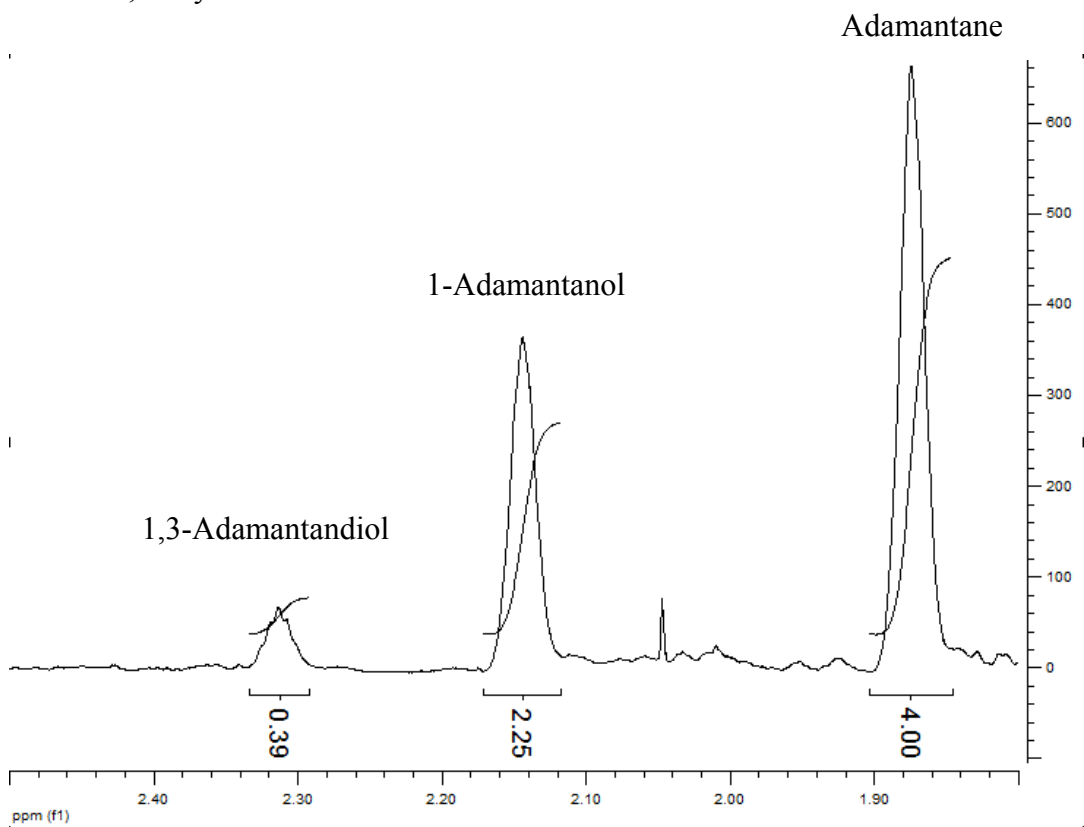


Table 2.4, entry 4

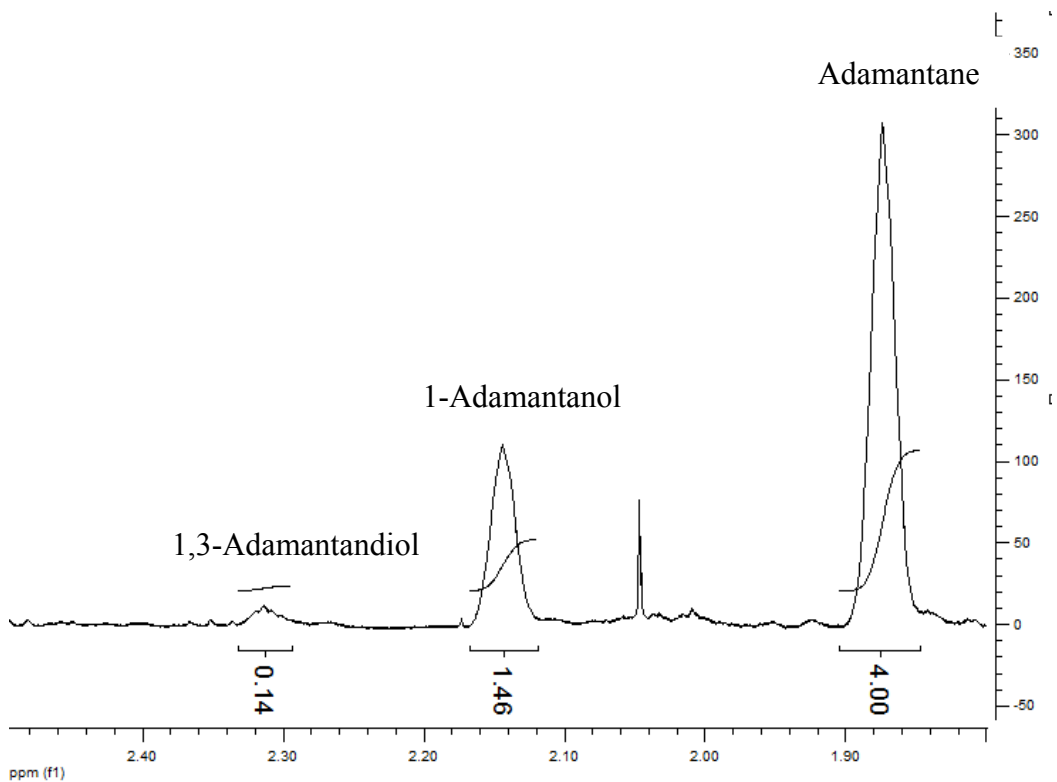


Table 2.5, entry 2

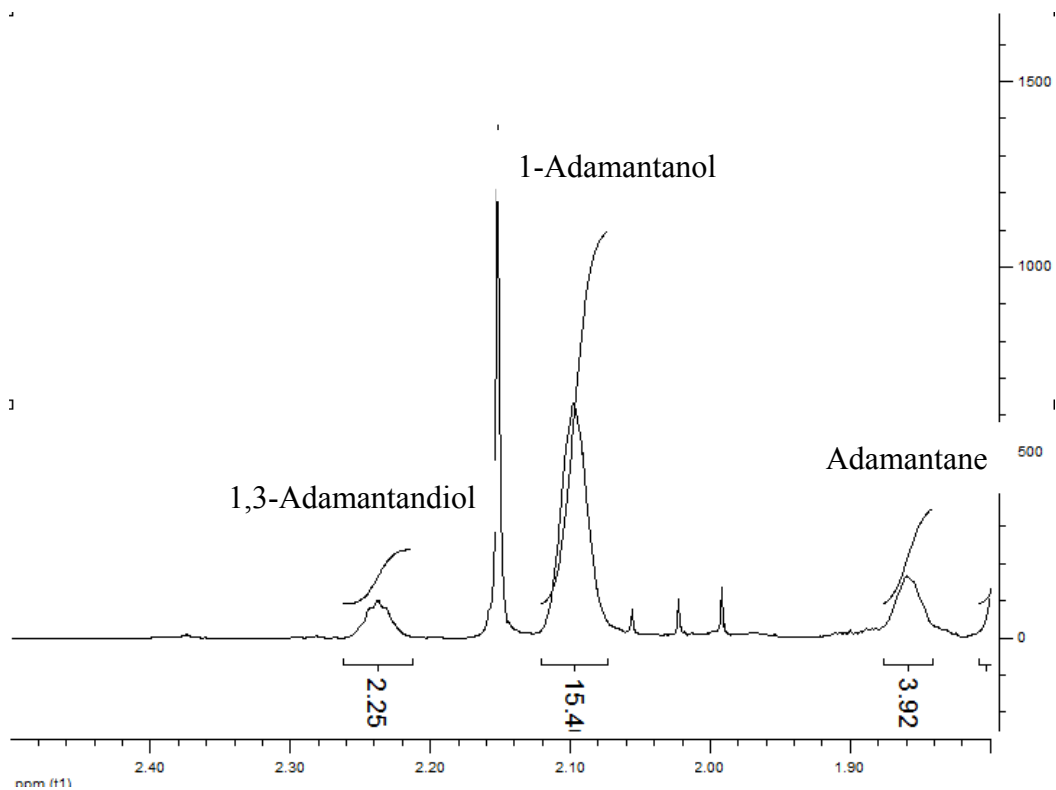


Table 2.5, entry 3

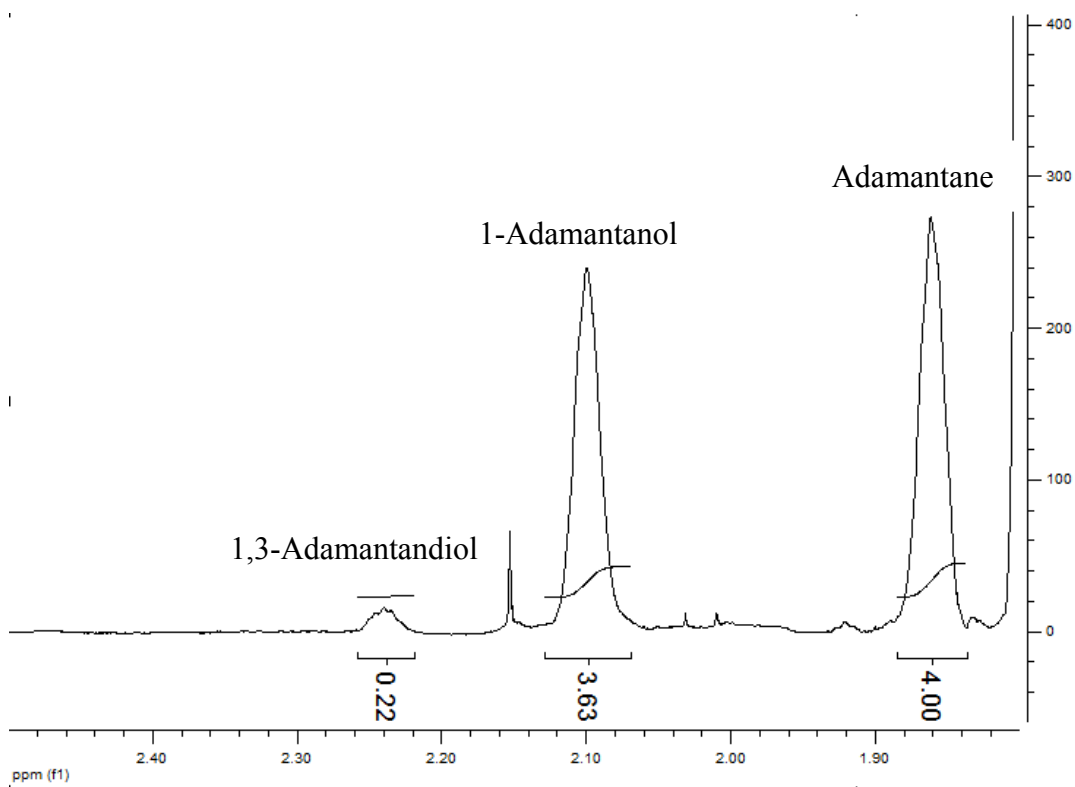


Table 2.5, entry 4

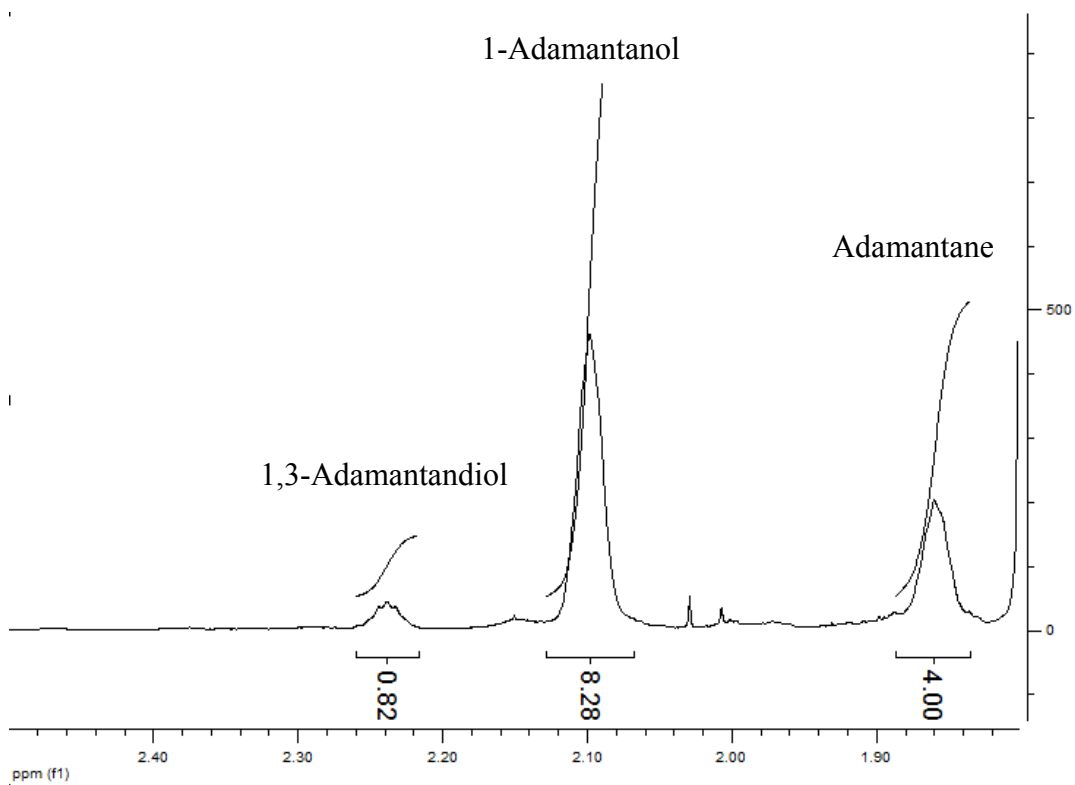


Table 2.5, entry 5

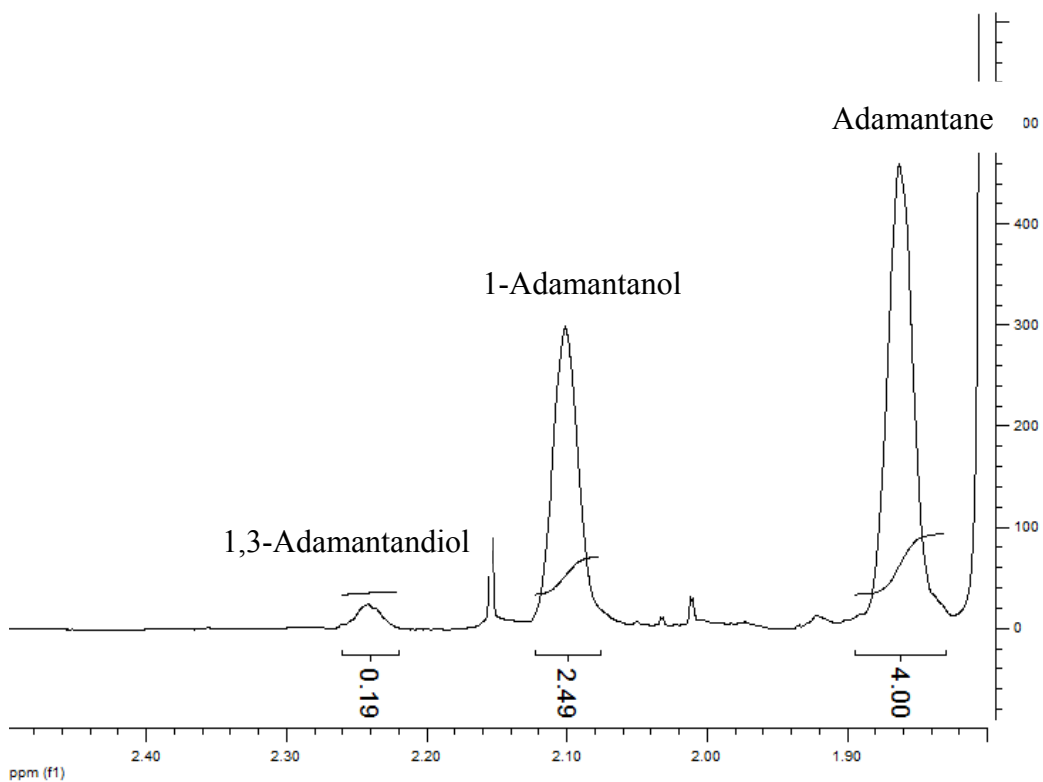


Table 2.5, entry 6

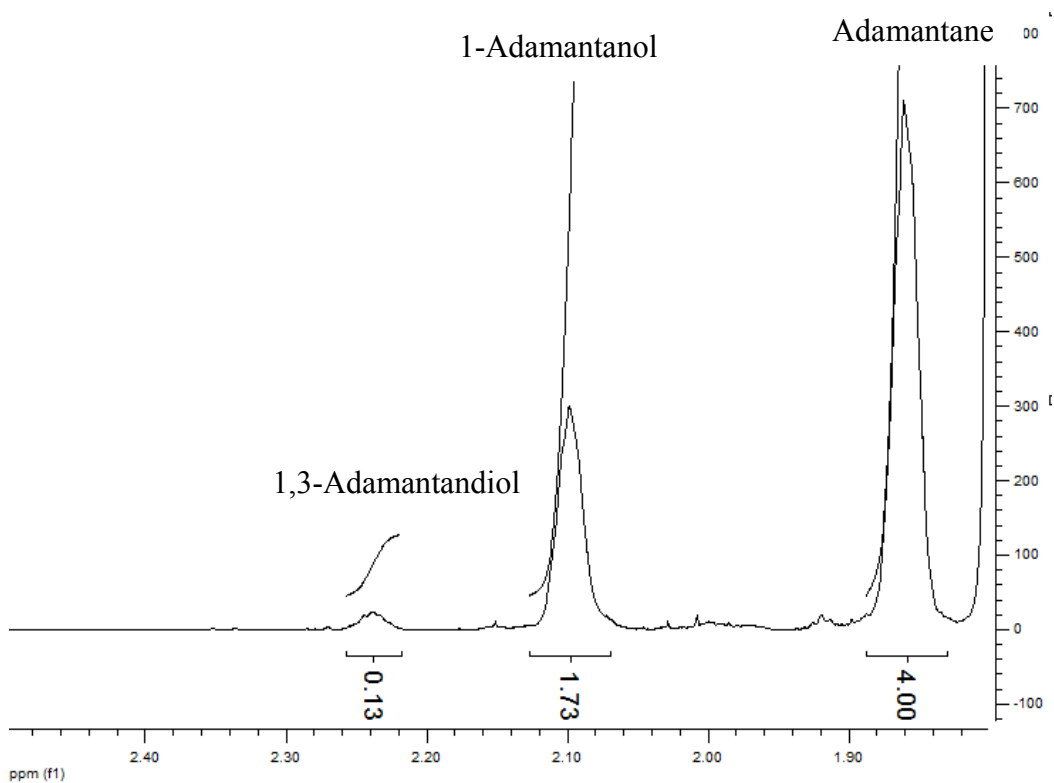


Table 2.5, entry 7

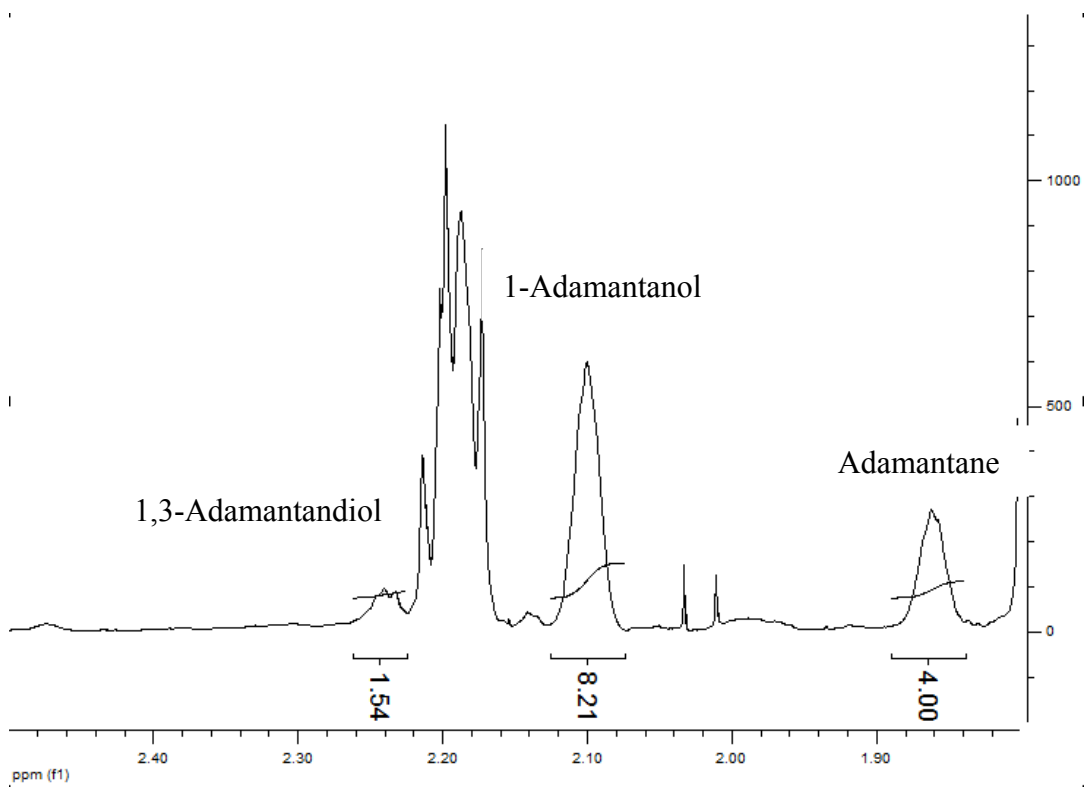


Table 2.5, entry 8

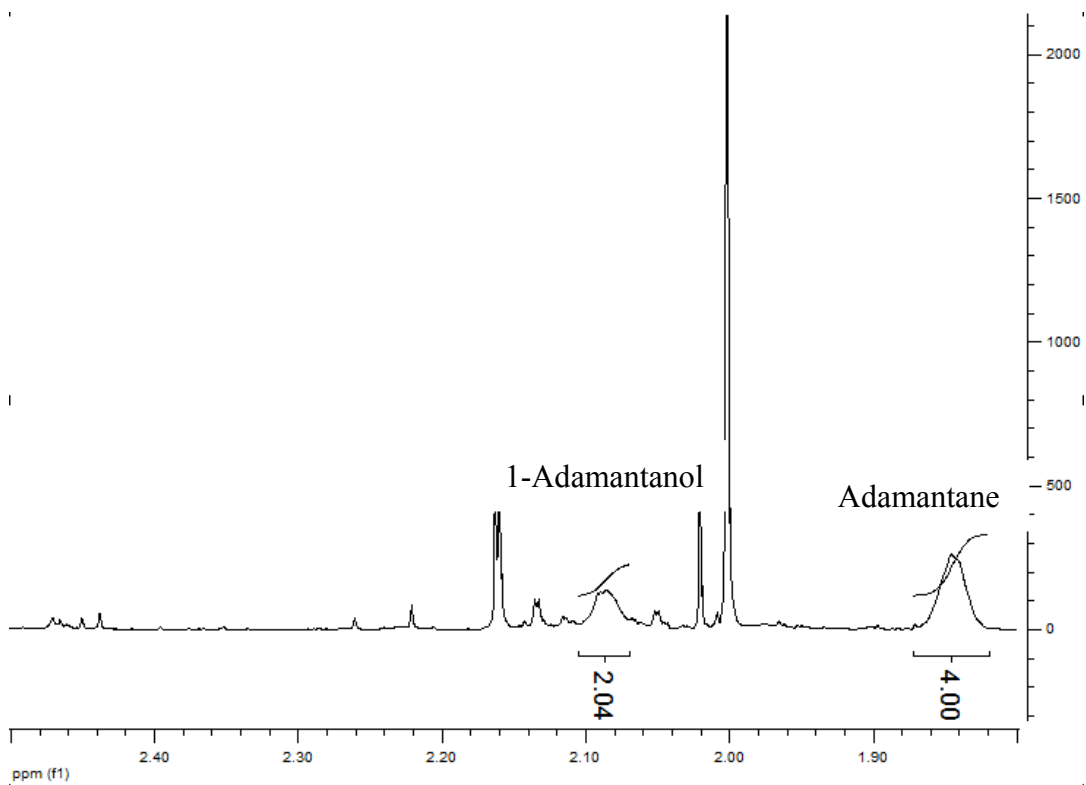


Table 2.5, entry 9

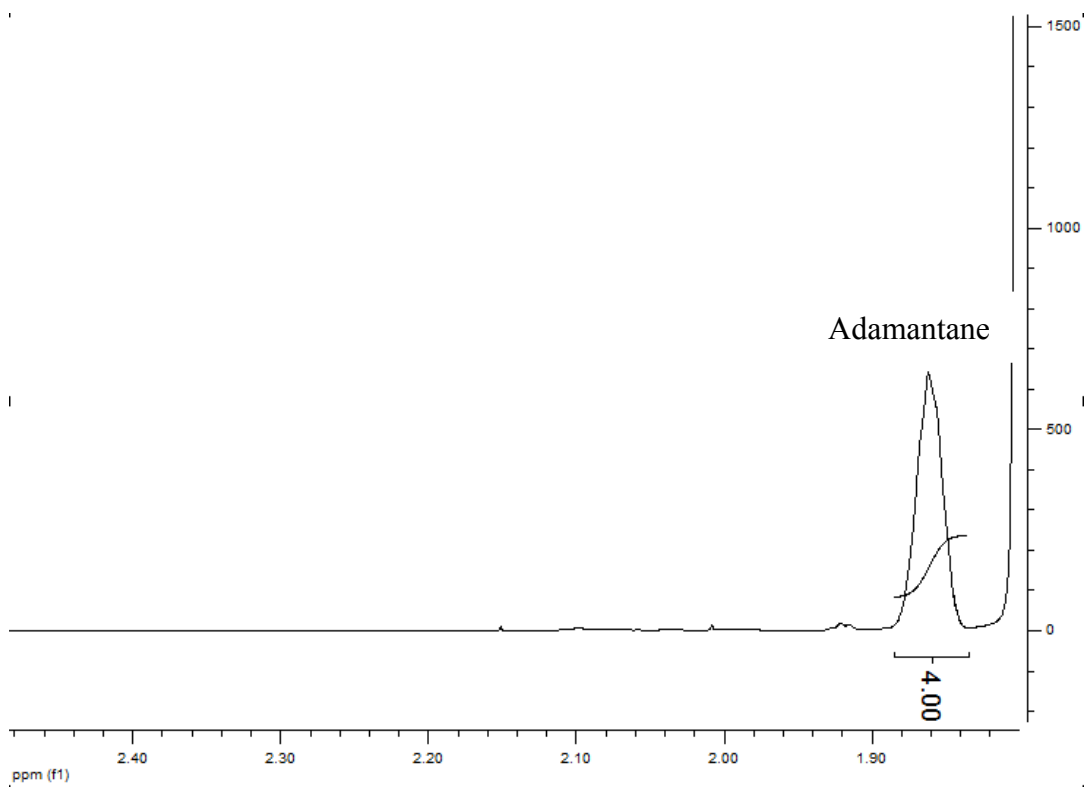
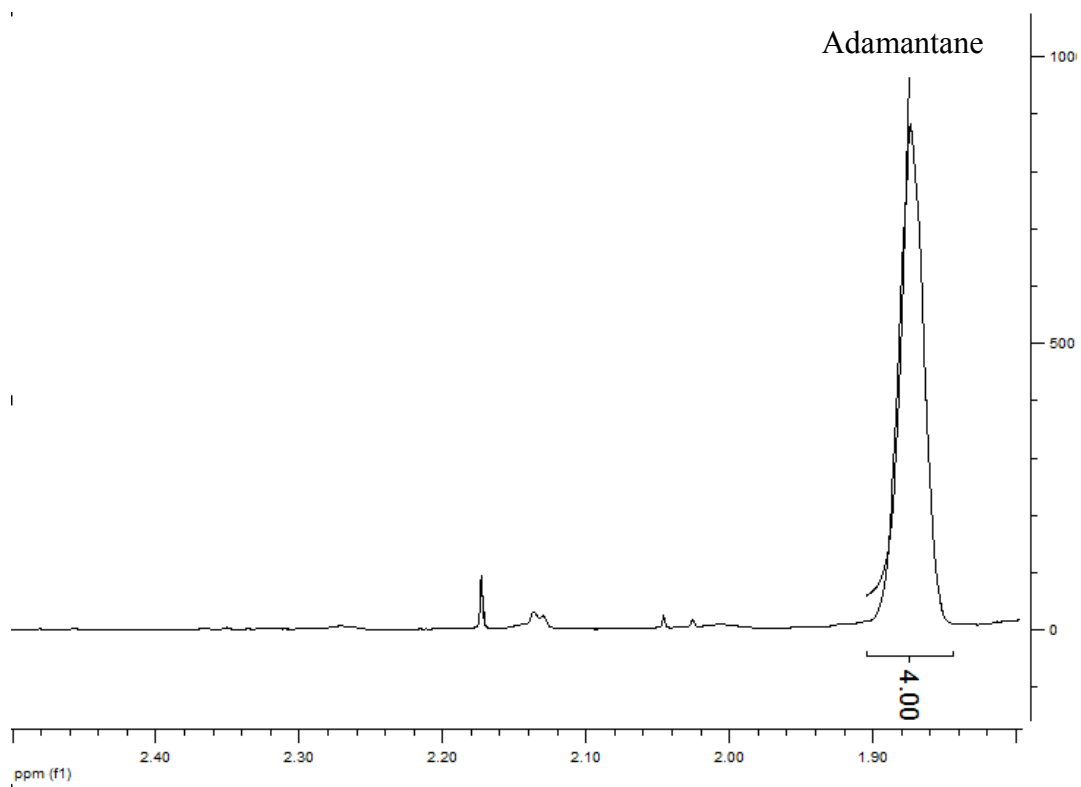


Table 2.5, entry 10



## 2.6 References

- (1) Review for dioxirane based C-H bond oxidation: a) Curci, R.; D'Accolti, L.; Fusco, C. *Acc. Chem. Res.* **2006**, *39*, 1
- (2) Examples for dioxirane based C-H bond oxidation from Curci and co-workers: a) Mello, R.; Fiorentino, M.; Fusco, Caterina and Curci, R. *J. Am. Chem. Soc.* **1989**, *111*, 6749-6757. b) Bovicelli, P.; Lupattelli, P.; Mincione, E.; Prencipe, T. and Curci, R. *J. Org. Chem.* **1992**, *57*, 5052-5054. c) Kuck, D.; Schuster, A.; Fusco, C.; Fiorentino, M.; Curci, R. *J. Am. Chem. Soc.* **1994**, *116*, 2375. d) Curci, R.; Detomaso, A.; Prencipe, T.; Carpenter, G. B. *J. Am. Chem. Soc.* **1994**, *116*, 8112. e) Fusco, C.; Fiorentino, M.; Dinoi, A. and Curci, R. *J. Org. Chem.* **1996**, *61*, 8681-8684. f) Curci, R.; Detomaso, A.; Lattanzio, M. E.; Carpenter, G. B. *J. Am. Chem. Soc.* **1996**, *118*, 11089. g) D'Accolti, L.; Fusco, C.; Lucchini, V.; Carpenter, G. B.; Curci, R. *J. Org. Chem.* **2001**, *66*, 9063. h) D'Accolti, L.; Dinoi, A.; Fusco, C.; Russo, A. and Curci, R. *J. Org. Chem.* **2003**, *68*, 7806-7810. i) D'Accolti, L.; Fiorentino, M.; Fusco, C.; Capitelli, F.; Curci, R. *Tetrahedron Lett.* **2007**, *48*, 3575. j) D'Accolti, L.; Fusco, C.; Lampignano, G.; Capitelli, F.; Curci, R. *Tetrahedron Lett.* **2008**, *49*, 5614. k) Annese, C.; D'Accolti, L.; Fusco, C.; Gandolfi, R.; Eaton, P. E. and Curci, R. *Organic Letters* **2009**,



11(16),3574-3577.

- (3) Examples for methyl(trifluoromethyl)dioxirane based C-H bond oxidation from Asensio and co-workers: a) Asensio, G.; Nunez, M. E. G.; Bernardini, C. B.; Mello, R.; Adam, W. *J. Am. Chem. Soc.* **1993**, *115*, 7250. b) Nunez, M. E. G.; Royo, J.; Castellano, G.; Andreu, C.; Boix, C.; Mello, R.; Asensio, G. *Org. Lett.* **2000**, *2*, 831. c) Nunez, M. E. G.; Castellano, G.; Andreu, C.; Royo, J.; Bagueña, M.; Mello, R.; Asensio, G. *J. Am. Chem. Soc.* **2001**, *123*, 7487. d) González-Núñez, M. E.; Royo, J.; Mello, R.; Bagueña, M.; Martínez Ferrer, J.; Ramírez de Arellano, C.; Asensio, G.; Surya Prakash, G. K. *J. Org. Chem.* **2005**, *70*, 7919. e) Mello, R.; Royo, J.; Andreu, C.; Bagueña-Añó, M.; Asensio, G.; González-Núñez, M. E. *Eur. J. Org. Chem.* **2008**, 455.
- (4) Murray, R. W.; Jeyaraman, R.; Mohan, L. *J. Am. Chem. Soc.* **1986**, *108*, 2470.
- (5) Chen, K.; Baran, P. S. *Nature* **2009**, *459*, 824.
- (6) First example for oxidation by dioxirane generated *in situ*: Yang, D.; Wong, M. K. and Yip, Y. C. *J. Org. Chem.* **1995**, *60*, 3887-3889. Reviews for oxidation by dioxirane generated *in situ*: a) Yang, D. *Acc. Chem. Res.* **2004**, *37*, 497-505. b) Shi, Y. *Acc. Chem. Res.*, **2004**, *37* (8), 488-496. c) Wong, O.

- A. and Shi, Y. *Top Curr Chem*, **2010**, *291*, 201–232.
- (7) Edwards, J. O.; Pater, R. H.; Curci, R.; DiFuria, F. *Photochem. Photobiol.* **1979**, *30*, 63.
- (8) Denmark, S. E.; Forbes, D. C.; Hays, D. S.; DePue, J. S.; Wilde, R. G. *J. Org. Chem.* **1995**, *60*, 1391.
- (9) Yang, D.; Wong, M. K.; Wang, X. C. and Tang Y. C. *J. Am. Chem. Soc.* **1998**, *120*, 6611-6612.
- (10) Yang, D.; Yip, Y. C.; Tang, M. W.; Wong, M. K.; Zheng, J. H. and Cheung, K. K. *J. Am. Chem. Soc.* **1996**, *118*, 491-492.
- (11) Adam, W.; Saha-Moller, C. R.; Ganeshpure, P. A. *Chem. Rev.* **2001**, *101*, 3499-3548.
- (12) Casy, G.; Sutherland, A. G.; Taylor, R. J. K.; Urban, P. G. *Synthesis* **1989**, 767.
- (13) Yang, D.; Yip, Y. C.; Jiao, G. S.; Wong, M. K. *J. Org. Chem.*, **1998**, *63*, 8952-8956.

## Chapter 3

### Site-Selective C-H Bond Oxidation through Supramolecular

### Control by Cyclodextrins

#### 3.1 Introduction

Cyclodextrins are supramolecular compounds. They can form inclusion complexes with organic compounds in water. The hydroxyl groups located at the two rims of cyclodextrins can react with substrates directly or be attached to other catalytic centres. All these advantages make cyclodextrins widely used as ideal hosts in biomimetic catalysis. Well documented in literatures, supramolecular catalysts based on cyclodextrins<sup>1</sup> mainly achieve selectivity in reactions by positioning the target site of the substrates in close proximity to the active reaction centre in order to facilitate the reactions, or by obstructing the approach of undesirable sites to the active reaction centre in order to increase the relative reactivity of the desirable target sites.

For C-H bond oxidation by cyclodextrin-based catalysts, Breslow and co-workers reported the pioneer work<sup>2</sup> on selective C-H bond oxidations of steroid compounds. Reported by Breslow, the catalyst was designed by attaching cyclodextrins to the manganese porphyrin (Figure 3.1). As shown in Scheme 3.1,

oxidation of the substrates was conducted with 10 mol% of cyclodextrin-linked manganese porphyrin and 5 mM iodosobenzene (5 equiv.) in aqueous solution with 10 equivalent of pyridine at room temperature for 2 h. Instead of the electron-rich tertiary C-H bonds, the secondary C-H bond of the steroid backbone was regioselectively oxidized by positioning the target C-H bond to the active catalytic center of the catalyst. After hydrolysis with 25% KOH, triol was obtained in 40% conversion. Indicated in this paper, the two *tert*-butylphenyl groups would bind to CDs at *trans*-position in the catalyst.

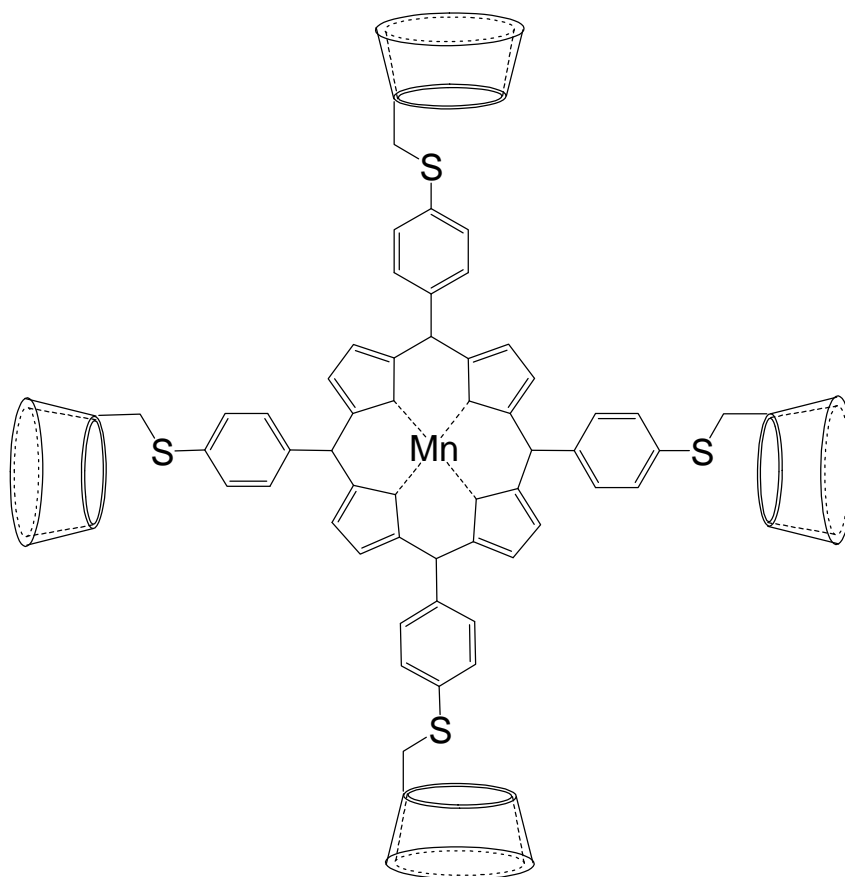
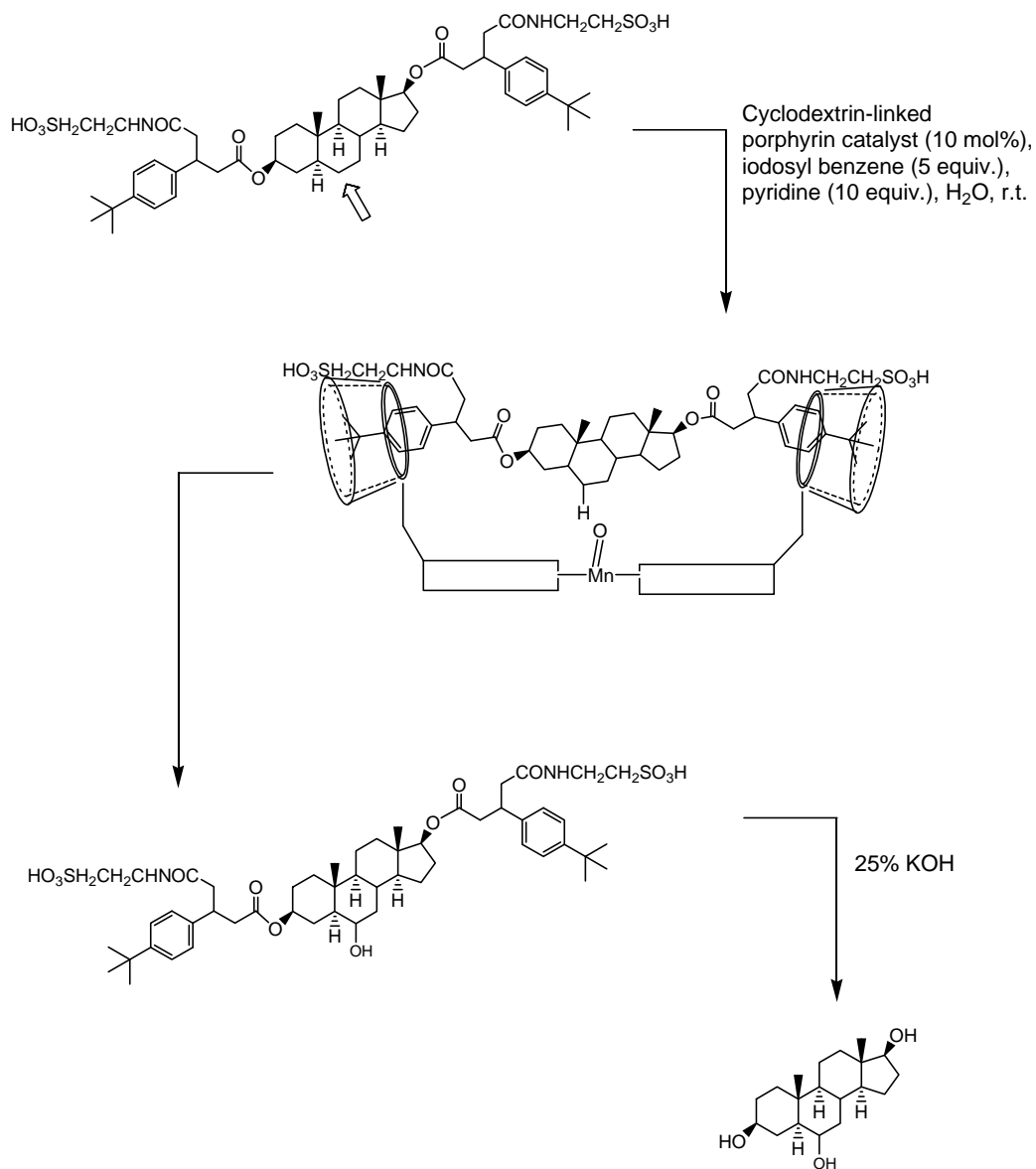
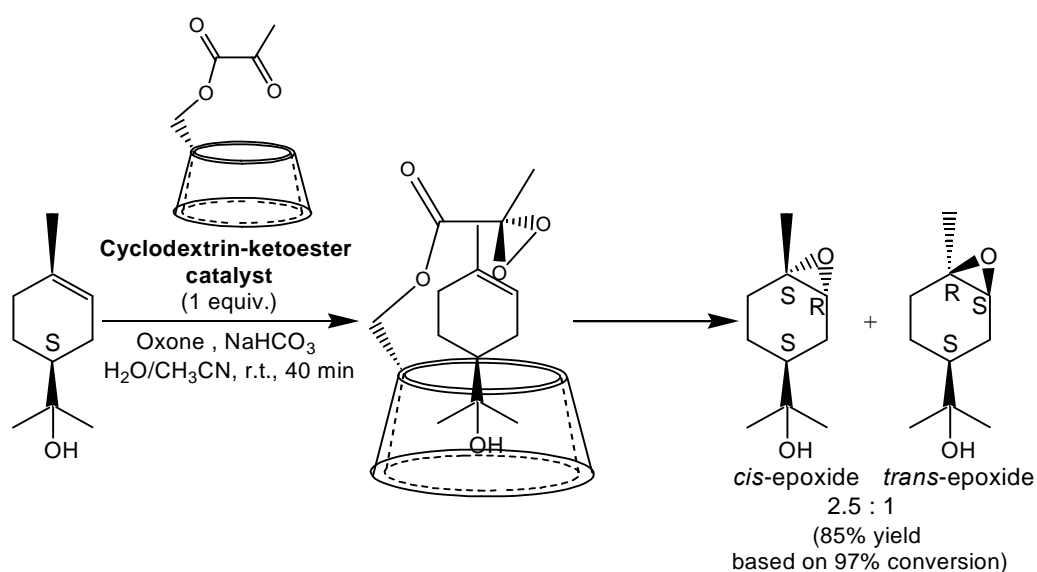


**Figure 3.1** Cyclodextrin-attached manganese porphyrin catalyst.



**Scheme 3.1** Regioselective C-H bond oxidation by cyclodextrin-attached catalyst.

In 2003, Wong's group has developed cyclodextrin-ketoester as supramolecular catalyst for stereoselective alkene epoxidation.<sup>3</sup> As shown in Scheme 3.2, using 0.1 mmol of terpene as substrate, the reaction was carried out with 0.1 mmol of cyclodextrin-ketoester, 0.1 mmol of Oxone and 0.31 mmol of NaHCO<sub>3</sub> in a mixture of H<sub>2</sub>O and CH<sub>3</sub>CN at room temperature for 40 min. As a result, epoxide was obtained in 85% yield based on 97% conversion. The product ratio of *cis*-epoxide to *trans*-epoxide was 2.5 : 1. According to <sup>1</sup>H NMR study, inclusion complex of the substrate and the catalyst was formed.



**Scheme 3.2** Stereoselective epoxidation with cyclodextrin-ketoester catalyst.

In this work, cyclodextrins were used as supramolecular hosts to promote site-selective C-H bond oxidation of 3,7-dimethyloctyl ester in water with *in-situ* generated methyl (trifluoromethyl) dioxirane as oxidant. Overriding the electronic effect, and beyond the control by steric and substrate-based directing effects, site-selectivity in C-H bond oxidation has been achieved by supramolecular control through inclusion complex formation between the substrates and cyclodextrins.

### 3.2 Design of Substrates

Tertiary C-H bond is of higher activity among unactivated C-H bonds towards electrophilic oxidation carried out by dioxiranes. To investigate the effect of cyclodextrins on the site selectivity of C-H bond oxidation, 3,7-dimethyloctyl esters with two tertiary C-H bonds (Figure 3.2) were chosen as the substrate. The tertiary C-H bonds are located at the terminal and internal positions of the substrate.

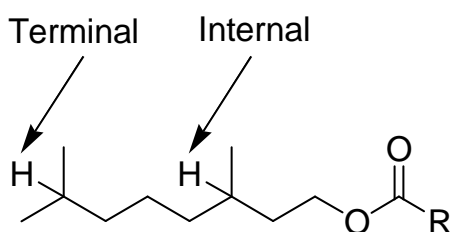
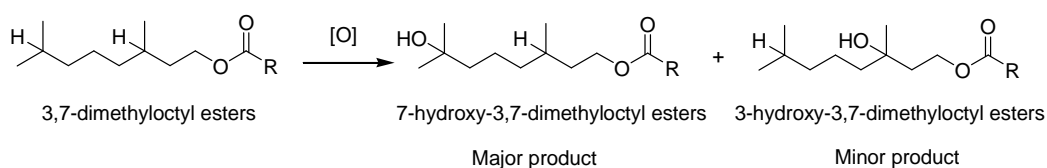


**Figure 3.2** Structure of 3,7-dimethyloctyl ester.

Due to the electronic effect imposed by the electron withdrawing ester moiety, electrophilic oxidation of the internal C-H bond is not favored. As a result, 7-hydroxy-3,7-dimethyloctyl ester is the major product through oxidation at the terminal C-H bond (Scheme 3.3).<sup>4a</sup>



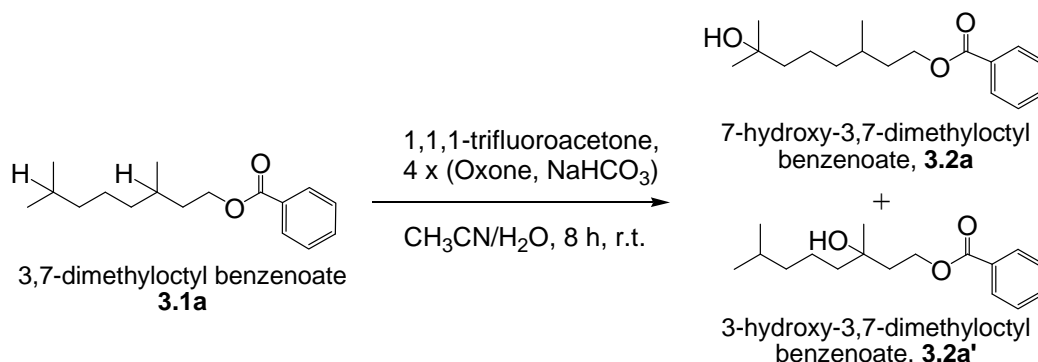
**Scheme 3.3** Oxidation of 3,7-dimethyloctyl ester.



### 3.3 Optimization of Reaction Conditions for Site-Selective C-H Bond

#### Oxidation

In order to increase the substrate conversion of site-selective C-H bond oxidation, the optimized reaction conditions used for adamantane oxidation was further modified. 3,7-Dimethyloctyl benzoate,<sup>5</sup> **3.1a**, was used as the substrate. The oxidation of **3.1a** was performed by stirring 0.2 mmol of substrate and 0.2 mmol of 1,1,1-trifluoroacetone in a mixture of H<sub>2</sub>O (4 mL) and CH<sub>3</sub>CN (6 mL) at 25 °C, followed by four additions of 1 mmol of Oxone and 3.1 mmol of NaHCO<sub>3</sub> at 0 h, 2 h, 4 h and 6 h. The products were separated by flash column chromatography and analyzed by <sup>1</sup>H NMR (Figure 3.3). It was found that 3,7-dimethyloctyl benzoate, **3.1a** was oxidized to 7-hydroxy-3,7-dimethyloctyl benzoate,<sup>5</sup> **3.2a** and 3-hydroxy-3,7-dimethyloctyl benzoate,<sup>6</sup> **3.2a'** (Scheme 3.4).



**Scheme 3.4** Dioxirane-based oxidation of 3,7-dimethyloctyl benzoate.

Based on  $^1\text{H}$  NMR analysis of the crude reaction mixture, the ratio of **3.1a** to **3.2a** to **3.2a'** was found to be 69 : 27 : 4 (Entry 1, Table 3.1).

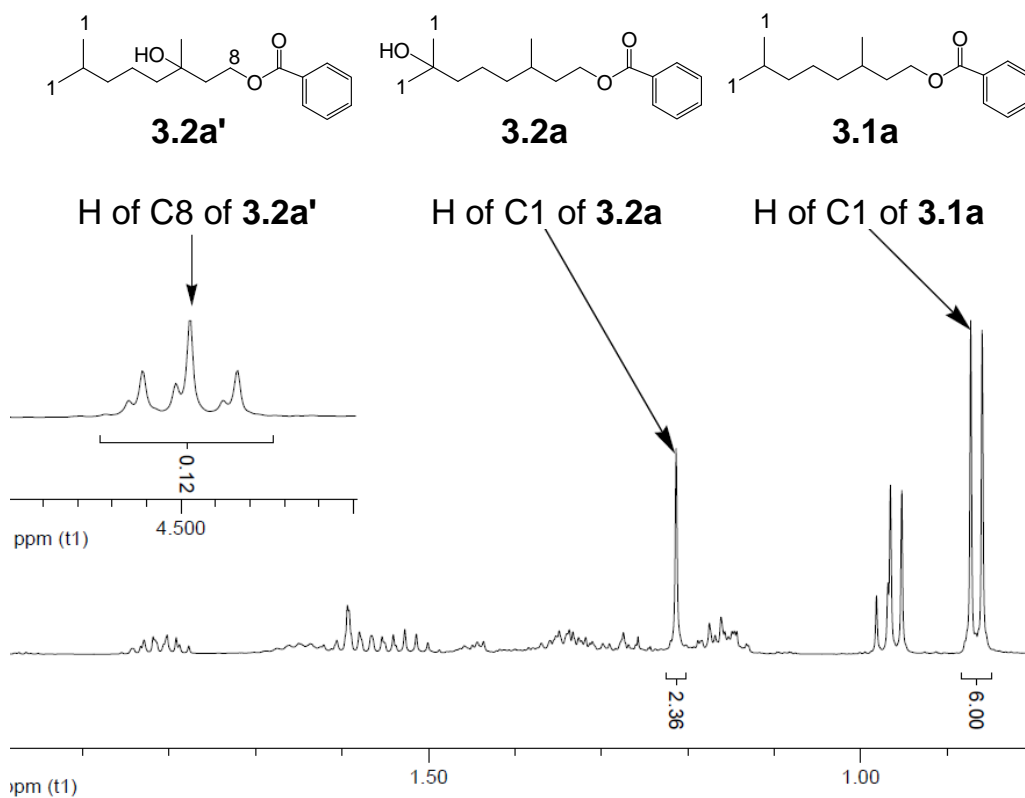


**Figure 3.3** Partial  $^1\text{H}$  NMR spectrum of the crude reaction mixture of oxidation of **3.1a**.

**Calculation of the ratio of 3,7-dimethyloctyl benzoate to products**

(entry 1, table 3.1)

**3.1a : 3.2a : 3.2a'**

= integral of H of C1 of **3.1a**/6 : integral of H of C1 of **3.2a**/6 : integral of H of C8 of **3.2a'**/2

= 6/6 : 2.36/6 : 0.12/2

= 1 : 0.39 : 0.06

When the reaction was performed with 8 additions of 0.5 mmol of Oxone and 1.55 mmol of NaHCO<sub>3</sub> at 0 h, 1 h, 2 h, 3 h, 4 h, 5 h, 6 h and 7 h, the conversion of 3,7-dimethyloctyl benzenoate increased (**3.1a** : **3.2a** : **3.2a'** = 1 : 0.99 : 0.17) (Entry 1, Table 3.1), compared to that given by the reaction carried out with four additions of Oxone and NaHCO<sub>3</sub> at 0 h, 2 h, 4 h and 6 h (**3.1a** : **3.2a** : **3.2a'** = 1 : 0.39 : 0.06) (Entry 2, Table 3.1).

Monitored by using iodine-starch test paper, the time for consuming 1 mmol of Oxone (Entry 1) and that for consuming 0.5 mmol of Oxone (Entry 2) both were one hour. This reveals that 0.5 mmol of Oxone in each Oxone addition of entry 2 was excess and lowered the conversion of the oxidation of **3.1a**.

**Table 3.1** Oxidation of **3.1a** with different loading of Oxone and NaHCO<sub>3</sub><sup>a</sup>

Entry	Oxone (mmol)	NaHCO <sub>3</sub> (mmol)	Time	<b>3.1a</b> : <b>3.2a</b> : <b>3.2a'</b> <sup>b</sup>
1	1×4	3.1×4	8 h	1 : 0.39 : 0.06
2 <sup>c</sup>	0.5×8	1.55×8	8 h	1 : 0.99 : 0.17

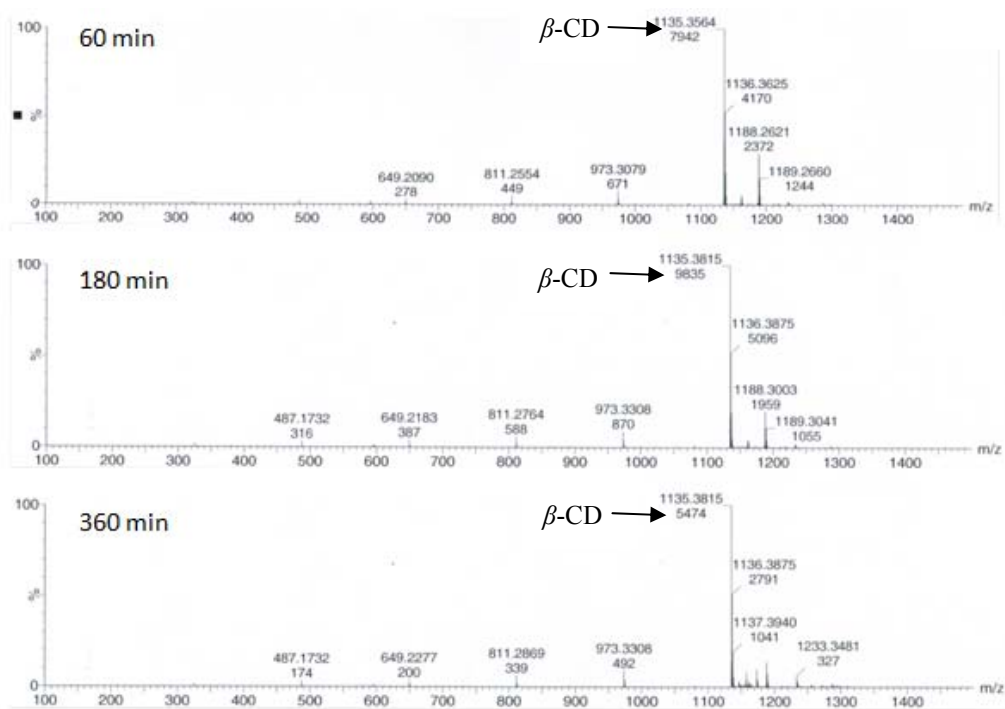
<sup>a</sup> Unless otherwise indicated, reactions were carried out by stirring 0.2 mmol of **3.1a** and 0.2 mmol of 1,1,1-trifluoroacetone in a mixture of 4 mL of H<sub>2</sub>O and 6 mL of CH<sub>3</sub>CN at room temperature with 4 additions of 1 mmol of Oxone and 3.1 mmol of NaHCO<sub>3</sub> at 0 h, 2 h, 4 h and 6 h. <sup>b</sup> Determined by <sup>1</sup>H NMR analysis of the crude reaction mixture. <sup>c</sup> The reaction was conducted with 8 additions of 0.5 mmol of Oxone and 1.55 mmol of NaHCO<sub>3</sub> at 0 h, 1 h, 2 h, 3 h, 4 h, 5 h, 6 h and 7 h.

The improvement of the conversion of oxidation of **3.1a** in entry 1 would be due to less decomposition of dioxiranes by excess amount of Oxone (see Scheme 2.1) when Oxone was added in a portion-wise manner. In order to maintain a neutral reaction condition, NaHCO<sub>3</sub> was added in a portion-wise manner as Oxone. For 0.2 mmol of substrate, 8 additions of 0.5 mmol of Oxone and 1.55 mmol of NaHCO<sub>3</sub> at 0 h, 1 h, 2 h, 3 h, 4 h, 5 h, 6 h and 7 h were chosen as a general protocol for selective C-H bond oxidation in Chapters 3 and 4.

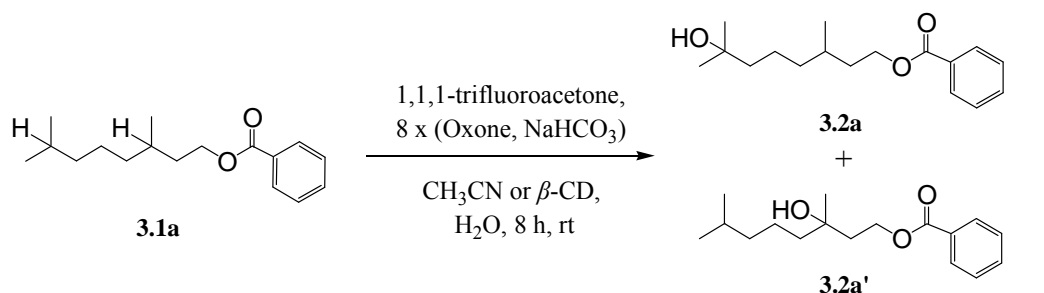
### 3.4 Effect of $\beta$ -CD on Site Selectivity of C-H Bond Oxidation of **3.1a**

Initially,  $\beta$ -cyclodextrin ( $\beta$ -CD) was chosen for studying the effect of cyclodextrins on site selective C-H bond oxidation, with **3.1a** as substrate. The reaction was carried out by stirring a mixture of **3.1a** and  $\beta$ -CD in water, followed by 8 additions of Oxone and NaHCO<sub>3</sub> at 0 h, 1 h, 2 h, 3 h, 4 h, 5 h, 6 h and 7 h (Table 3.2, entry 1). **3.1a** was oxidized to **3.2a** and **3.2a'**. Based on the <sup>1</sup>H NMR analysis of the crude product mixture, the ratio of **3.2a** to **3.2a'** was 20 : 1 with 71% yield based on 40% conversion in 8 h.

The experiment was repeated without the addition of substrate **3.1a**. 0.1 mL of the reaction mixture was withdrawn at 60 min, 180 min and 360 min during the reaction. After being quenched by Na<sub>2</sub>SO<sub>3</sub> solution, the withdrawn samples were analyzed by LC-MS. The results showed that no significant change on  $\beta$ -CD in during the course of the reaction was observed, indicating that  $\beta$ -CD is stable under the oxidation reaction conditions.



**Figure 3.4** LC-MS (ESI+) spectra of  $\beta$ -CD in dioxirane-based oxidation of **3.1a**

**Table 3.2** Oxidation of 3,7-dimethyloctyl benzenoate <sup>a</sup>

Entry	β-CD	H <sub>2</sub> O	CH <sub>3</sub> CN	%Conv <sup>n</sup> . <sup>b</sup>	% Yield <sup>c</sup>	<b>3.2a</b> : <b>3.2a'</b> <sup>d</sup>
1	1.1 equiv.	10 mL	---	40	71	20 : 1
2 <sup>e</sup>	---	4 mL	6 mL	35	96	7 : 1
3 <sup>f</sup>	1.1 equiv.	4 mL	6 mL	34	75	7 : 1
4 <sup>g</sup>	---	10 mL	---	4	34	5 : 1

<sup>a</sup> Unless otherwise indicated, reactions were conducted by stirring 0.2 mmol of **3.1a**, 0.2 mmol of 1,1,1-trifluoroacetone and 0.22 mmol of β-CD in 10 mL of water at room temperature with 8 additions of 0.5 mmol of Oxone and 1.55 mmol of NaHCO<sub>3</sub> at 0 h, 1 h, 2 h, 3 h, 4 h, 5 h, 6 h and 7 h. <sup>b</sup> Conversion was calculated from the amount of unreacted substrate recovered by flash column chromatography. <sup>c</sup> Yield based on conversion. <sup>d</sup> Determined by <sup>1</sup>H NMR. <sup>e</sup> The reaction was performed in a mixture of 4 mL of water and 6 mL of CH<sub>3</sub>CN without β-CD. <sup>f</sup> The reaction was performed in a mixture of 4 mL of water and 6 mL of CH<sub>3</sub>CN. <sup>g</sup> The reaction was performed in water without β-CD.

Then, the oxidation was conducted in a mixture of water and CH<sub>3</sub>CN with  $\beta$ -CD (entry 2). The conversion and yield (96% yield based on 35% conversion) was found to be similar to that in water with addition of  $\beta$ -CD (entry 1, 71% yield based on 40% conversion). However, the ratio of **3.2a** to **3.2a'** decreased from 20 : 1 (entry 1) to 7 : 1 (entry 2). The preferential formation of **3.2a** would be attributed to the decreased activity of the internal C-H bond towards electrophilic oxidation by the strong electron-withdrawing benzoate moiety and the inherent steric hindrance caused by the ester group.

When the reaction was carried out in the mixture of water and CH<sub>3</sub>CN with addition of  $\beta$ -CD (entry 3), the ratio of **3.2a** to **3.2a'** was not improved (**3.2a** : **3.2a'** = 7 : 1), without significant changes of conversion and yield (75% yield based on 34% conversion). In the presence of CH<sub>3</sub>CN, **3.1a** was well dissolved in CH<sub>3</sub>CN, and would not bind to the hydrophobic cavity of  $\beta$ -CD. Therefore, the site-selectivity of C-H bond oxidation was not enhanced.

According to the above experiments, it is proposed that  $\beta$ -CD could provide enhanced site-selectivity on C-H bond oxidation (20 : 1) by obstructing the approach of dioxirane to the internal C-H bond of the substrate through inclusion complex formation in water.

A control experiment was performed in water without addition of  $\beta$ -CD



(entry 4), only poor conversion could be obtained (34% yield based on 4% conversion). The low conversion would be attributed to the low solubility of the substrate in water. Based on the results of the experiment, it is proposed that  $\beta$ -CD could act as a reaction vessel to improve the conversion and yield of C-H bond oxidation by increasing the solubility of the substrate in H<sub>2</sub>O.

### 3.5 $^1\text{H}$ NMR titration for binding of 3.1a to $\beta$ -CD

As the result shown in Table 3.2, it is proposed that  $\beta$ -CD enhances the site-selectivity of C-H bond oxidation by obstructing the approach of dioxiranes to the internal C-H bond of the substrate in water and acts as reaction vessel to improve the conversion and yield of C-H bond oxidation. This could be attributed to inclusion complex formation by binding the substrate into the cavity of  $\beta$ -CD. To support this supposition, it was decided to study the inclusion complex formation between  $\beta$ -CD and **3.1a** by  $^1\text{H}$  NMR titration.<sup>8</sup>

As depicted in Figure 3.5, H3 and H5 are located inside the cavity of  $\beta$ -CD when H2 and H4 are located outside  $\beta$ -CD, H6 represents the protons of the methylene moiety of the primary hydroxyl groups which are located at the rim of the primary face.

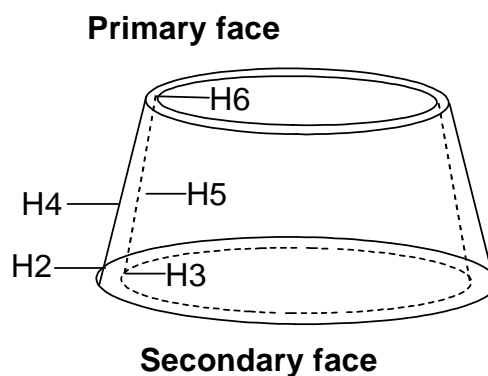


**Figure 3.5** Positions of protons located in  $\beta$ -cyclodextrin

The inclusion complexation between **3.1a** and  $\beta$ -CD was confirmed by  $^1\text{H}$  NMR titration (Figure 3.6). The signals of H3 and H5 were shifted upfield significantly when the amount of **3.1a** presented in the aqueous solution of  $\beta$ -CD increased, whereas the signals of H2 and H4 remained unchanged. This reflects that **3.1a** only interacts with the protons inside  $\beta$ -CD. The upfield shift of signals of H3 and H5 is attributed to the increased shielding effect during inclusion complexation, as the water molecules in the cavity are replaced by the apolar guest.<sup>8</sup>

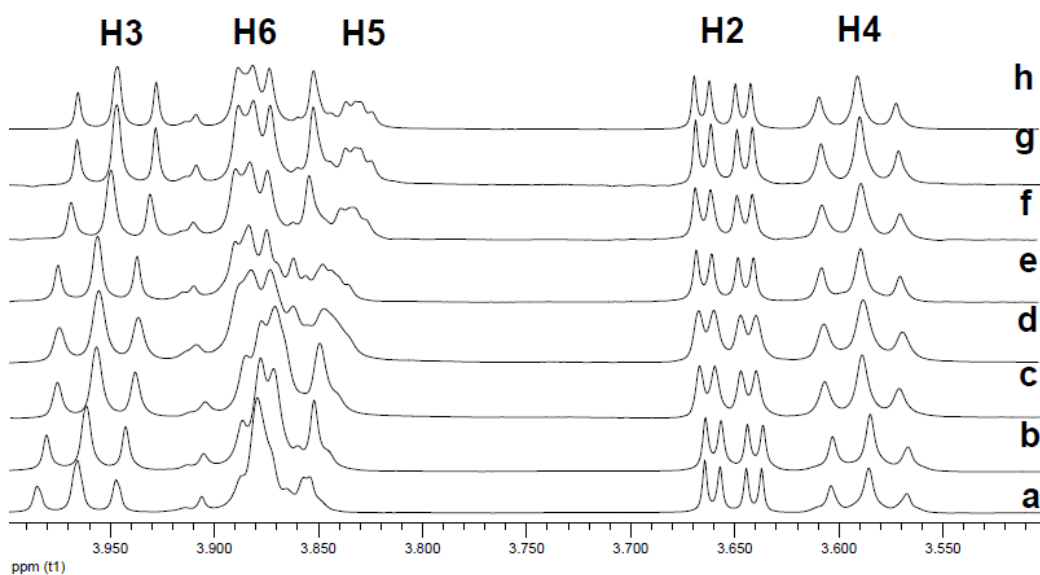


**Figure 3.6** Partial  $^1\text{H}$  NMR spectra of a mixture of **3.1a** and  $\beta$ -CD in  $\text{D}_2\text{O}$  (signals of  $\beta$ -CD). Ratios of **3.1a** :  $\beta$ -CD: (a) 0 : 10, (b) 1 : 9, (c) 2 : 8, (d) 3 : 7, (e) 4 : 6, (f) 5 : 5, (g) 6 : 4, (h) 7 : 3.

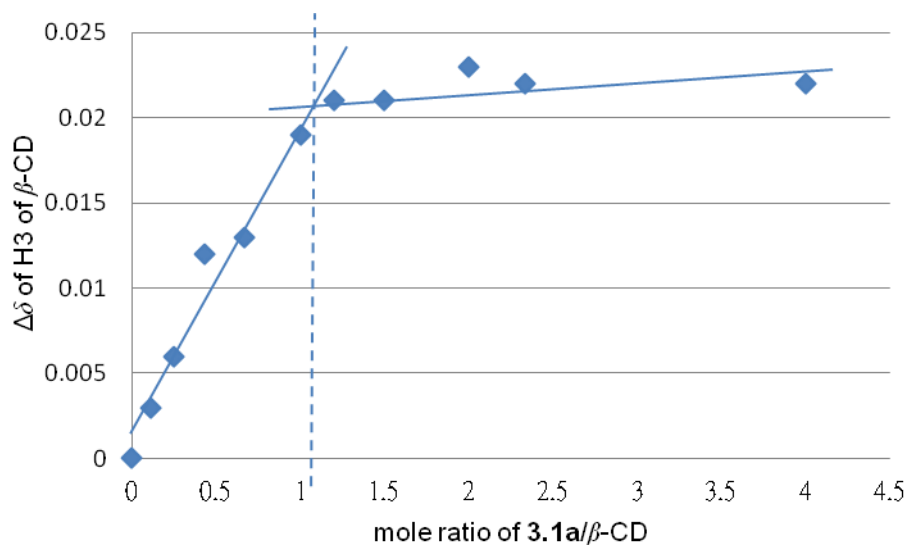


**Figure 3.7**  $^1\text{H}$  NMR titration curve for **3.1a** and  $\beta$ -CD

A  $^1\text{H}$  NMR titration curve was obtained by plotting the change of chemical shifts of H-3 against the ratio of **3.1a** to  $\beta$ -CD (Figure 3.7). The stoichiometry for the formation of inclusion complex was 1:1, determined by extrapolating the curve. The association constant of the inclusion complex was  $210 \text{ M}^{-1}$ , determined by Scott's method.<sup>10</sup>

### 3.6 Effect of Loading of $\beta$ -CD on the Yield and Site Selectivity of C-H Bond

#### Oxidation of **3.1a**

The effect of loading of  $\beta$ -CD on the C-H bond oxidation of **3.1a** has been investigated. The oxidation of **3.1a** carried out with 1.1 equivalents of  $\beta$ -CD gave 71% yield based on 40% conversion (Table 3.3, entry 3). When the loading of  $\beta$ -CD decreased, the conversion, yield, and selectivity also decreased. The reaction performed by using 0.1 equivalent of  $\beta$ -CD (entry 1) gave 40% yield based on 23% conversion with product ratio of 7 : 1, and the reaction performed by using 0.5 equivalents of  $\beta$ -CD (entry 2) gave 50% yield based on 32% conversion with product ratio of 8 : 1. Increasing the amount of  $\beta$ -CD to 2, 5, and 10 equivalent led to enhanced selectivity yet with reduced yield. The reaction performed with 2 equivalents of  $\beta$ -CD gave 42% yield based on 34% conversion with product ratio of 25 : 1 (entry 4); the reaction performed with 5 equivalents of  $\beta$ -CD gave 20% yield based on 49% conversion with product ratio of 29 : 1 (entry 5); and the reaction performed with 10 equivalents of  $\beta$ -CD gave 29% yield based on 47% conversion with product ratio of 30 : 1 (entry 6).

Based on the 1 : 1 stoichiometry of the inclusion complex between **3.1a** and  $\beta$ -CD, only one **3.1a** molecule can be included in each  $\beta$ -CD cavity. Reviewing the experimental results presented in Table 3.2, only poor conversion was

obtained when the C-H bond oxidation of **3.1a** was performed in water without addition of  $\beta$ -CD (Table 3.2, 34% yield based on 4% conversion). Thus, with less than 1.1 equivalents of  $\beta$ -CD, the conversion of C-H bond oxidation decreases, as not all substrate molecules are included in  $\beta$ -CD cavities and could not be oxidized efficiently. This further supports that  $\beta$ -CD acts as reaction vessel; only the substrate bound to  $\beta$ -CD cavity could be oxidized efficiently.

Excess amount of  $\beta$ -CD than 1.1 equivalents gave higher site selectivity, it may because more  $\beta$ -CD can form inclusion complex with **3.1a**, the steric hindrance induced by  $\beta$ -CD become more efficient. Excess  $\beta$ -CD lowered the yield of the reaction, it may because the aliphatic chain of **3.1a** would binding to the cavity of excess  $\beta$ -CD, this obstructs the approach of dioxirane to the terminal C-H bond of **3.1a**.

**Table 3.3** Oxidation of **3.1a** with different amounts of  $\beta$ -CD <sup>a</sup>

Entry	$\beta$ -CD	% Convn. <sup>b</sup>	% Yield <sup>c</sup>	<b>3.2a : 3.2a'</b> <sup>d</sup>
1	0.1	23	40	7 : 1
2	0.5	32	50	8 : 1
<b>3</b>	<b>1.1</b>	<b>40</b>	<b>71</b>	<b>20 : 1</b>
4	2	34	42	25 : 1
5	5	49	20	29 : 1
6	10	47	29	30 : 1

<sup>a</sup> Unless otherwise indicated, reactions were conducted by stirring 0.2 mmol of **3.1a**, 0.2 mmol of 1,1,1-trifluoroacetone and different loadings of  $\beta$ -CD in 10 mL of water at room temperature with 8 additions of 0.5 mmol of Oxone and 1.55 mmol of NaHCO<sub>3</sub> at 0 h, 1 h, 2 h, 3 h, 4 h, 5 h, 6 h and 7 h. <sup>b</sup> Conversion was calculated from the amount of unreacted substrate recovered by flash column chromatography. <sup>c</sup> Yield based on conversion. <sup>d</sup> Determined by <sup>1</sup>H NMR.

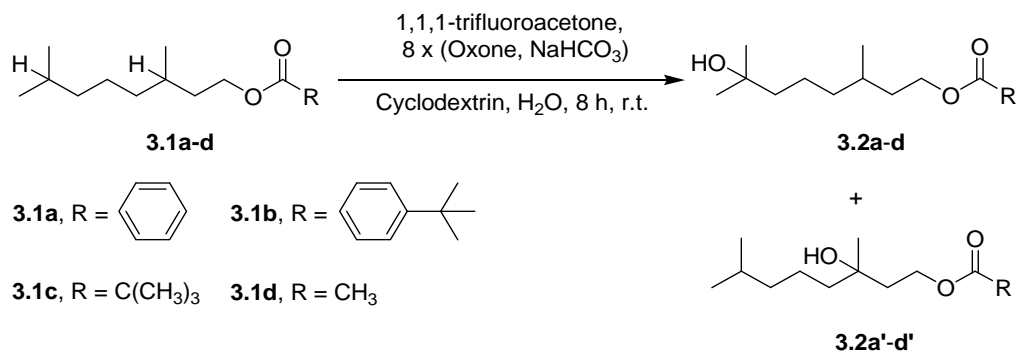
### 3.7 Effect of Different Substituents on the Site-Selectivity of C-H Bond

#### Oxidation of 3,7-Dimethyloctyl Ester in the Presence of $\beta$ -CD

Upon confirmation of the inclusion complex formation between 3,7-dimethyloctyl benzoate (**3.1a**) and  $\beta$ -CD, the effect of  $\beta$ -CD on the C-H bond oxidations of 4-*tert*-butylbenzoate (**3.1b**), pivalate<sup>7</sup> (**3.1c**) and acetate<sup>4b</sup> (**3.1d**) were studied. 4-*tert*-butylbenzoate, pivalate and acetate moieties are usually used as the aromatic and aliphatic binding groups to  $\beta$ -CD cavity.<sup>1,2</sup> The reactions were performed by stirring 0.2 mmol of substrate and 0.22 mmol of  $\beta$ -CD in 10 mL of water, followed by 8 additions of 0.5 mmol of Oxone and 1.55 mmol of NaHCO<sub>3</sub> at 0 h, 1 h, 2 h, 3 h, 4 h, 5 h, 6 h and 7 h. The results are summarized in Table 3.4.



**Table 3.4** Effect of different substituents and  $\alpha$ -,  $\beta$ - and  $\gamma$ - CDs on the site-selectivity of oxidation of 3,7-dimethyloctyl ester <sup>a</sup>



Entry	Substrate	CD	% Convn. <sup>c</sup>	% Yield <sup>d</sup>	3.2a-d : 3.2a'-d' <sup>e</sup>
1	<b>3.1a</b>	$\alpha$	6	55	6 : 1
2	<b>3.1a</b>	$\beta$	40	71	20 : 1
3	<b>3.1a</b>	$\gamma$	17	81	7 : 1
4 <sup>b</sup>	<b>3.1a</b>	-	35	96	7 : 1
5	<b>3.1b</b>	$\alpha$	34	23	11 : 1
6	<b>3.1b</b>	$\beta$	40	40	12 : 1
7	<b>3.1b</b>	$\gamma$	28	22	5 : 1
8 <sup>b</sup>	<b>3.1b</b>	-	52	56	7 : 1
9	<b>3.1c</b>	$\alpha$	41	18	3 : 1
10	<b>3.1c</b>	$\beta$	61	20	12 : 1
11	<b>3.1c</b>	$\gamma$	45	19	4 : 1
12 <sup>b</sup>	<b>3.1c</b>	-	54	39	4 : 1

13	<b>3.1d</b>	$\alpha$	64	5	n.d.
14	<b>3.1d</b>	$\beta$	68	24	5 : 1
15	<b>3.1d</b>	$\gamma$	73	39	10 : 1
16 <sup>b</sup>	<b>3.1d</b>	-	54	61	4 : 1

<sup>a</sup> Unless otherwise indicated, reactions were conducted by stirring 0.2 mmol of substrate, 0.2 mmol of 1,1,1-trifluoroacetone and 0.22 mmol of  $\alpha$ -,  $\beta$ - or  $\gamma$ -CD in 10 mL of water at room temperature with 8 additions of 0.5 mmol of Oxone and 1.55 mmol of NaHCO<sub>3</sub> at 0 h, 1 h, 2 h, 3 h, 4 h, 5 h, 6 h and 7 h. <sup>b</sup> The reaction was carried out in a mixture of 4 mL of H<sub>2</sub>O and 6 mL of CH<sub>3</sub>CN. <sup>c</sup> Conversion was calculated from the amount of unreacted substrate recovered by flash column chromatography. <sup>d</sup> Yield based on conversion. <sup>e</sup> Determined by <sup>1</sup>H NMR.

In the presence of  $\beta$ -CD, **3.1a-d** (Table 3.4, entries 2, 6, 10 and 14) were oxidized to **3.2a-d** and **3.2a'-d'** respectively. Except **3.1d** (entry 14, **3.2d**<sup>d</sup> : **3.2d'**<sup>d</sup> = 5 : 1; entry 16, **3.2d** : **3.2d'** = 4 : 1),  $\beta$ -CD gave enhancement on the site selectivity of C-H bond oxidations of **3.1a**, **3.1b** and **3.1c** (entries 2, 6 and 10). Compared to the control experiments performed in a mixture of water and CH<sub>3</sub>CN without  $\beta$ -CD (entries 4, 8 and 12), the ratio of **3.2a** to **3.2a'** increased from 7 : 1 (entry 4) to 20 : 1 (entry 2); the ratio of **3.2b** to **3.2b'** increased from 7 :

1 (entry 8) to 12 : 1 (entry 6); and the ratio of **3.2c**<sup>7</sup> to **3.2c'** increased from 4 : 1 (entry 12) to 12 : 1 (entry 10).

As reported in literatures,<sup>4</sup> the oxidation of 3,7-dimethyloctyl ester gives 7-hydroxy-3,7-dimethyloctyl ester and 3-hydroxy-3,7-dimethyloctyl ester in a ratio of 5 : 1 based on the inherent electronic effect of the substrate. Compared to the literature reports, the site selectivity of C-H bond oxidation of 3,7-dimethyloctyl ester obtained in the presence of  $\beta$ -CD is two-to-four fold higher than that just controlled by electronic effect.

As illustrated in Table 3.4, the site-selectivity of C-H bond oxidation of 3,7-dimethyloctyl ester was affected by different substituents of the esters. The stoichiometry for formation of inclusion complex of **3.1b** and  $\beta$ -CD and that of **3.1c** and  $\beta$ -CD were found to be 1 : 1, and the association constants were 220 M<sup>-1</sup> and 325 M<sup>-1</sup>, respectively, which were similar to that of inclusion complex of **3.1a** and  $\beta$ -CD (210 M<sup>-1</sup>). The difference in site-selectivity could not be related to their comparable association constants. Thus, we decided to study the binding geometry of esters with different substituents to  $\beta$ -CD by 2D ROESY experiments<sup>8</sup> in order to provide hints on the difference in site-selectivity.

### 3.8 Studies of the Binding Geometry between 3,7-Dimethyloctyl Esters and $\beta$ -CD through 2D ROESY Experiments

Owing to the low solubility of the substrates (3,7-dimethyloctyl ester) in water, attempts to perform 2D ROESY experiments<sup>8</sup> for the inclusion complexes between the substrates and  $\beta$ -CD were not successful (the signals of the substrates in 2D ROESY spectra are very weak). Therefore, we used methyl esters of different substituted groups as models to study the binding geometry of the anchors to  $\beta$ -CD. Methyl benzenoate (**3.3a**), methyl 4-*tert*-butylbenzoate (**3.3b**) and methyl pivalate (**3.3c**) are selected as the model compounds of **3.1a**, **3.1b** and **3.1c**, respectively (Figure 3.8).

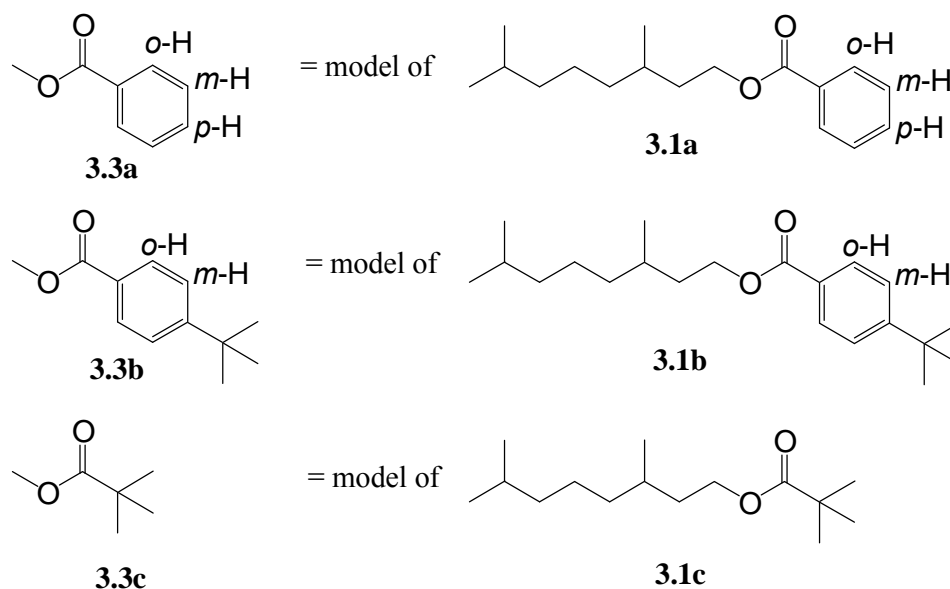


**Figure 3.8** Model compounds of 3,7-dimethyloctyl ester for 2D ROESY experiments

Figure 3.9 shows the 2D ROESY spectrum of the binding of **3.3a** to  $\beta$ -CD. Both *o*-H and *m*-H of the phenyl group in **3.3a** have strong NOE correlation signals with H-3 and H-5 of  $\beta$ -CD, whereas *p*-H of **3.3a** shows no correlation signal with any protons of  $\beta$ -CD, suggesting that the phenyl group deeply inserts into the  $\beta$ -CD cavity and *p*-H is exposed outside the cavity. Besides, as H-6 of  $\beta$ -CD shows no NOE correlation signal with any protons of the phenyl group in **3.3a**, this reveals that *p*-H of **3.3a** is exposed outside the secondary face of  $\beta$ -CD. Considering the 1 : 1 stoichiometry of the inclusion complexation between **3.1a** and  $\beta$ -CD, the possible binding geometry of benzenoate group of **3.3a** is proposed as shown in Figure 3.10.

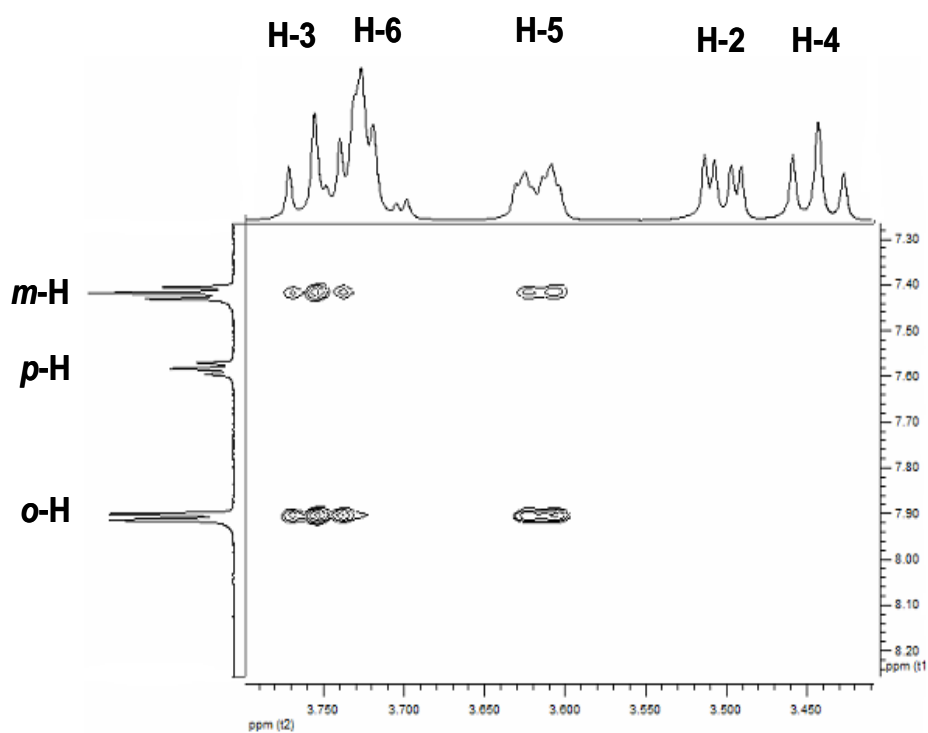


**Figure 3.9** Partial contour plot of 600 MHz 2D ROESY spectrum for binding of **3.3a** to  $\beta$ -CD in  $D_2O$

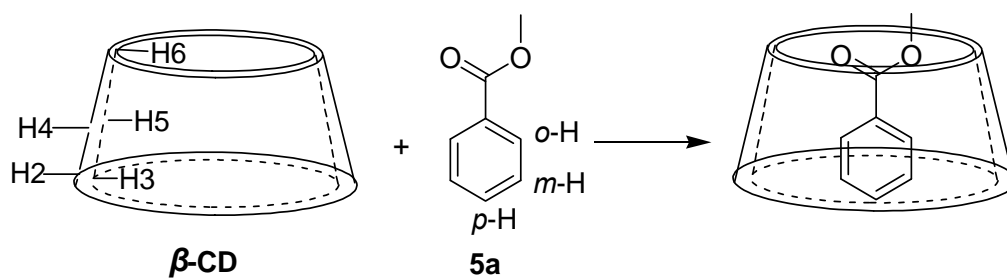


**Figure 3.10** Proposed binding geometry for the inclusion of **3.3a** and -CD.

In the 2D ROESY spectrum for binding of **3.3b** to  $\beta$ -CD (Figure 3.11a and 3.11b), the protons of the *tert*-butyl group and the protons at the *m*-position of the phenyl ring part have strong NOE correlation signals with H-3 and H-5 of  $\beta$ -CD while the protons at the *o*-position of the phenyl ring only shows the weak correlation signal with H-6 of  $\beta$ -CD. This suggests that the 4-*tert*-butylbenzenoate inserts into  $\beta$ -CD from the primary face. The *tert*-butyl group is completely included in the  $\beta$ -CD cavity, and just half of the phenyl ring inserts to the  $\beta$ -CD cavity. As the stoichiometry for the formation of inclusion complex of **3.2b** and  $\beta$ -CD is 1 : 1, the possible binding geometry of 4-*t*-butylbenzenoate moiety of **3.3b** is proposed as depicted in Figure 3.12.

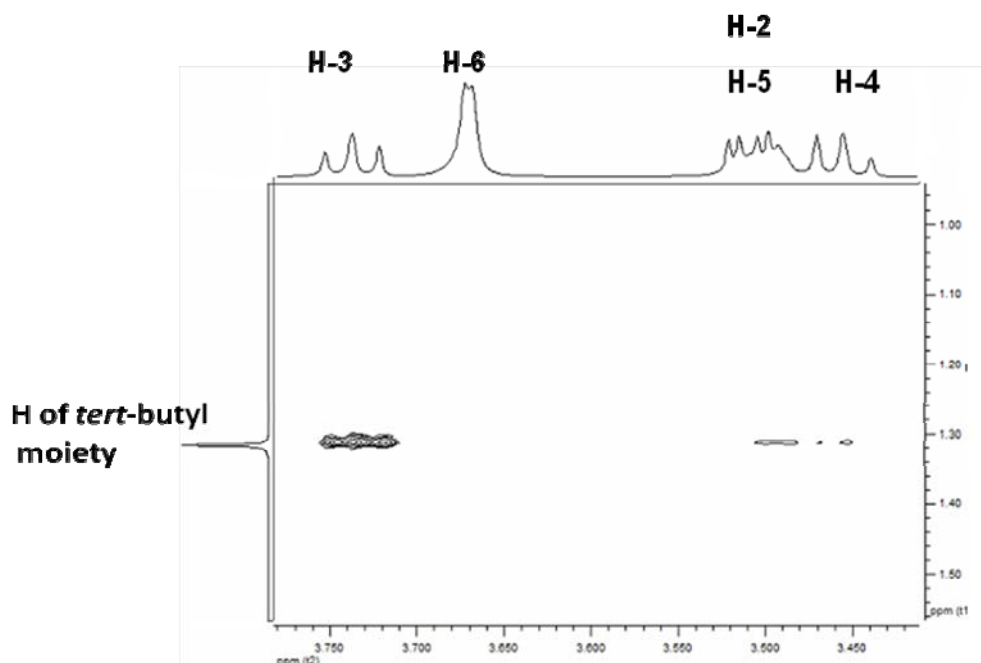


**Figure 3.11a** Partial contour plot of 600 MHz 2D ROESY spectrum for binding of **3.3b** (*tert*-butyl moiety) to  $\beta$ -CD in  $D_2O$

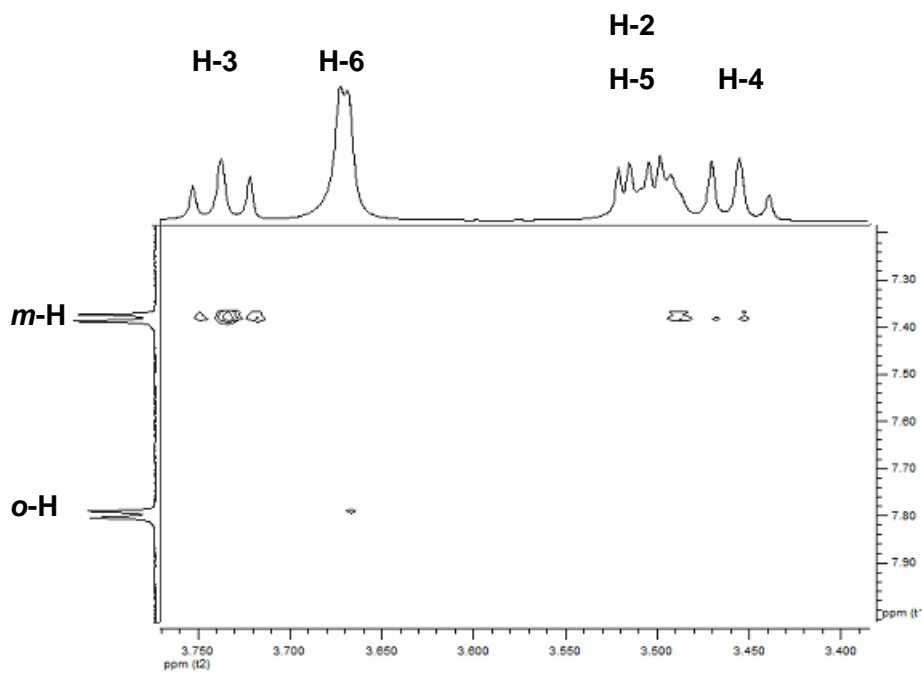


**Figure 3.11b** Partial contour plot of 600 MHz 2D ROESY spectrum for binding of **3.3b** (phenyl ring moiety) to  $\beta$ -CD in  $D_2O$

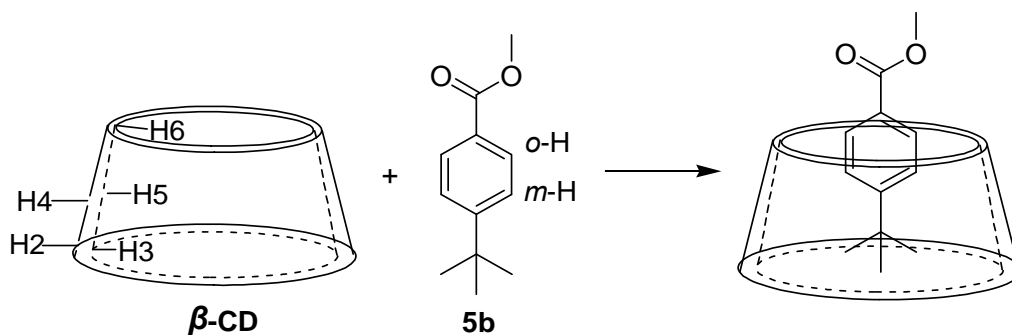


**Figure 3.12** Proposed binding geometry for the inclusion of **3.3b** and  $\beta$ -CD.



From the 2D ROESY spectrum for binding of **3.3c** to  $\beta$ -CD (Figure 3.13), the protons of the *tert*-butyl group have NOE correlation signal with H-3, H-5 and H-6 of  $\beta$ -CD with different intensities. The NOE signal between the protons of the *tert*-butyl group and H-3 is the strongest, and that between the protons of the *tert*-butyl group and H-5 is moderate, while that between the protons of the *tert*-butyl group and H-5 is the weakest. Based on these findings, it was predicted that the *tert*-butyl group enters the cavity of  $\beta$ -CD from the secondary face, unlike **3.3a** and **3.3b**. As the stoichiometry for formation of inclusion complex of **3.2c** and  $\beta$ -CD is 1 : 1, the possible binding geometry of *tert*-butyl group of **3.3c** to  $\beta$ -CD is proposed as shown in Figure 3.14.

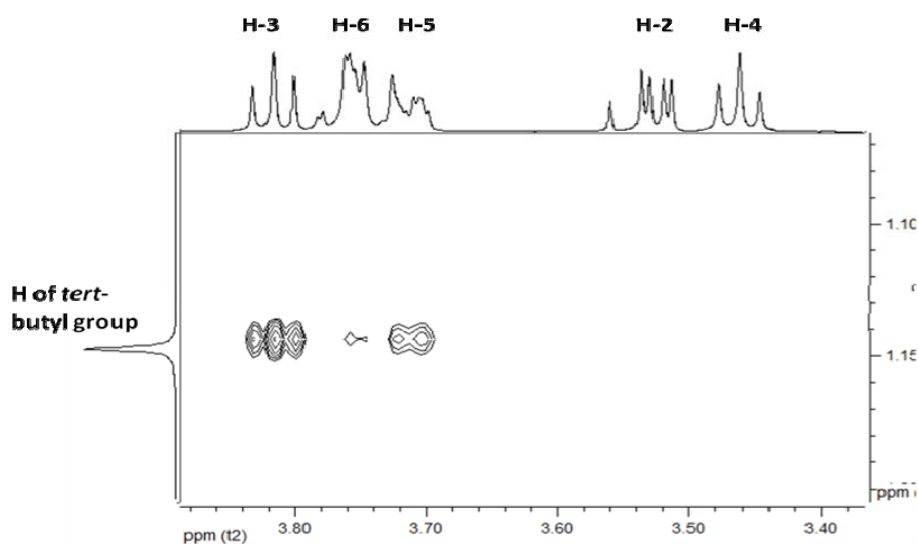


**Figure 3.13** Partial contour plot of 600 MHz 2D ROESY spectrum for binding of **3.3c** to  $\beta$ -CD in D<sub>2</sub>O.

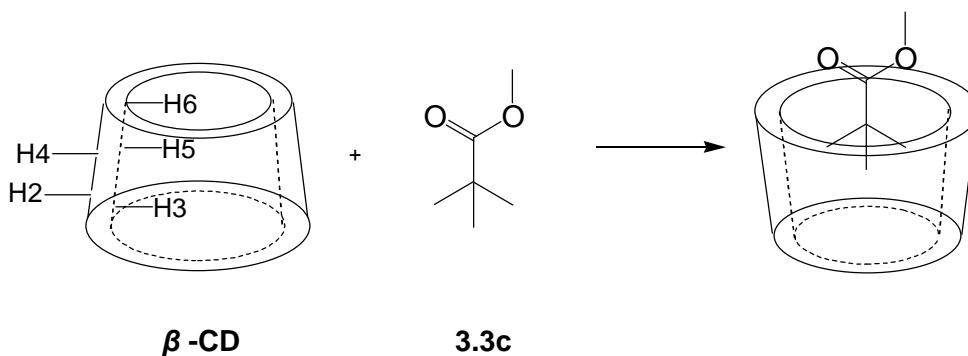


**Figure 3.14** Proposed binding geometry for the inclusion of **3.3c** and  $\beta$ -CD.

### 3.9 The Effect of Different Binding Geometries of the Substituents on the Site-Selective C-H Bond Oxidation of 3,7-Dimethyloctyl Esters

As mentioned in the previous sections, in the presence of  $\beta$ -CD, the site-selectivity of C-H bond oxidation of 3,7-dimethyloctyl ester varied with different substituents. Based on the 2D ROESY study of the binding geometries between the model compounds of **3.1a-c** and  $\beta$ -CD, it could be reasoned that the different binding geometries of the substituents to  $\beta$ -CD would affect the site-selectivity of C-H bond oxidation of 3,7-dimethyloctyl esters (Figure 3.15).

Due to the deep inclusion of the benzenoate group of **3.1a** into the cavity of  $\beta$ -CD, the internal tertiary C-H bond of **3.1a** would be well protected by steric hindrance induced by  $\beta$ -CD, the dioxirane would preferentially oxidize the more exposed tertiary C-H bond at the terminal position, leading to highly site-selective C-H bond oxidation (Table 3.4, entry 2, **3.2a** : **3.2a'** = 20 : 1).

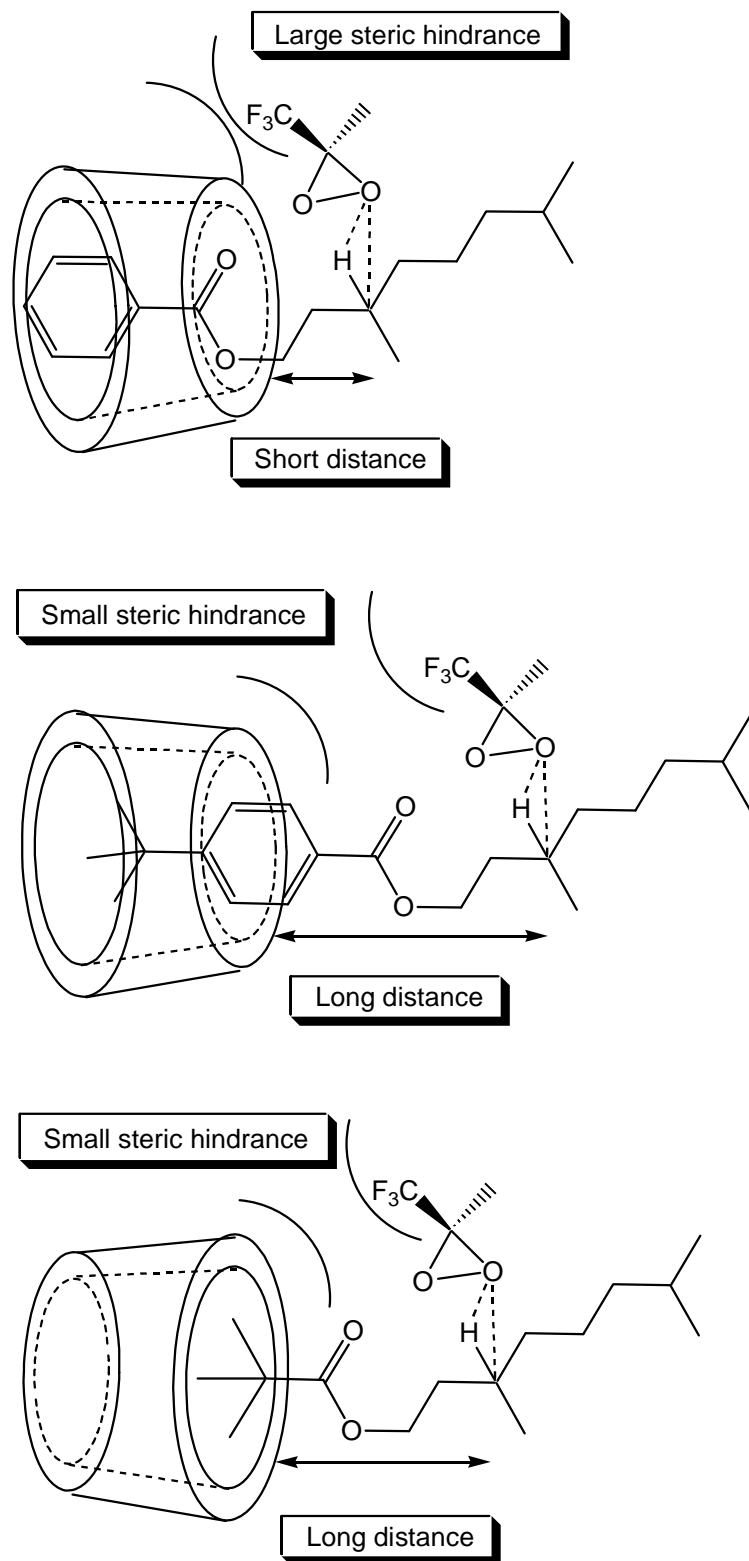


**Figure 3.15** Schematic diagrams for site selective C-H bond oxidation of **3.1a-c**

Referring to the binding geometry of **3.3b** to  $\beta$ -CD, only the *tert*-butyl moiety and half of the phenyl ring were included in the cavity of  $\beta$ -CD during the inclusion complex formation with 4-*tert*-butyl benzoate. Based on this binding mode, in the case of **3.1b**, the internal tertiary C-H bond was more distant from  $\beta$ -CD. Thus, the steric hindrance induced by  $\beta$ -CD was smaller, and dioxirane could more easily oxidize the internal tertiary C-H bond, leading to the decrease in the site-selectivity of C-H bond oxidation (Table 3.4, entry 6, **3.2b** : **3.2b'** = 12 : 1).

The reason for the lower site-selectivity induced by  $\beta$ -CD in the oxidation of **3.1c** is similar to that of **3.1b**. The *tert*-butyl group of **3.1b** was in proximity to H-3 located at the rim of  $\beta$ -CD and not to be included in the  $\beta$ -CD as deep as the phenyl group of **3.1a**. The distance between  $\beta$ -CD and the internal tertiary C-H bond of **3.1c** was longer. The protection of the internal tertiary C-H bond by the induced steric hindrance of  $\beta$ -CD was less significant. Hence, the site-selectivity of the oxidation of **3.1c** decreased (Table 3.4, entry 10, **3.2c** : **3.2c'** = 12 : 1).

### 3.10 Effect of different CDs on the site-selective C-H bond oxidation

Apart from  $\beta$ -CD, the effect of  $\alpha$ -CD and  $\gamma$ -CD on the site-selective oxidation of 3,7-dimethyloctyl esters has been examined, and the results are shown in Table 3.4.

In the presence of  $\alpha$ -CD, **3.1a** was oxidized to **3.2a** and **3.2a'** with 55% yield based on 6% conversion (entry 1, **3.2a** : **3.2a'** = 6 : 1); **3.1b** was oxidized to **3.2b** and **3.2b'** with 23% yield based on 34% conversion (entry 5, **3.2b** : **3.2b'** = 11 : 1); **3.1c** was oxidized to **3.2c** and **3.2c'** with 18% yield based on 41% conversion (entry 9, **3.2c** : **3.2c'** = 3 : 1); **3.1d** was oxidized to **3.2d** and **3.2d'** with 5% yield based on 64% conversion (entry 13, the ratio of **3.2d** : **3.2d'** was not determined as the signal of products in  $^1\text{H}$  NMR spectrum was not observable).

In the presence of  $\gamma$ -CD, **3.1a** was oxidized to **3.2a** and **3.2a'** with 81% yield based on 17% conversion (entry 3, **3.2a** : **3.2a'** = 7 : 1); **3.1b** was oxidized to **3.2b** and **3.2b'** with 22% yield based on 28% conversion (entry 7, **3.2b** : **3.2b'** = 11 : 1); **3.1c** was oxidized to **3.2c** and **3.2c'** with 19% yield based on 45% conversion (entry 11, **3.2c** : **3.2c'** = 3 : 1); **3.1d** was oxidized to **3.2d** and **3.2d'** with 39% yield based on 73% conversion (entry 15, **3.2d** : **3.2d'** = 10 : 1).

Generally, the oxidation of 3,7-dimethyloctyl esters performed in the presence of  $\alpha$ -CD and  $\gamma$ -CD gave poor conversion and yield, and the site-selectivity was not significantly enhanced. This would be attributed to the low binding constants of the substrates to  $\alpha$ -CD and  $\gamma$ -CD, which were supported by  $^1\text{H}$  NMR titration. The poor binding of the substrates to the cavities of  $\alpha$ -CD and  $\gamma$ -CD could not increase solubility of the substrates in water, and hence lower the conversion and yield were resulted. Moreover, owing to the weak binding of the substrates to the CD cavity, the dioxirane could not be efficiently obstructed to oxidize the internal C-H bond, leading to no enhancement on the site-selectivity.

### 3.11 Conclusion

In summary, site-selective C-H bond of 3,7-dimethyloctyl esters was achieved by supramolecular approach using  $\beta$ -CD. In the presence of  $\beta$ -CD in water, 3,7-dimethyloctyl esters were oxidized to 7-hydroxy-3,7-dimethyloctyl esters and 3-hydroxy-3,7-dimethyloctyl esters smoothly in water by dioxirane generated *in situ*, with site selectivity enhancement. The product ratios of 7-hydroxy-3,7-dimethyloctyl ester to 3-hydroxy-3,7-dimethyloctyl ester were found to be 12 : 1 to 20 : 1, as determined by  $^1\text{H}$  NMR analysis of the crude reaction mixtures. These product ratios were two to three-fold higher than the product ratios (4 : 1 to 7 : 1) given by the reactions performed in a mixture of water and acetonitrile. As indicated by 2D ROESY experiments, the site selectivity would be related to the binding geometries.

## 3.12 Experimental Section

### 3.12.1 Experimental Procedure

#### (a) General Procedure for Site-selective C-H Bond Oxidation of 3,7-Dimethyloctyl Esters with Two Tertiary C-H Bonds with Cyclodextrins

To a mixture of 0.2 mmol of 3,7-dimethyloctyl ester and 0.22 mmol of cyclodextrin, 10 mL of water was added, followed by addition of 0.2 mmol of 1,1,1-trifluoroacetone. Then, the reaction mixture was treated with 8 additions of 0.5 mmol of Oxone and 1.55 mmol of NaHCO<sub>3</sub> at 0 h, 1 h, 2 h, 3 h, 4 h, 5 h, 6 h and 7 h. After stirring for 8 h at room temperature, the resulting mixture was extracted by ethyl acetate (3 × 20 mL). The combined organic extract was dried over anhydrous Na<sub>2</sub>SO<sub>4</sub>, and the organic solvent was evaporated under reduced pressure. The residue was then dissolved in CDCl<sub>3</sub> for the analysis of the product ratio by <sup>1</sup>H NMR spectroscopy. The yield and conversion were obtained by flash column chromatography.

#### (b) <sup>1</sup>H NMR titration experiments and Scott's plots of 3a-c

The mixtures of **3a-c** and β-CD for the <sup>1</sup>H NMR titration experiments were prepared by mixing indicated volume of (i) **3a-c** stock solutions (0.5 M, 0.25 mmol of **3a-c** in 0.5 mL of D<sub>6</sub>-acetone), (ii) β-CD stock solution (0.01 M, 0.1



mmol of  $\beta$ -CD in 10 mL of D<sub>2</sub>O), and (iii) D<sub>2</sub>O according to Table 3.5. The final volumes of the mixtures were  $\sim$  0.5 mL.

**Table 3.5** Amount of **3.1a-c**,  $\beta$ -CD, and D<sub>2</sub>O for <sup>1</sup>H NMR titration.

Entry	Ratio of <b>3.1a-c</b> : $\beta$ -CD	Volume of <b>3.1a-c</b> stock solutions ( $\mu$ L)	Volume of $\beta$ -CD stock solution (mL)	Volume of D <sub>2</sub> O (mL)
1	0 : 10	0	0.50	0
2	1 : 9	1	0.45	0.05
3	2 : 8	2	0.40	0.10
4	3 : 7	3	0.35	0.15
5	4 : 6	4	0.30	0.20
6	5 : 5	5	0.25	0.25
7	5.5 : 4.5	6	0.25	0.25
8	6 : 4	6	0.20	0.30
9	6.7 : 3.3	6	0.15	0.35
10	7 : 3	7	0.15	0.35

Remarks: In general, the mixtures with high ratio of  $\beta$ -CD are opaque and viscous (entries 1-7) while transparent solutions are observed in the mixtures with low ratio of  $\beta$ -CD (entries 8-10).

The mixtures were subjected to  $^1\text{H}$  NMR analysis. The changes of the chemical shift of H3 of  $\beta$ -CD (with the chemical shift of H4 of  $\beta$ -CD as the internal reference) are obtained as  $\Delta\delta_{\text{obs}}$  which is used for the calculation of the binding constant (shown as tables 3.6, 3.7 and 3.8).

**Table 3.6**  $\Delta\delta_{\text{obs}}$  of H3 of  $\beta$ -CD in  $^1\text{H}$  NMR titration of **3.1a** and  $\beta$ -CD.

Entry	Ratio of <b>3.1a</b> : $\beta$ -CD	$\delta_{\text{H3}} - \delta_{\text{H4}}$	$\Delta\delta_{\text{obs}} = (\delta_{\text{H3}} - \delta_{\text{H4}})_i - (\delta_{\text{H3}} - \delta_{\text{H4}})_f$
1	0 : 10	0.380	0
2	1 : 9	0.377	0.003
3	2 : 8	0.374	0.006
4	3 : 7	0.368	0.012
5	4 : 6	0.367	0.013
6	5 : 5	0.361	0.019
7	5.5 : 4.5	0.359	0.021
8	6 : 4	0.359	0.021
9	6.7 : 3.3	0.357	0.023
10	7 : 3	0.358	0.022

**Table 3.7**  $\Delta\delta_{\text{obs}}$  of H3 of  $\beta$ -CD in  $^1\text{H}$  NMR titration of **3.1b** and  $\beta$ -CD.

Entry	Ratio of <b>3.1b</b> : $\beta$ -CD	$\delta_{\text{H3}} - \delta_{\text{H4}}$	$\Delta\delta_{\text{obs}} = (\delta_{\text{H3}} - \delta_{\text{H4}})_i - (\delta_{\text{H3}} - \delta_{\text{H4}})_f$
1	0 : 10	0.381	0
2	1 : 9	0.378	0.003
3	2 : 8	0.376	0.005
4	3 : 7	0.369	0.012
5	4 : 6	0.368	0.013
6	5 : 5	0.365	0.016
7	5.5 : 4.5	0.359	0.022
8	6 : 4	0.358	0.023
9	6.7 : 3.3	0.358	0.023
10	7 : 3	0.360	0.021

**Table 3.8**  $\Delta\delta_{\text{obs}}$  of H3 of  $\beta$ -CD in  $^1\text{H}$  NMR titration of **3.1c** and  $\beta$ -CD.

Entry	Ratio of <b>3.1c</b> : $\beta$ -CD	$\delta_{\text{H3}} - \delta_{\text{H4}}$	$\Delta\delta_{\text{obs}} = (\delta_{\text{H3}} - \delta_{\text{H4}})_i - (\delta_{\text{H3}} - \delta_{\text{H4}})_f$
1	0 : 10	0.382	0
2	1 : 9	0.377	0.005
3	2 : 8	0.370	0.012
4	3 : 7	0.368	0.014
5	4 : 6	0.363	0.019
6	5 : 5	0.356	0.026
7	5.5 : 4.5	0.353	0.029
8	6 : 4	0.354	0.028
9	6.7 : 3.3	0.352	0.030
10	7 : 3	0.349	0.033

The binding constants (K) of **3.1a-c** to  $\beta$ -CD were calculated by fitting  $\Delta\delta_{\text{obs}}$  into Scott's plot as the equation shown below: <sup>7</sup>

$$[\mathbf{3.1a-c}]_{\text{normal}} / \Delta\delta_{\text{obs}} = [\mathbf{3.1a-c}]_{\text{normal}} / \Delta\delta_{\text{max}} + \Delta\delta_{\text{max}} / K$$

where  $[\mathbf{3.1a-c}]_{\text{normal}}$  is the concentration of **3.1a-c** with normalized concentration of  $\beta$ -CD,  $\Delta\delta_{\text{obs}}$  is the observed change of the chemical shift of H3 of  $\beta$ -CD at different concentrations of **3.1a-c**,  $\Delta\delta_{\text{max}}$  is the maximum change of the chemical shift of H3 of  $\beta$ -CD.

**Table 3.9** Data of Scott's plot of <sup>1</sup>H NMR titration of **3.1a** and  $\beta$ -CD

$[\mathbf{3.1a}]_{\text{normal}}$ (M)	$\Delta\delta_{\text{obs}}$	$[\mathbf{3.1a}]_{\text{normal}} / \Delta\delta_{\text{obs}}$	$[\mathbf{3.1a}]_{\text{normal}} / \Delta\delta_{\text{max}}$ ( $\Delta\delta_{\text{max}} = 0.021$ )
$5 \times 10^{-7}$	0.003	$2.38 \times 10^{-5}$	$1.67 \times 10^{-4}$
$1.125 \times 10^{-6}$	0.006	$5.36 \times 10^{-5}$	$1.88 \times 10^{-4}$
$1.929 \times 10^{-6}$	0.012	$9.18 \times 10^{-5}$	$1.61 \times 10^{-4}$
$3 \times 10^{-6}$	0.013	$1.43 \times 10^{-4}$	$2.31 \times 10^{-4}$
$4.5 \times 10^{-6}$	0.019	$2.14 \times 10^{-4}$	$2.37 \times 10^{-4}$
$5.4 \times 10^{-6}$	0.021	$2.57 \times 10^{-4}$	$2.57 \times 10^{-4}$
$6.75 \times 10^{-6}$	0.021	$3.21 \times 10^{-4}$	$3.21 \times 10^{-4}$
$9 \times 10^{-6}$	0.023	$4.29 \times 10^{-4}$	$3.91 \times 10^{-4}$
$1.05 \times 10^{-5}$	0.022	$5.00 \times 10^{-4}$	$4.77 \times 10^{-4}$

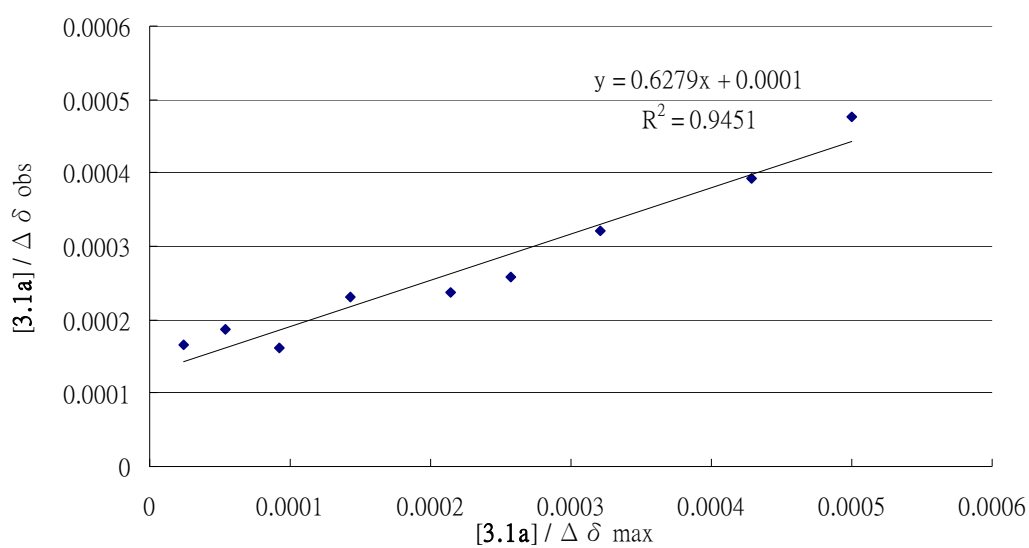


**Figure 3.16** Scott's plot of  $^1\text{H}$  NMR titration of **3.1a** and  $\beta$ -CD

**Table 3.10** Data of Scott's plot of  $^1\text{H}$  NMR titration of **3.1b** and  $\beta$ -CD

$[\mathbf{3.1b}]_{\text{normal}}$ (M)	$\Delta\delta_{\text{obs}}$	$[\mathbf{3.1b}]_{\text{normal}} / \Delta\delta_{\text{obs}}$	$[\mathbf{3.1b}]_{\text{normal}} / \Delta\delta_{\text{max}}$ ( $\Delta\delta_{\text{max}} = 0.026$ )
$5 \times 10^{-7}$	0	$3.13 \times 10^{-5}$	$1.67 \times 10^{-4}$
$1.125 \times 10^{-6}$	0.003	$7.03 \times 10^{-5}$	$2.25 \times 10^{-4}$
$1.929 \times 10^{-6}$	0.005	$1.21 \times 10^{-4}$	$1.61 \times 10^{-4}$
$3 \times 10^{-6}$	0.012	$1.88 \times 10^{-4}$	$2.31 \times 10^{-4}$
$4.5 \times 10^{-6}$	0.013	$2.81 \times 10^{-4}$	$2.81 \times 10^{-4}$
$5.4 \times 10^{-6}$	0.016	$3.38 \times 10^{-4}$	$2.25 \times 10^{-4}$
$6.75 \times 10^{-6}$	0.022	$4.22 \times 10^{-4}$	$2.93 \times 10^{-4}$
$9 \times 10^{-6}$	0.023	$5.63 \times 10^{-4}$	$3.91 \times 10^{-4}$
$1.05 \times 10^{-5}$	0.023	$6.56 \times 10^{-4}$	$5.00 \times 10^{-4}$

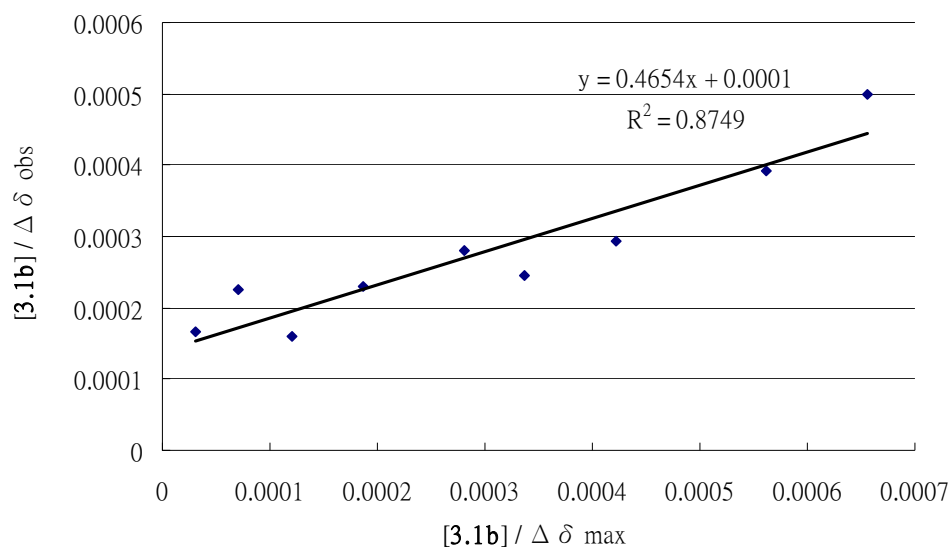


**Figure 3.17** Scott's plot of  $^1\text{H}$  NMR titration of **3.1b** and  $\beta$ -CD

**Table 3.11** Data of Scott's plot of  $^1\text{H}$  NMR titration of **3.1c** and  $\beta$ -CD

$[\mathbf{3.1c}]_{\text{normal}}$ (M)	$\Delta\delta_{\text{obs}}$	$[\mathbf{3.1c}]_{\text{normal}} / \Delta\delta_{\text{obs}}$	$[\mathbf{3.1c}]_{\text{normal}} / \Delta\delta_{\text{max}}$ ( $\Delta\delta_{\text{max}} = 0.026$ )
$5 \times 10^{-7}$	0	$1.92 \times 10^{-5}$	$1.00 \times 10^{-4}$
$1.125 \times 10^{-6}$	0.005	$4.33 \times 10^{-5}$	$9.37 \times 10^{-5}$
$1.929 \times 10^{-6}$	0.012	$7.42 \times 10^{-4}$	$1.38 \times 10^{-4}$
$3 \times 10^{-6}$	0.014	$1.15 \times 10^{-4}$	$1.58 \times 10^{-4}$
$4.5 \times 10^{-6}$	0.019	$1.73 \times 10^{-4}$	$1.73 \times 10^{-4}$
$5.4 \times 10^{-6}$	0.026	$2.08 \times 10^{-4}$	$1.86 \times 10^{-4}$
$6.75 \times 10^{-6}$	0.029	$2.60 \times 10^{-4}$	$2.41 \times 10^{-4}$
$9 \times 10^{-6}$	0.028	$3.46 \times 10^{-4}$	$3.00 \times 10^{-4}$
$1.05 \times 10^{-5}$	0.030	$4.04 \times 10^{-4}$	$3.18 \times 10^{-4}$

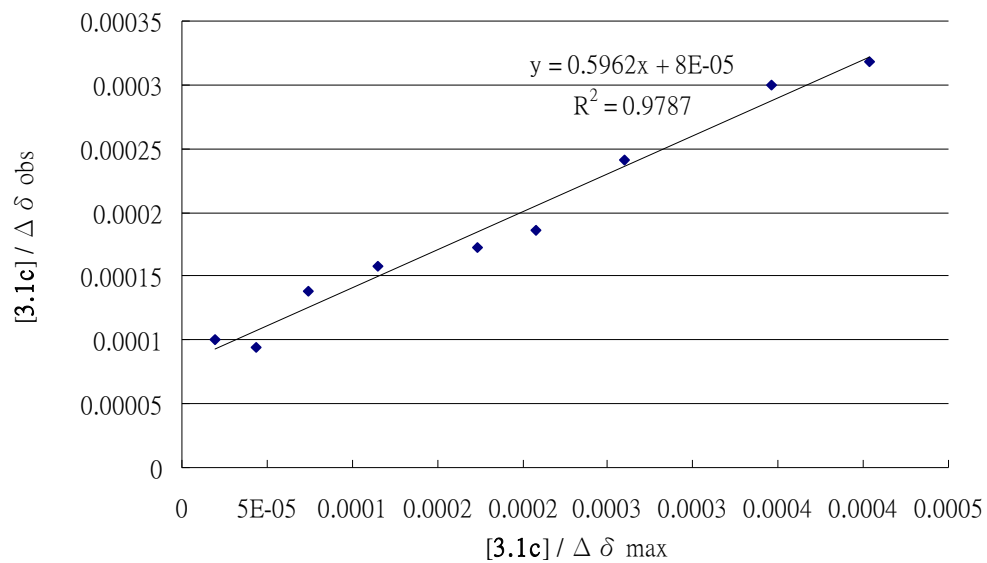
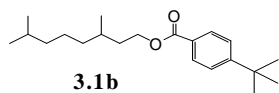


**Figure 3.18** Scott's plot of  $^1\text{H}$  NMR titration of **3.1c** and  $\beta$ -CD



### 3.12.3 Characterization Data of 3,7-Dimethyloctyl Esters 3.1b, 3.2b, 3.2b'

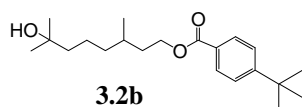
and 3.2c'



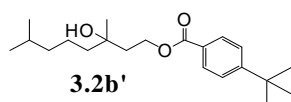
**Synthesis:** To 0.1 mmol of DMAP in 5 mL of distilled dichloromethane under nitrogen atmosphere, 1 mmol of 3,7-dimethyl 1-octanol was added, followed by addition of 5 mmol of triethylamine and dropwise addition of 1.2 mmol of 4-*tert*-butylbenzoyl chloride. After stirring the reaction mixture overnight under nitrogen atmosphere, the reaction was quenched by addition of 10 mL of water. The resulting solution was extracted with 10 mL of dichloromethane. The organic extract was then washed with 10 mL of 3.7% hydrochloric acid, 10 mL of saturated solution of sodium bicarbonate and 10 mL of brine. The organic solvent was evaporated under reduced pressure. The resulted product was purified by flash column chromatography, dissolved in CDCl<sub>3</sub> and analyzed by <sup>1</sup>H NMR spectroscopy.

**Characterization:** Colorless liquid; analytical TLC (silica gel 60) (2% EtOAc in *n*-hexane),  $R_f = 0.54$ ; <sup>1</sup>H NMR (500 MHz, CDCl<sub>3</sub>)  $\delta$  7.98–7.96 (d, 2H), 7.46–7.44 (d, 2H), 4.38–4.30 (m, 2H), 1.83–1.76 (m, 1H), 1.67–1.60 (m, 1H), 1.59–1.49 (m, 1H), 1.38–1.22 (m, 12H), 1.18–1.13 (m, 3H), 0.96–0.95 (d, 3H), 0.87–0.86 (d, 6H); <sup>13</sup>C NMR (75.47 MHz, CDCl<sub>3</sub>)  $\delta$  166.64, 156.61, 129.39, 127.46, 125.35,

72.04, 61.59, 44.78, 42.87, 39.85, 39.44, 35.08, 31.11, 29.70, 27.97, 27.19, 22.58, 21.75; HRMS (ESI)  $m/z$  calcd.  $C_{21}H_{34}O_2Na$   $[M + Na]^+$ : 341.2457, found 341.2466.



Colorless liquid; analytical TLC (silica gel 60) (20% EtOAc in hexane),  $R_f = 0.48$ ;  $^1H$  NMR (500 MHz,  $CDCl_3$ )  $\delta$  7.98–7.96 (d, 2H), 7.46–7.44 (d, 2H), 4.39–4.31 (m, 2H), 1.84–1.78 (m, 1H), 1.71–1.62 (m, 1H), 1.61–1.54 (m, 1H), 1.47–1.32 (m, 15H), 1.27–1.22 (m, 1H), 1.21 (s, 6H), 0.98–0.96 (d, 3H);  $^{13}C$  NMR (75.47 MHz,  $CDCl_3$ )  $\delta$  166.69, 156.42, 129.39, 127.70, 125.28, 70.94, 63.25, 44.11, 37.41, 35.60, 31.12, 29.98, 29.29, 29.22, 21.64, 19.57; HRMS (ESI)  $m/z$  calcd.  $C_{21}H_{35}O_3$   $[M + H]^+$ : 335.2586, found 335.2598.



Colorless liquid; analytical TLC (silica gel 60) (20% EtOAc in hexane),  $R_f = 0.52$ ;  $^1H$  NMR (500 MHz,  $CDCl_3$ )  $\delta$  7.96–7.94 (d, 2H), 7.46–7.44 (d, 2H), 4.49–4.47 (t, 2H), 2.00–1.91 (m, 2H), 1.64–1.48 (m, 5H), 1.35–1.32 (m, 12H), 1.26–1.27 (s, 3H), 0.88–0.84 (dd, 6H);  $^{13}C$  NMR (75.47 MHz,  $CDCl_3$ )  $\delta$  166.82,

156.82, 129.61, 127.71, 125.56, 72.24, 61.80, 43.09, 40.08, 39.66, 35.28, 31.33,

28.18, 27.41, 22.79, 21.95; HRMS (ESI) m/z calcd.  $C_{21}H_{35}O_3$   $[M + H]^+$ :

335.2586, found 335.2573.

### 3.12.4 $^1\text{H}$ NMR Spectra of Site-selective C-H Bond Oxidation of Aliphatic

#### Esters with Two Tertiary C-H Bonds

Table 3.1, entry 1

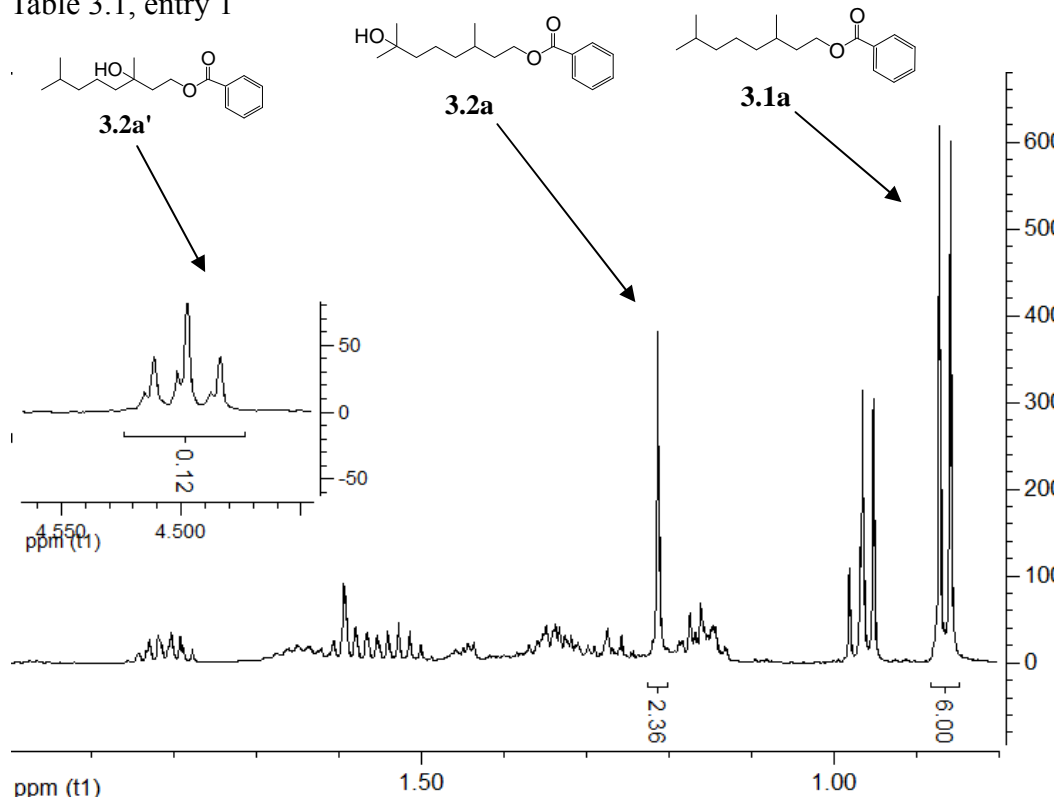


Table 3.1, entry 2

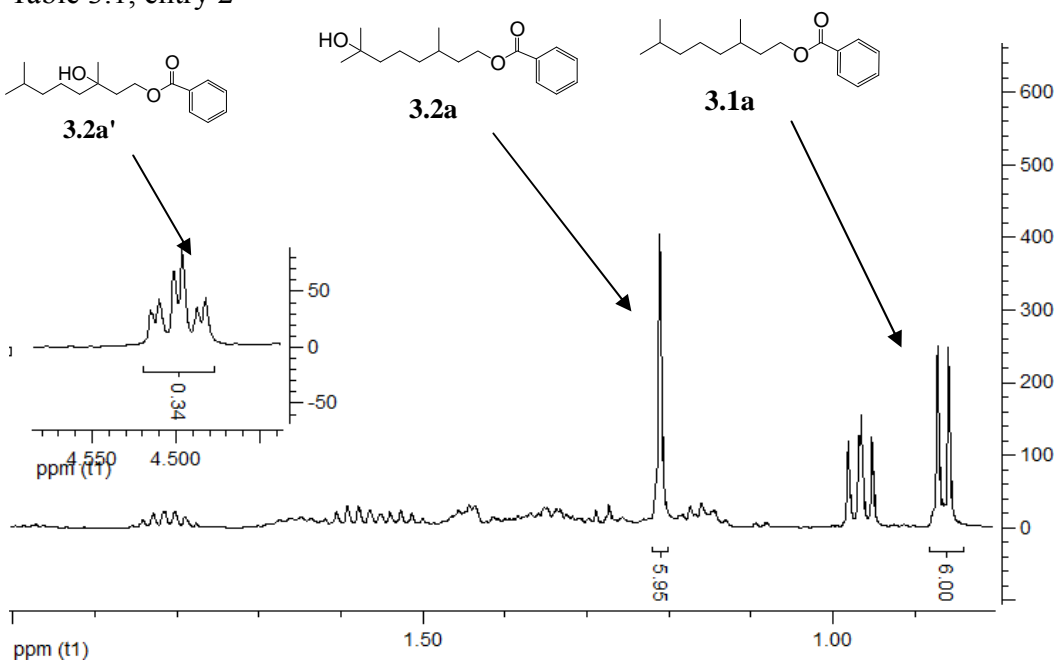


Table 3.2, entry 1

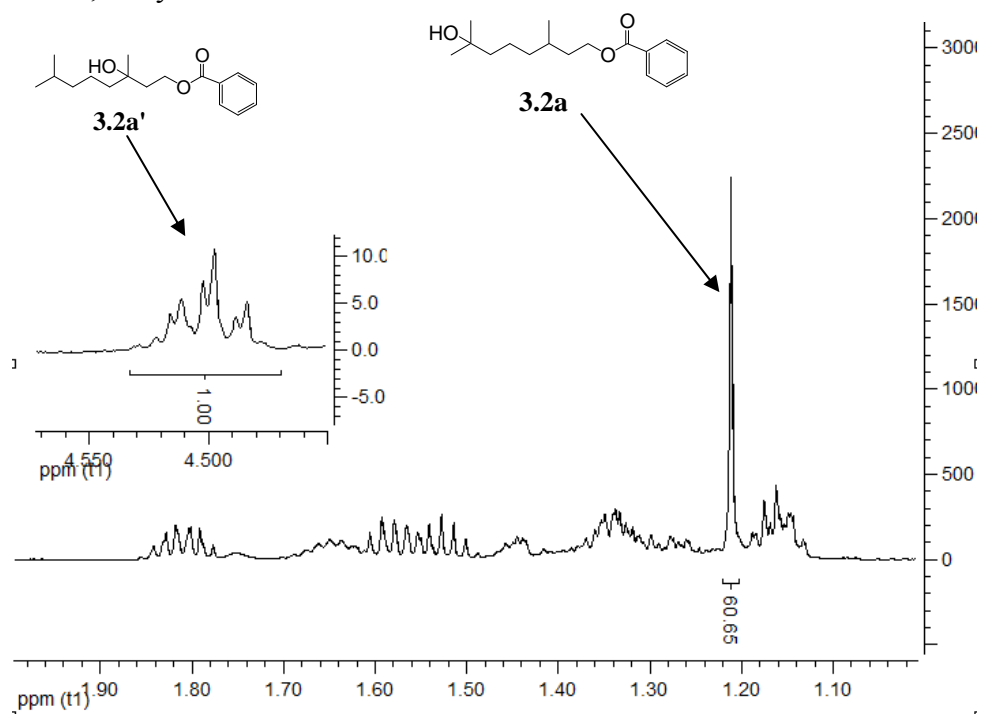


Table 3.2, entry 2

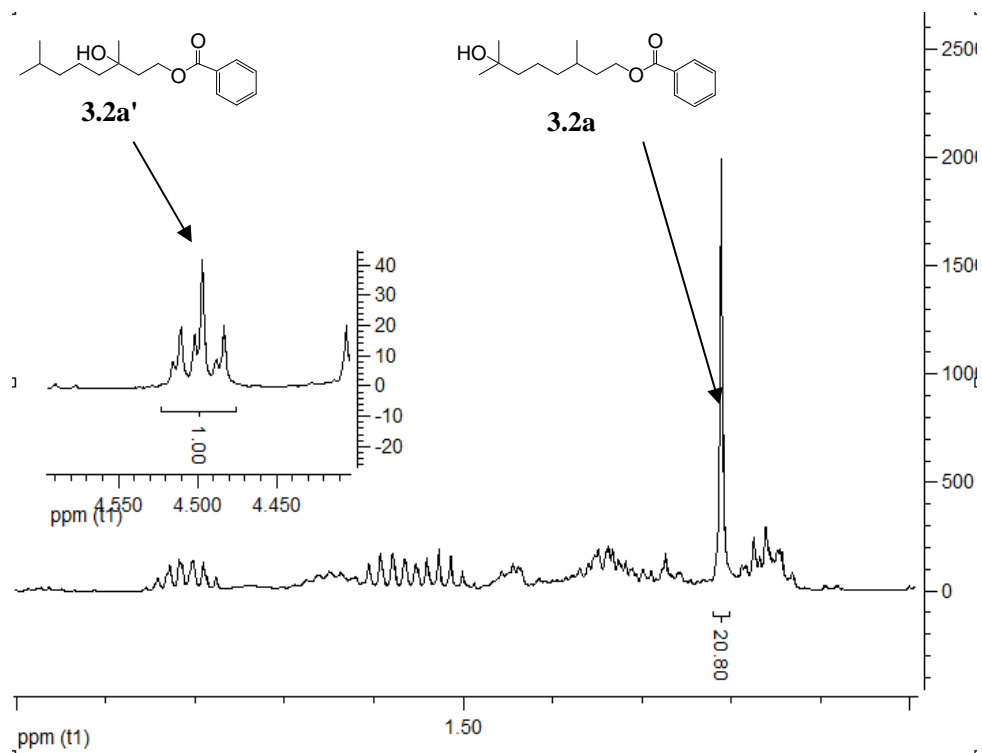


Table 3.2, entry 3

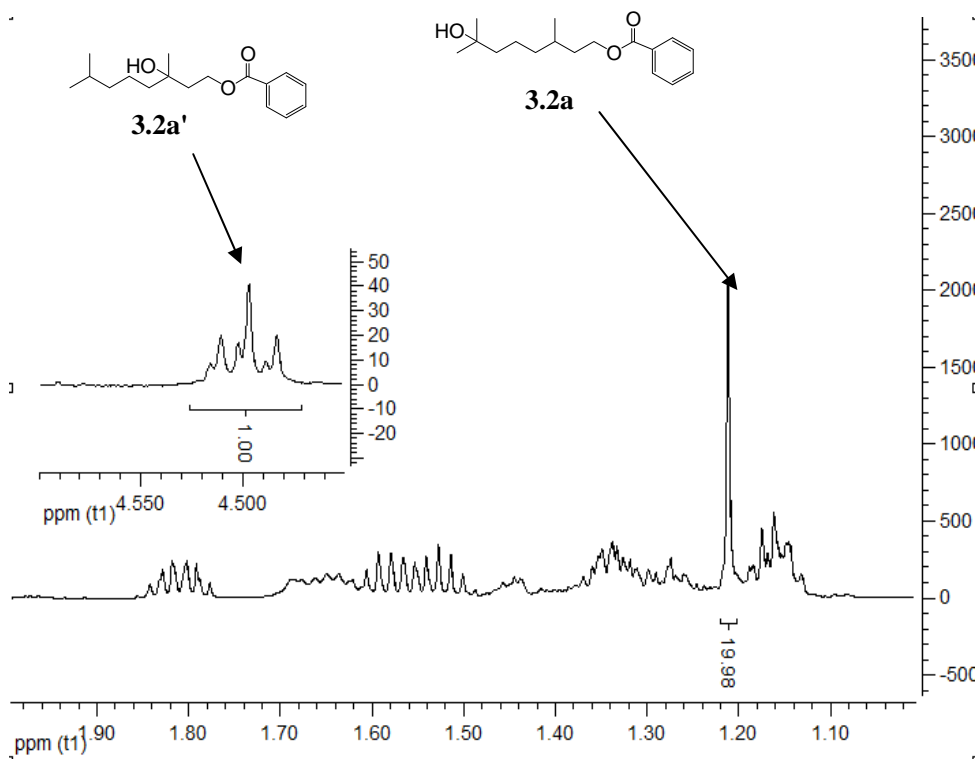


Table 3.2, entry 4

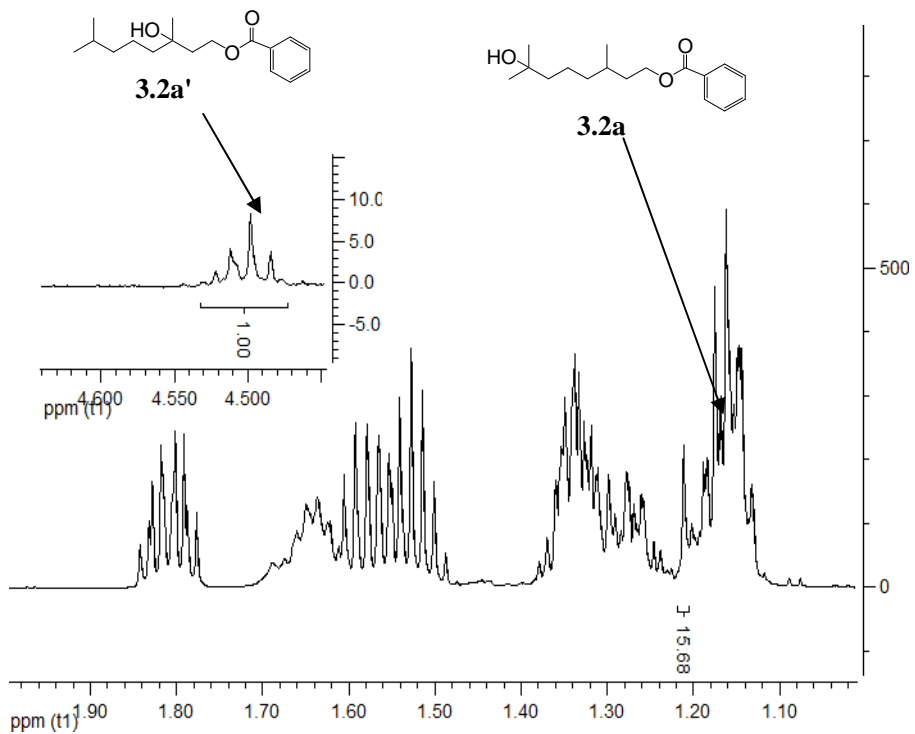


Table 3.3, entry 1

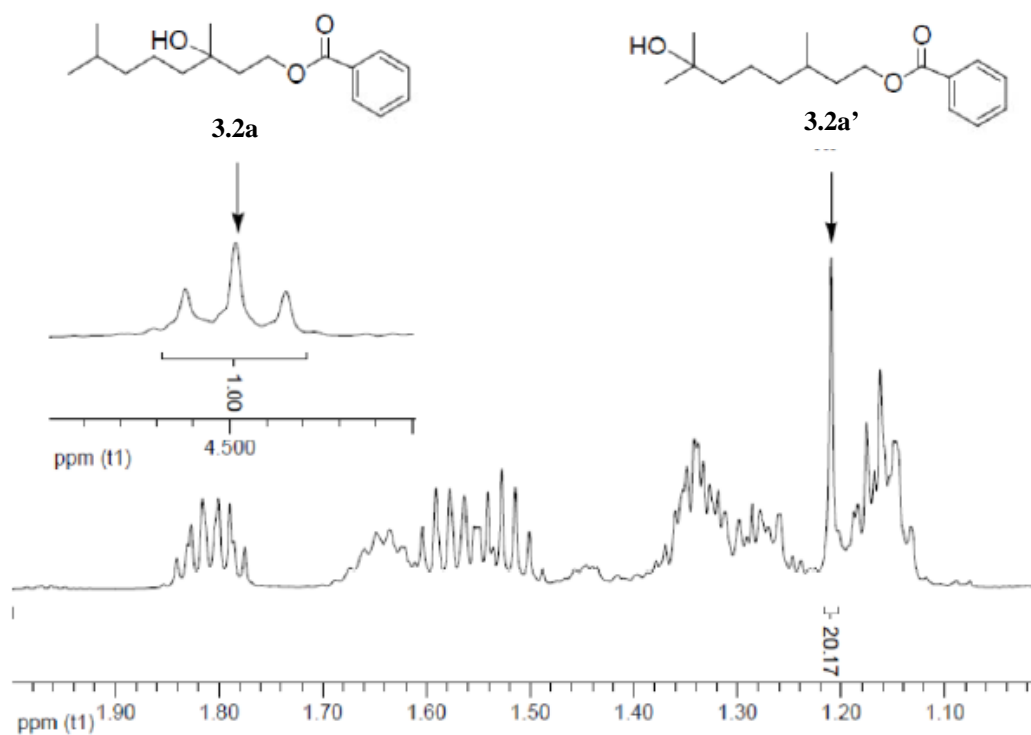


Table 3.3, entry 2

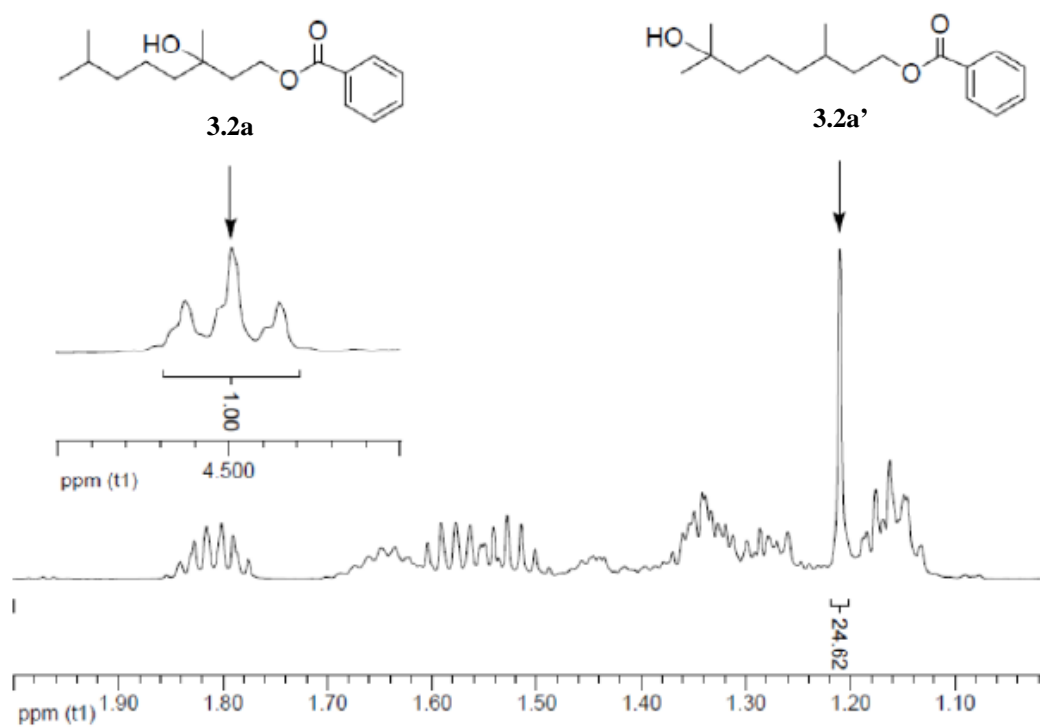


Table 3.3, entry 4

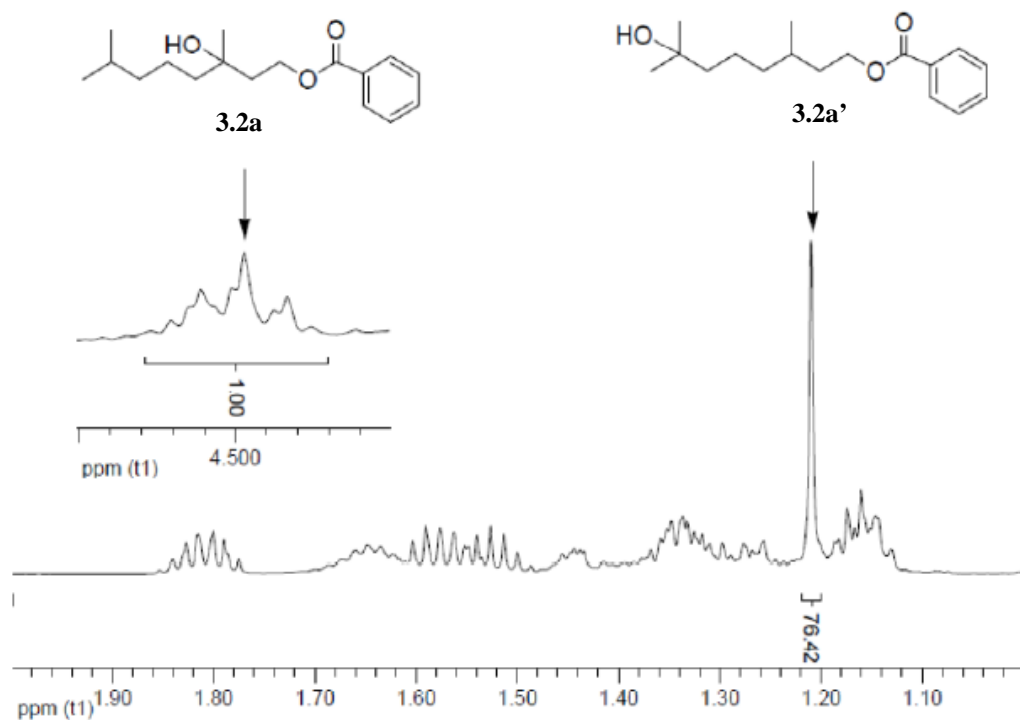


Table 3.3, entry 5

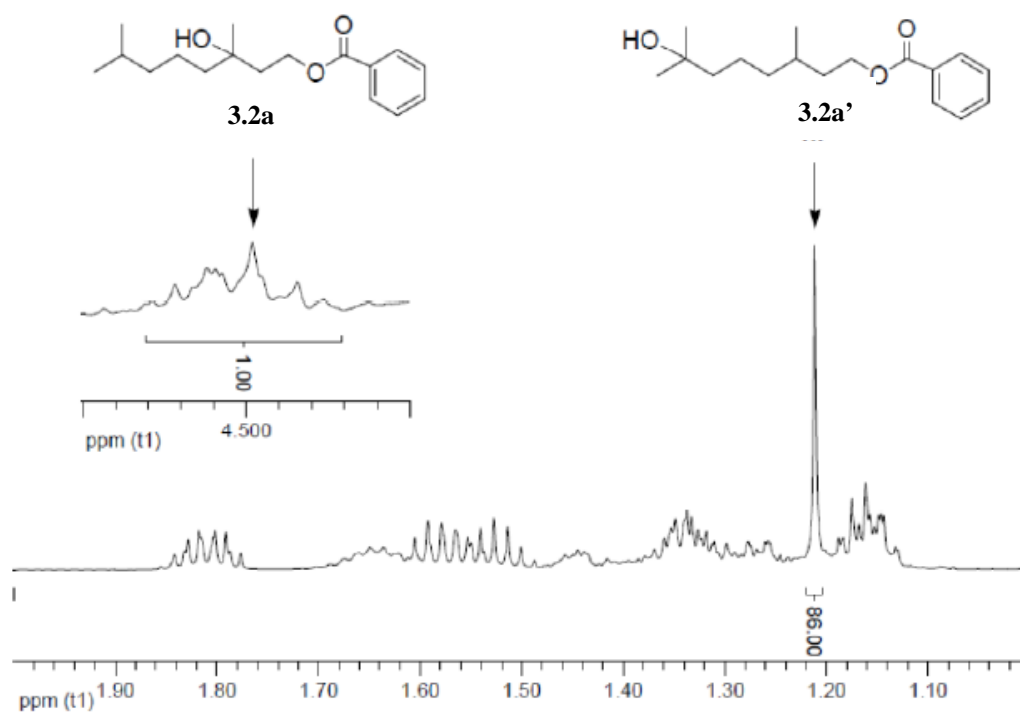




Table 3.3, entry 6

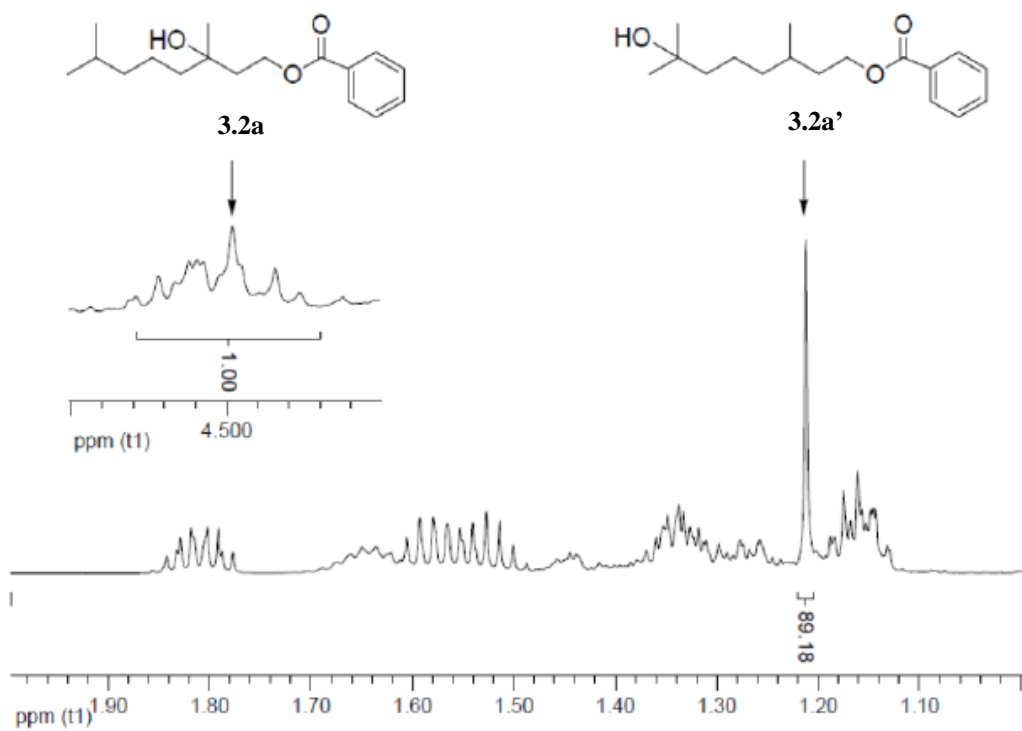


Table 3.4, entry 1

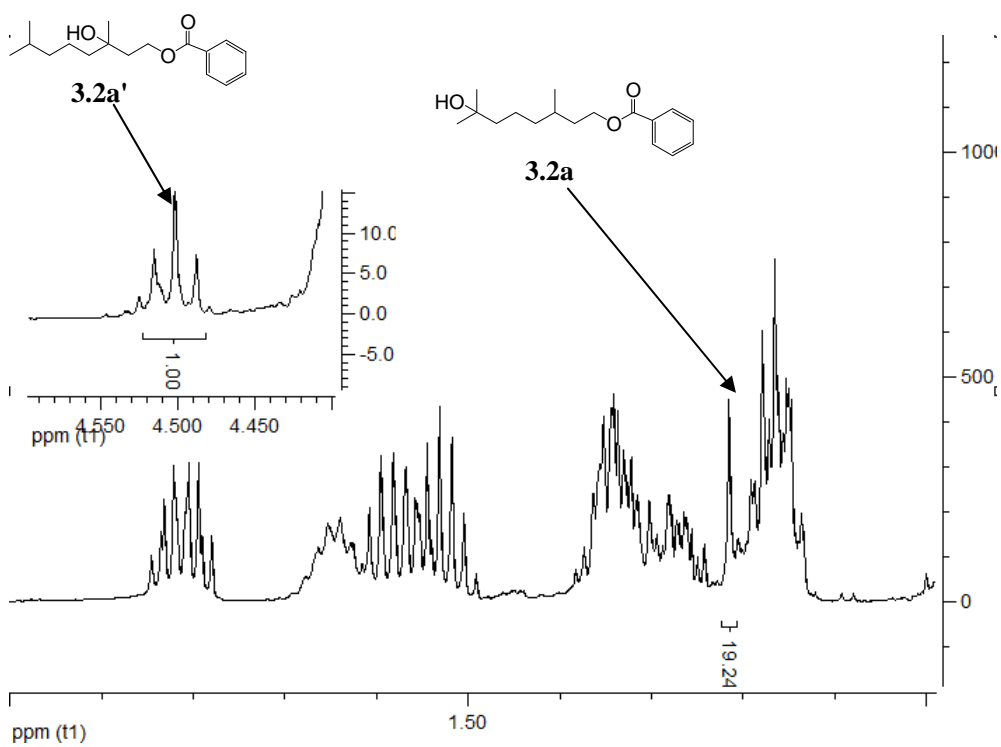


Table 3.4, entry 3

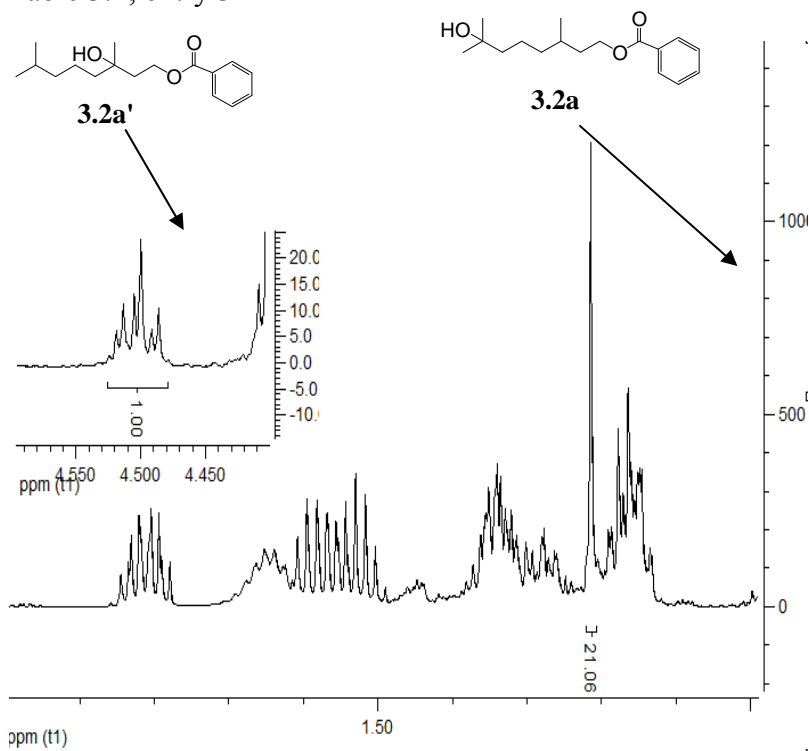


Table 3.4, entry 5

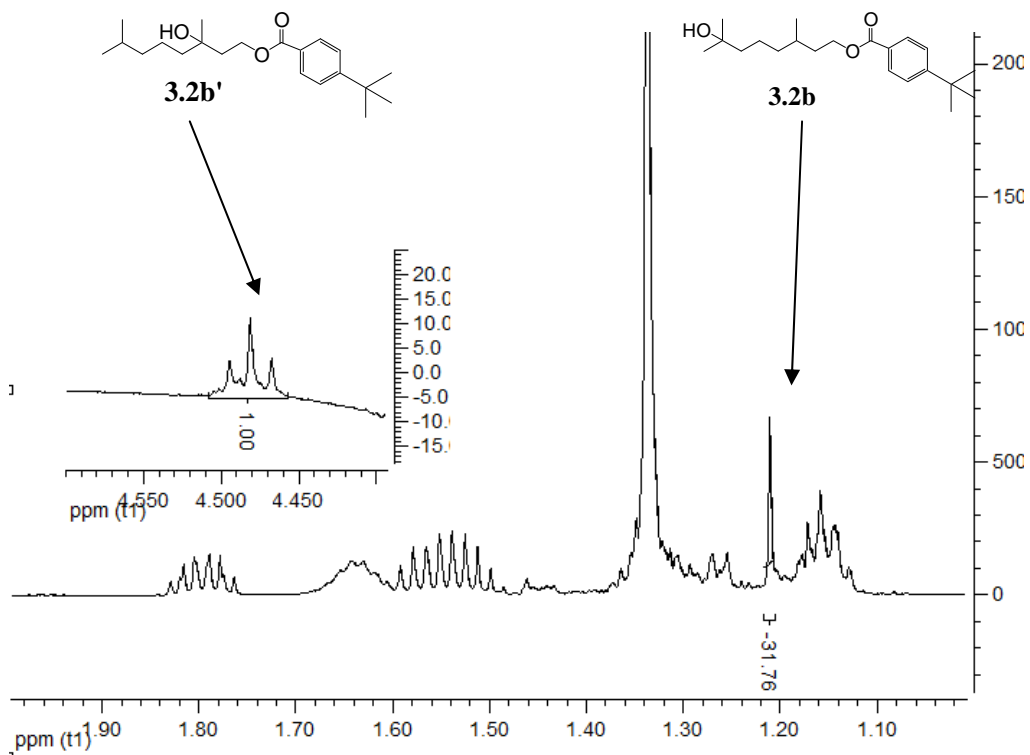


Table 3.4, entry 6

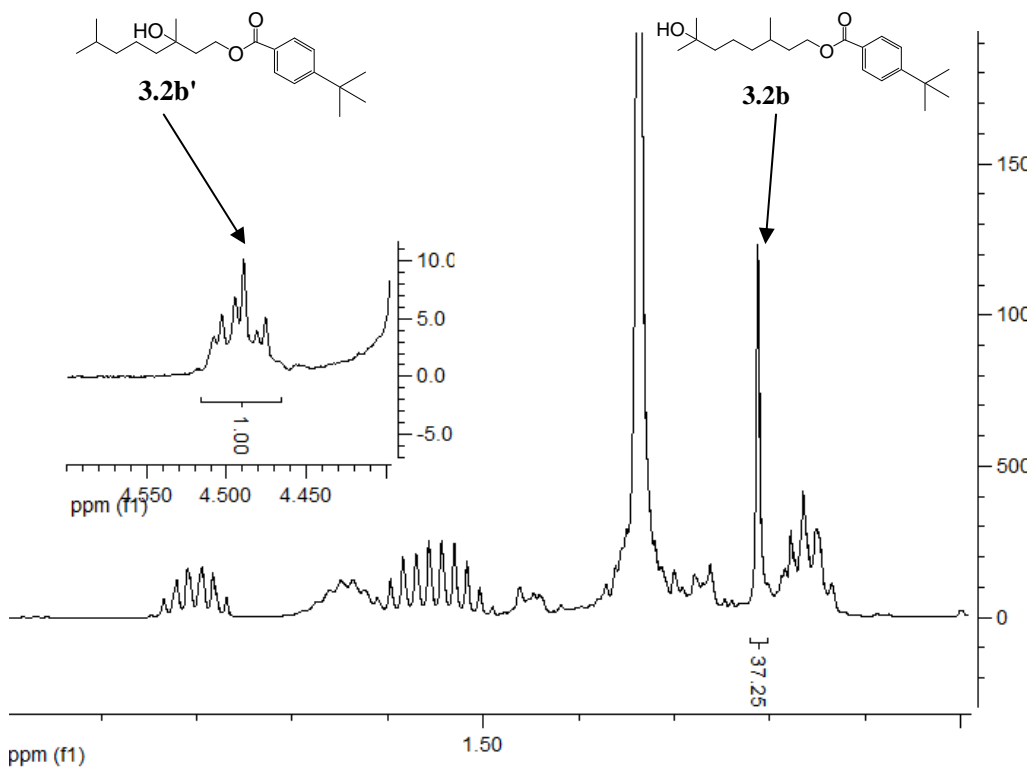


Table 3.4, entry 7

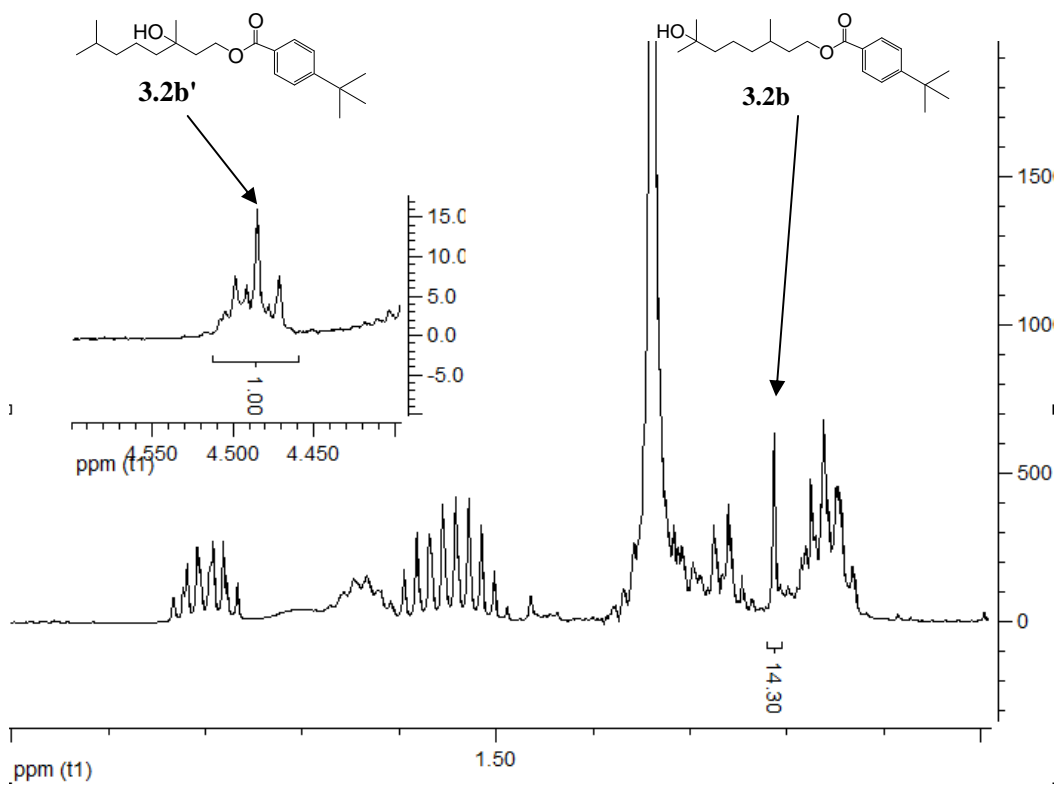


Table 3.4, entry 8

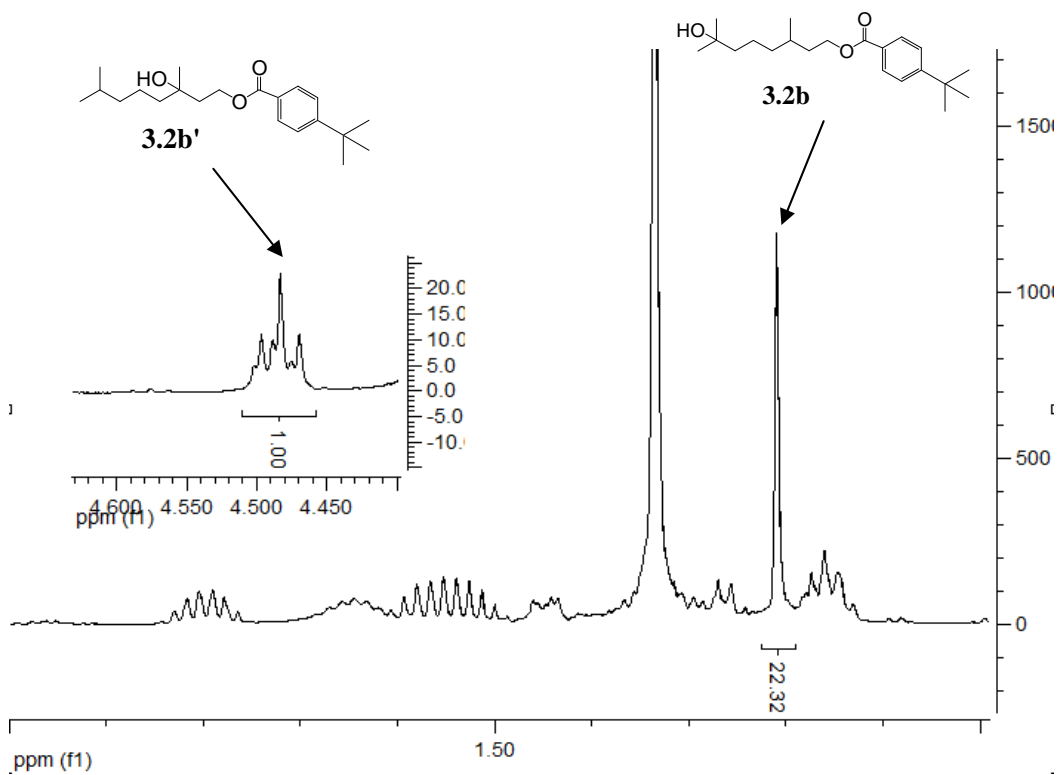


Table 3.4, entry 9

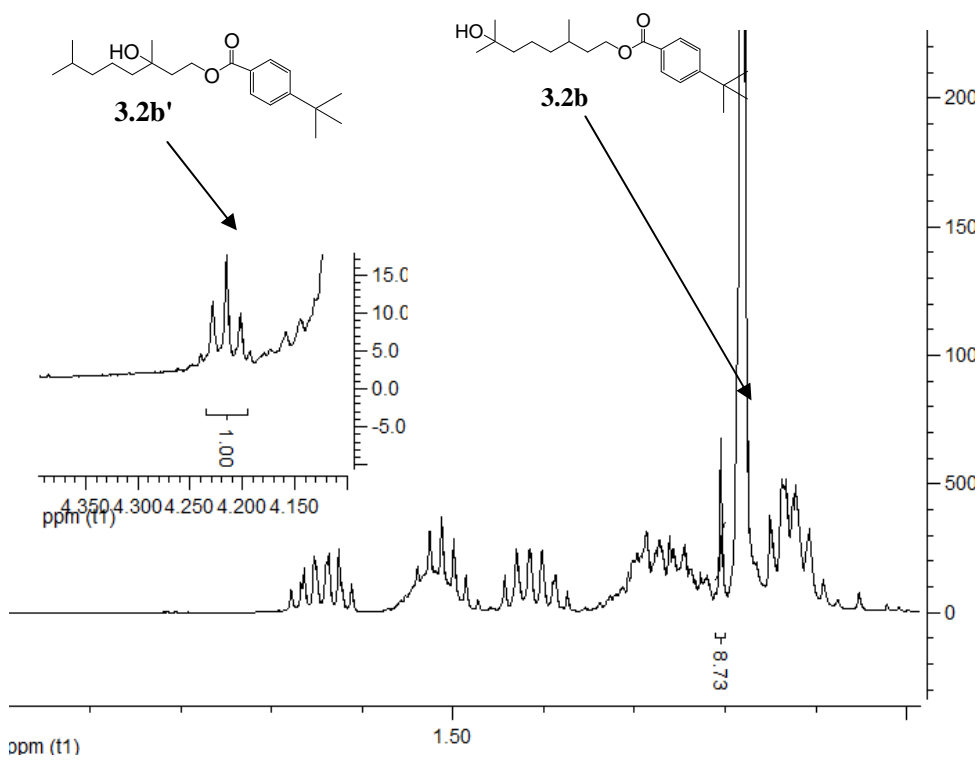


Table 3.4, entry 10

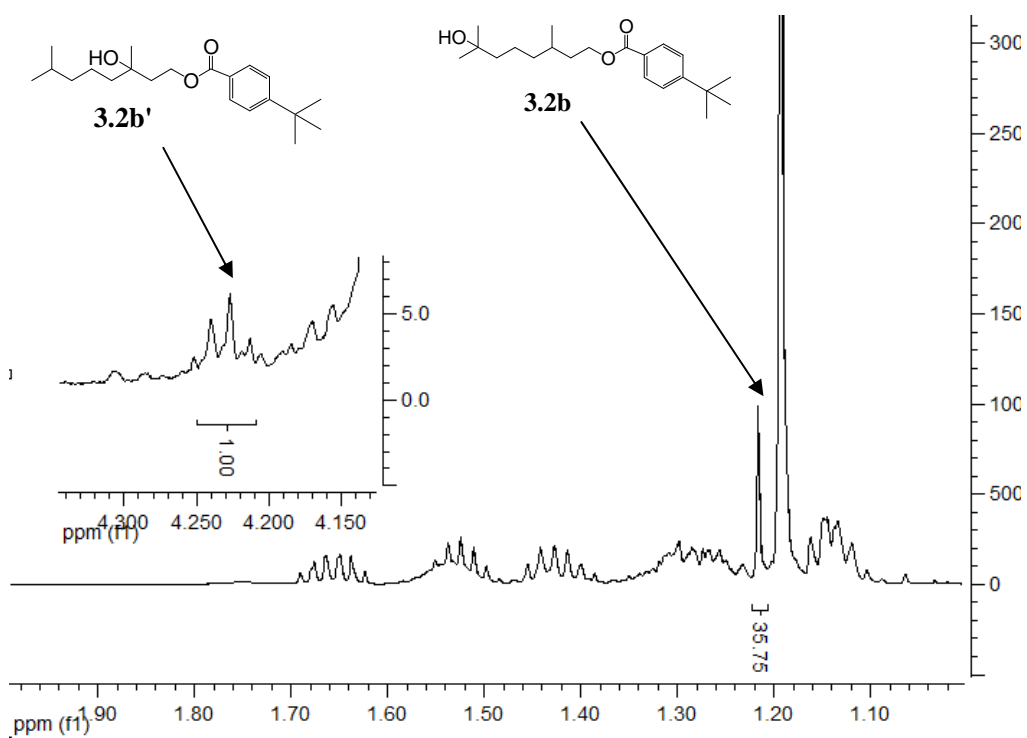


Table 3.4, entry 11

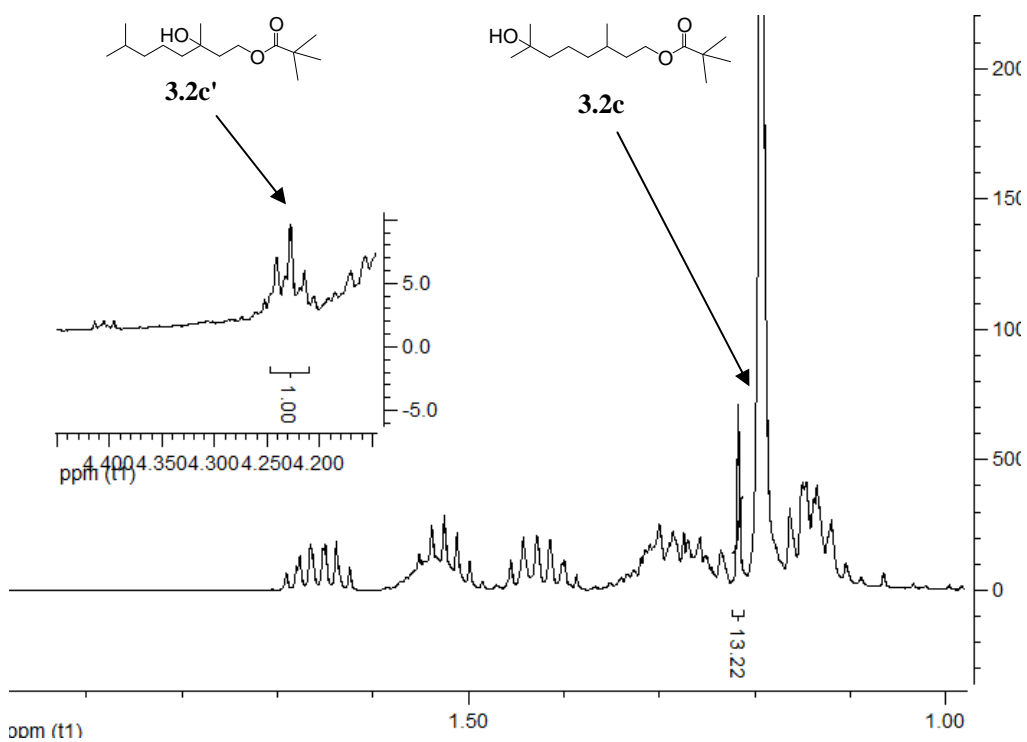


Table 3.4, entry 12

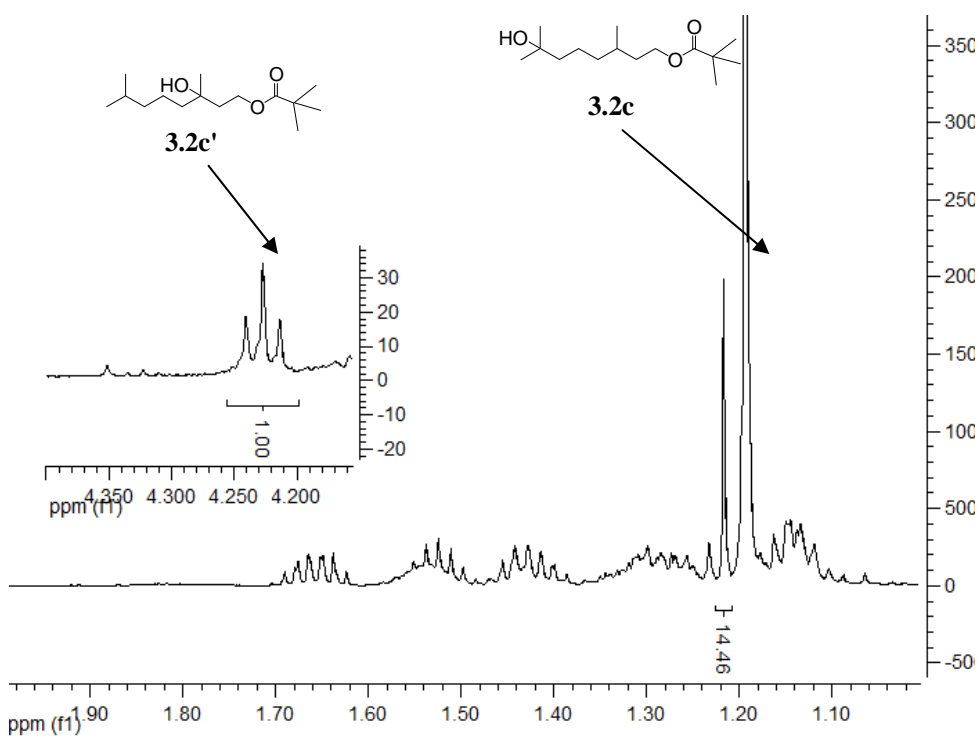


Table 3.4, entry 14

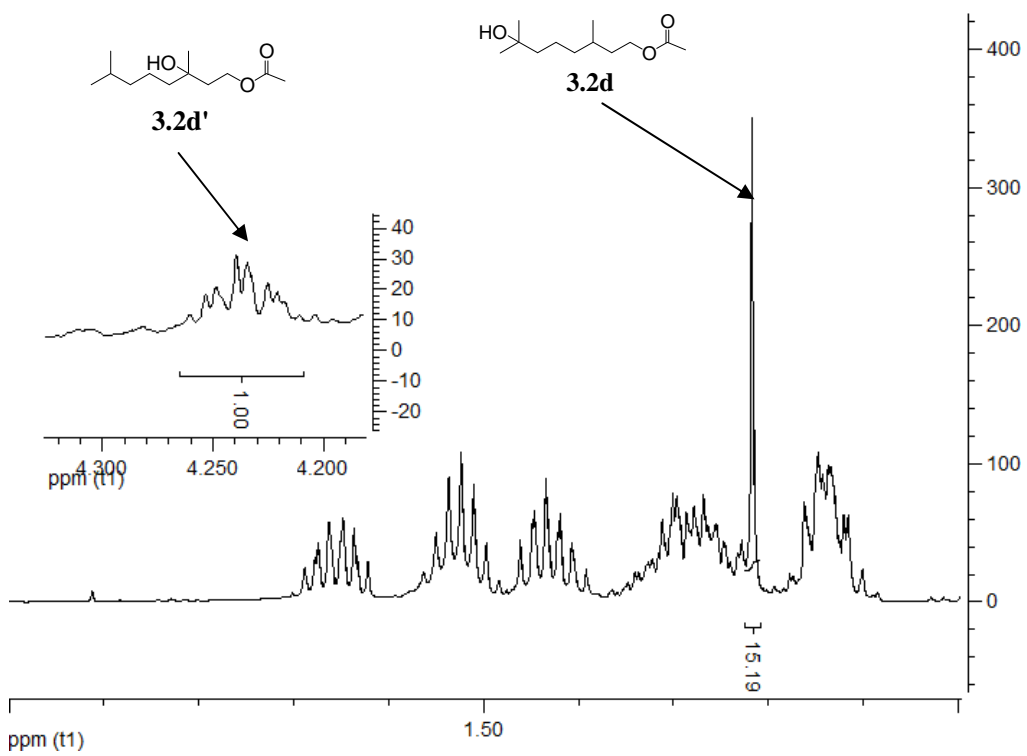


Table 3.4, entry 15

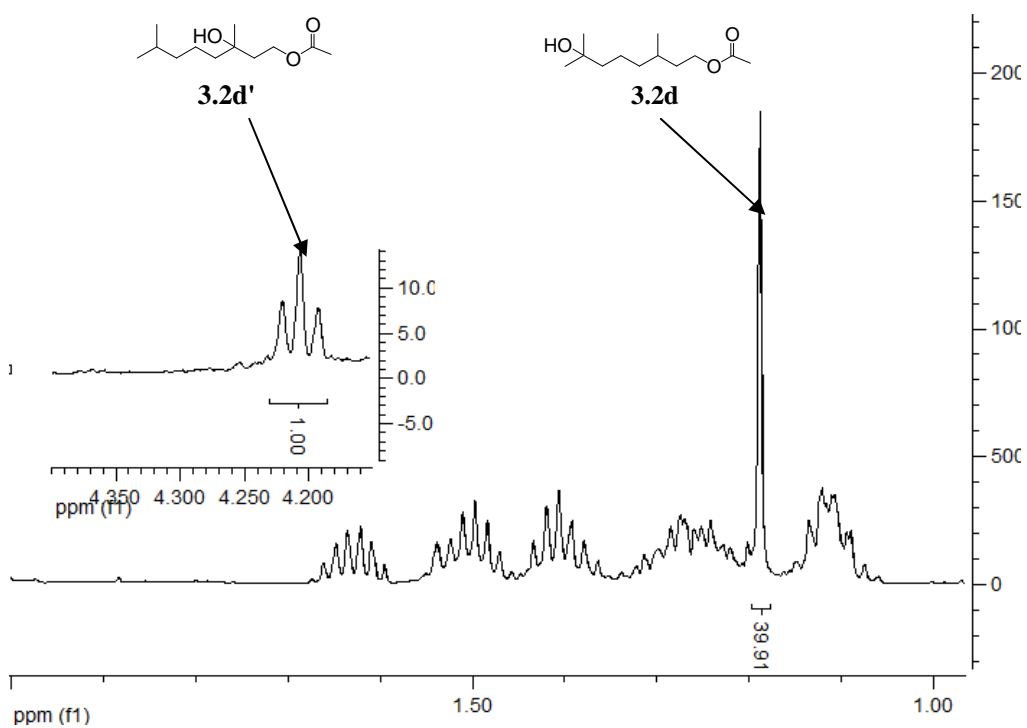
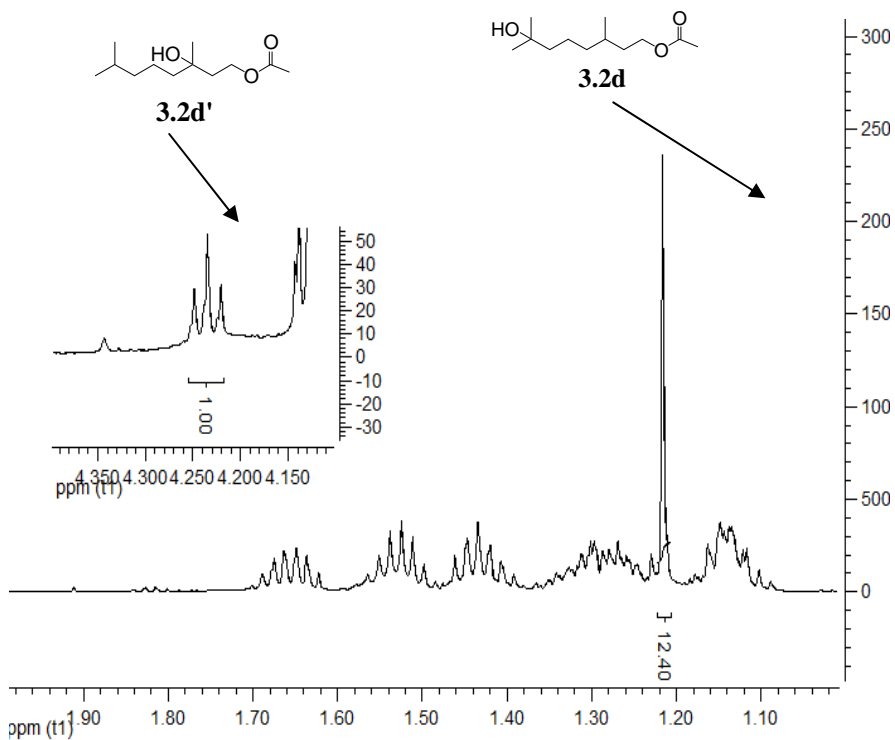


Table 3.4, entry 16





### 3.13 References

- (1) For the cyclodextrin-based supramolecular catalysis, see: (a) Szejtli, J.; Osa, T. Cyclodextrins. In *Comprehensive Supramolecular Chemistry*; Lehn, J.-M., Atwood, J. L., Davies, J. E. D., MacNicol, D. D., Vogtle, F., Eds.; Pergamon: New York, 1996; Vol. 3. (b) Szejtli, J. *Cyclodextrin Technology*; Kluwer Academic Publishers, 1988. (c) Breslow, R. and Dong, S. D. *Chem. Rev.* **1998**, *98*, 1997-2011 (d) Takahashi, K. *Chem. Rev.* **1998**, *98*, 2013-2033. (e) Bhosale, S. V.; Bhosale, S. V. *Mini-Reviews in Organic Chemistry*, **2007**, *4*, 231-242.
- (2) For the modified cyclodextrins working as mimics of cytochrome P450 by Breslow and co-workers: (a) Breslow, R.; Zhang, X.; Huang, Y. *J. Am. Chem. Soc.* **1997**, *119*, 4535. (c) Breslow, R.; Huang, Y.; Zhang, X. and Yang, J. *Proc. Natl. Acad. Sci. USA* **1997**, *94*, 11156-11158. (c) Breslow, R. and Dong, S. D. *Chem. Rev.* **1998**, *98*, 1997-2011. (d) Breslow, R.; Yang, J. and Yan, J. *Tetrahedron*, **2002**, *58*, 653-659; (e) Breslow, R. and Fang, Z. *Tetrahedron Lett.*, **2002**, *43*, 5197-5200; (f) Yang, J.; Gabriele, B.; Belvedere, S.; Huang, Y. and Breslow, R. *J. Org. Chem.*, **2002**, *67*, 5057-5067; (g) Fang, Z. and Breslow, R. *Org. Lett.*, **2006**, *8*, 251-254.
- (3) Chan, W. K.; Yu, Wing. Y.; Che, Chi. M. and Wong, M. K. *J. Org. Chem.*

**2003**, 68, 6576-6582.

- (4) (a) Chen, M. S. and White, M. C. *Science*, **2007**, 318, 783–787. (b) Gomez, L.; Bosch, I.G.; Company, A.; Buchholz, J. B.; Polo, A.; Sala, X.; Ribas, X. and Costas, M. *Angew. Chem. Int. Ed.* **2009**, 48, 5720-5723.
- (5) Brodsk, B. H. and Du Bois, J. *J. Am. Chem. Soc.* **2005**, 127, 15391-15393.
- (6) Tietze, L. F.; Biller, S.; Wolfram, T. *Synlett.* **2010**, 14, 230-2132.
- (7) McNeill, E. and Du Bois, J. *J. Am. Chem. Soc.* **2010**, 132, 10202–10204.
- (8) (a) Botsi, A.; Yannakopoulou, K.; Perly, B.; Hadjoudis, E. *J. Org. Chem.* **1995**, 60, 4017. (b) Salvatierra, D.; Jaime, C.; Virgili, A.; Sanchez-Ferrando, F. *J. Org. Chem.* **1996**, 61, 9578. (c) Botsi, A.; Perly, B.; Hadjoudis, E. *J. Chem. Soc., Perkin Trans. 2* **1997**, 89. (d) Salvatierra, D.; Sanchez-Ruiz, X.; Garduno, R.; Cervello, E.; Jaime, C.; Virgili, A.; Sanchez-Ferrando, F. *Tetrahedron* **2000**, 56, 3035. (e) Zubiaur, M.; Jaime, C. *J. Org. Chem.* **2000**, 65, 8139.
- (9) (a) Wilson, L. D.; Siddall, S. R.; Verrall, R. E. *Can. J. Chem.* **1997**, 75, 927-933. (b) Bojinova, T.; Coppel, Y.; Viguerie, N. L.; Milius, A.; Rico-Lattes, I. and Lattes A. *Langmuir* **2003**, 19, 5233-5239.
- (10) (a) Scott, R.L. *Recl Trav Chim Pays-Bas* **1956**, 75, 787-789. (b) Upadhyay, S. K. and Kumar, G. *Chemistry Central Journal* **2009**, 3, 9-17.

## Chapter 4

# Selective C-H Bond Oxidation of Hydrocarbon Mixtures by Supramolecular Approach

### 4.1 Introduction

In Chapter 3, the effects of CDs on site-selective C-H bond oxidation have been studied. In the presence of  $\beta$ -CD, 3,7-dimethyloctyl benzoate was oxidized to 7-hydroxy-3,7-dimethyloctyl benzoate and 3-hydroxy-3,7-dimethyloctyl benzoate in 71% yield based on 40% conversion with the product ratio of 20 : 1, by methyl (trifluoromethyl) dioxirane generated *in situ* in water. No reaction occurred without  $\beta$ -CD. By  $^1\text{H}$  NMR titration, inclusion complex formation between 3,7-dimethyloctyl benzoate and  $\beta$ -CD was confirmed. This reveals that  $\beta$ -CD would act as reaction vessel<sup>1</sup> in water to facilitate C-H bond oxidation by binding the substrate in its hydrophobic cavity (Figure 4.1).

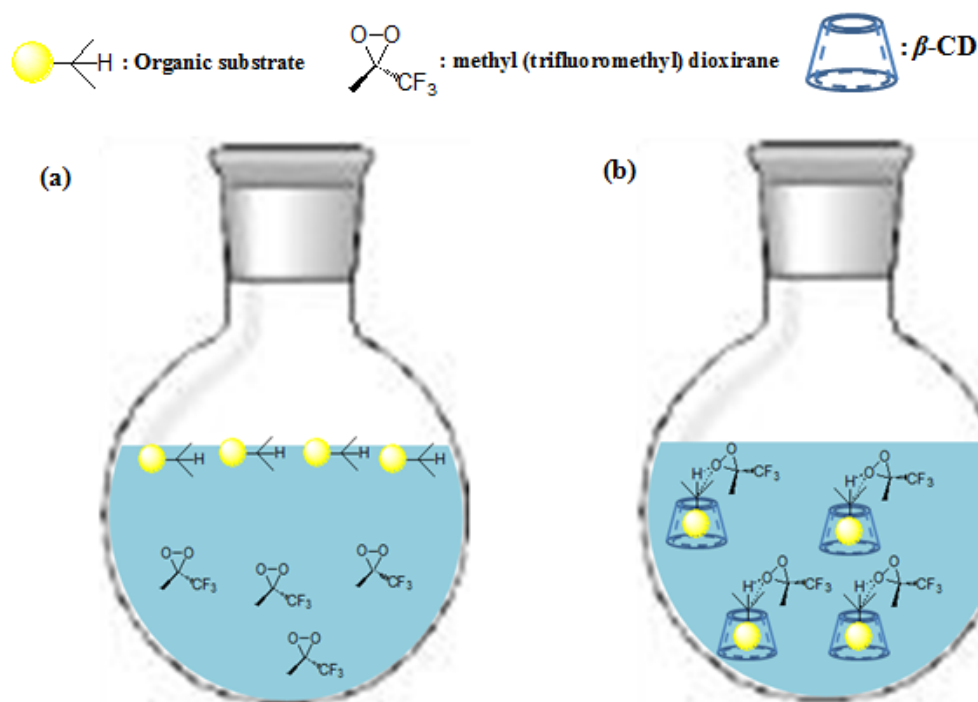


**Figure 4.1** (a) No C-H bond oxidation occurs in water in the absence of  $\beta$ -CD. (b) C-H bond oxidation occurs in water in the presence of  $\beta$ -CD.

After studying the effect of CDs on site-selective C-H bond oxidation, we would like to explore the possibility of selective C-H bond oxidation of hydrocarbon mixtures in water. As  $\beta$ -CD gave enhancement on C-H bond oxidation, it was interesting to see whether it would exhibit selectivity of C-H bond oxidation of hydrocarbon mixtures. As a proof-of concept, cumene and ethyl benzene were chosen as the substrates. Cumene is an aromatic compound with an isopropyl group while ethyl benzene is an aromatic compound with an ethyl group as the substituent.

## 4.2 Effect of $\beta$ -CD on the Oxidation of Cumene

Initially, the effect of  $\beta$ -CD on the oxidation of cumene was examined. The reaction was performed at room temperature by using 0.2 mmol of cumene, 0.22 mmol of  $\beta$ -CD and 0.2 mmol of 1,1,1-trifluoroacetone in 10 mL of water with eight additions of 0.5 mmol of Oxone and 1.55 mmol of  $\text{NaHCO}_3$  at 0 h, 1 h, 2 h, 3 h, 4 h, 5 h, 6 h and 7 h (Table 4.1, entry 1). By analysis of the crude reaction mixture by gas chromatography (GC) with n-decane as internal standard (Figure 4.2), it was found that cumyl alcohol in 32% yield was obtained with 38% recovery of cumene. Through  $^1\text{H}$  NMR titration experiment, the inclusion complex formation between cumene and  $\beta$ -CD in water was confirmed. According to the literatures, the stoichiometry of cumene- $\beta$ -CD inclusion complex is 1 : 1.<sup>11</sup>

Cumyl alcohol is a by-product in process of phenol production,<sup>2</sup> which can be utilized to synthesize alpha-methyl styrene (AMS) by dehydration.<sup>3</sup> AMS is starting material in the synthesis of heat resistant acrylonitrile butadiene styrene (ABS) resin.<sup>4</sup>

**Table 4.1** Oxidation of cumene <sup>a</sup>

Entry	Condition	% Yield <sup>b</sup>	% recovery of starting material <sup>b</sup>
1	H <sub>2</sub> O + $\beta$ -CD	32	38
2	H <sub>2</sub> O	0	3%
3	H <sub>2</sub> O + CH <sub>3</sub> CN	4	63

<sup>a</sup> Unless otherwise indicated, reactions were conducted by stirring 0.2 mmol of cumene, 0.2 mmol of 1,1,1-trifluoroacetone and 0.22 mmol of  $\beta$ -CD in 10 mL of water at room temperature with 8 additions of 0.5 mmol of Oxone and 1.55 mmol of NaHCO<sub>3</sub> at 0 h, 1 h, 2 h, 3 h, 4 h, 5 h, 6 h and 7 h. <sup>b</sup> Obtained by GC analysis of crude reaction mixture using authentic standards. <sup>c</sup> The reaction was performed without  $\beta$ -CD. <sup>d</sup> The reaction was performed in 4 mL of water and 6 mL of CH<sub>3</sub>CN without  $\beta$ -CD.

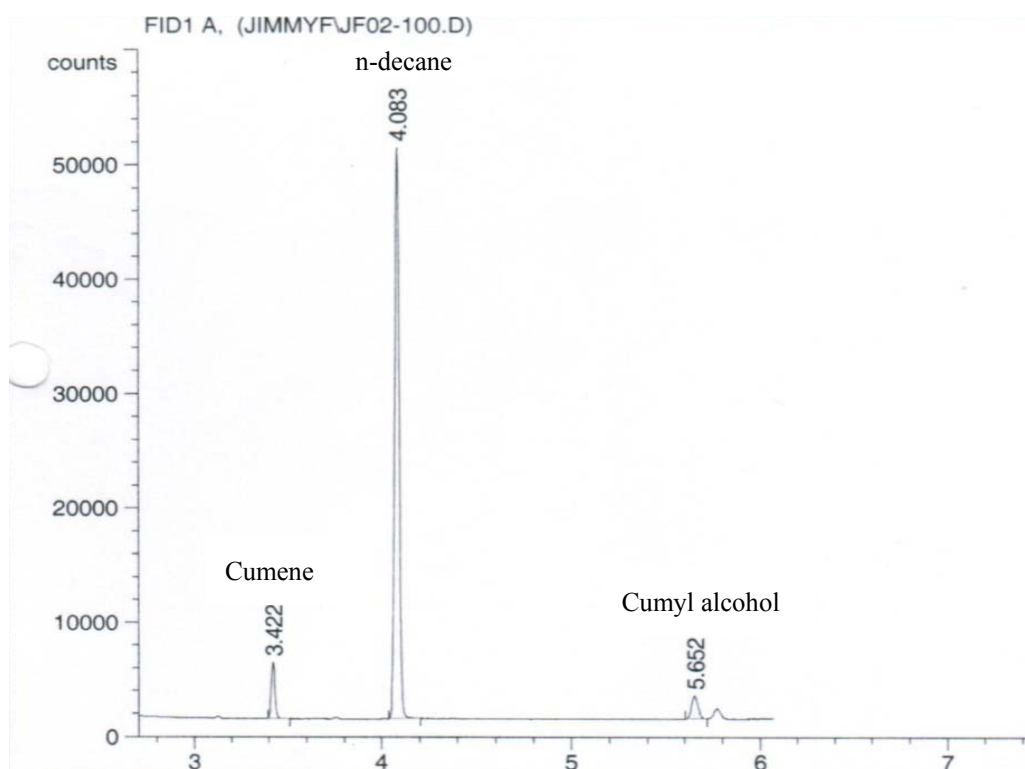


**Figure 4.2** GC-FID chromatograph of the crude product mixture of dioxirane-based cumene oxidation in the presence of  $\beta$ -CD.

The reaction was then performed in the absence of  $\beta$ -CD (Entry 2). Based on the GC analysis of the crude product mixture, no cumyl alcohol was obtained. This would be attributed to the low solubility of cumene in water. Noted that only 3% of cumene could be recovered. The low recovery of cumene is likely due to the evaporation of cumene during the reaction. These findings show that  $\beta$ -CD could reduce the loss of volatile substrates through inclusion complex formation.<sup>5</sup>

The dioxirane-based cumene oxidation in a mixture of water and CH<sub>3</sub>CN was examined (Entry 3). In a mixture of 4 mL of water and 6 mL of CH<sub>3</sub>CN in the absence of  $\beta$ -CD, cumyl alcohol in 4% yield with 63% cumene recovery was resulted. This result shows that the evaporation of cumene could be reduced in the presence of water-miscible CH<sub>3</sub>CN, but the oxidation of cumene would not be enhanced, although cumene was well dissolved in the solvent system. This would be due to the excessive formation of Na<sub>2</sub>SO<sub>4</sub> by the reaction of Oxone and NaHCO<sub>3</sub>. The high ionic strength induced by a large amount of Na<sub>2</sub>SO<sub>4</sub> would lead to biphasic separation of water and acetonitrile. In biphasic system, the dioxiranes in aqueous phase was decomposed rapidly by Oxone, and only small amount of dioxirane could pass to organic phase for cumene oxidation. As a result, poor conversion of cumene was obtained.

#### **4.3 Effect of $\beta$ -CD on the Oxidation of Ethyl Benzene**

Besides cumene, the effect of  $\beta$ -CD on the oxidation of ethyl benzene has been examined. The reaction was performed at room temperature by using 0.2 mmol of ethyl benzene, 0.22 mmol of  $\beta$ -CD and 0.2 mmol of 1,1,1-trifluoroacetone in 10 mL of water with eight additions of 0.5 mmol of Oxone and 1.55 mmol of NaHCO<sub>3</sub> at 0 h, 1 h, 2 h, 3 h, 4 h, 5 h, 6 h and 7 h



(Table 4.2, entry 1). The reaction gave acetophenone in 15% yield with 65% recovery of ethyl benzene, based on GC analysis of the crude reaction mixture.

Acetophenone mainly comes from the Hock process in phenol production from cumene.<sup>6</sup> It can also be produced from oxidation of ethyl benzene in oxygen at 130 °C and 0.5 MPa with magnesium salt or cobalt salt of fatty acids as catalysts in 25% conversion.<sup>7</sup> Our findings provide a new alternative for acetophenone production in H<sub>2</sub>O at ambient temperature without using metal catalyst. Acetophenone is mainly used to synthesize resin by the reaction with formaldehyde and base through Aldol condensation<sup>2,8</sup> and synthesize styrene.<sup>2,5</sup> It is also widely used in organic synthesis, particularly for pharmaceutical industry.<sup>9</sup> Moreover, it can be used as flavor additive for food.<sup>10</sup>

**Table 4.2** Oxidation of Ethyl Benzene <sup>a</sup>

Entry	Conditions	% Yield <sup>b</sup>	% Recovery of starting material <sup>b</sup>
1	H <sub>2</sub> O + $\beta$ -CD	15	65
2 <sup>c</sup>	H <sub>2</sub> O	0	3
3 <sup>d</sup>	H <sub>2</sub> O + CH <sub>3</sub> CN	4	73

<sup>a</sup> Unless otherwise indicated, reactions were conducted by stirring 0.2 mmol of ethyl benzene, 0.2 mmol of 1,1,1-trifluoroacetone and 0.22 mmol of  $\beta$ -CD in 10 mL of water at room temperature with 8 additions of 0.5 mmol of Oxone and 1.55 mmol of NaHCO<sub>3</sub> at 0 h, 1 h, 2 h, 3 h, 4 h, 5 h, 6 h and 7 h. <sup>b</sup> Obtained by GC analysis of crude reaction mixture using authentic standards. <sup>c</sup> The reaction was performed without  $\beta$ -CD. <sup>d</sup> The reaction was performed in 4 mL of water and 6 mL of CH<sub>3</sub>CN without  $\beta$ -CD.

Without  $\beta$ -CD, no oxidation of ethyl benzene occurred in water and only 3% of ethyl benzene was recovered (Entry 2). The poor recovery of ethyl benzene would be due to the loss of ethyl benzene by evaporation. Owing to the low solubility of ethyl benzene in water, no oxidation occurred.

The performance of dioxirane-based oxidation of ethyl benzene in a mixture

of water and CH<sub>3</sub>CN has also been examined (Entry 3). Without  $\beta$ -CD, the oxidation of ethyl benzene in the water-CH<sub>3</sub>CN solvent system gave acetophenone in 4% yield with 73% recovery of ethyl benzene. This shows that enhancement on oxidation of ethyl benzene which could not be achieved by using the water-CH<sub>3</sub>CN solvent system.

Through the above studies, the effects of  $\beta$ -CD on C-H bond oxidation of cumene and ethyl benzene are concluded as follows:

- 1)  $\beta$ -CD would act as reaction vessel and increase the solubility of organic compounds in water. This function is similar to that of water-CH<sub>3</sub>CN system.
- 2)  $\beta$ -CD would reduce the loss of volatile organic compounds in water by formation of inclusion complex and assisting to disperse the volatile organic compound in water.
- 3)  $\beta$ -CD gives enhancement on the C-H bond oxidation of cumene (32% yield, 38% cumene recovery) and ethyl benzene (15% yield, 65% ethyl benzene recovery) in water by confining them in the cavity of  $\beta$ -CD, this could not be achieved by the reaction performed in a mixture of water and CH<sub>3</sub>CN.

#### 4.4 Effect of $\beta$ -CD on the Selective Oxidation of a Hydrocarbon Mixture

After studying the effect of  $\beta$ -CD on the oxidation of cumene and ethyl benzene, respectively, the effect of  $\beta$ -CD on selective oxidation of a mixture of cumene and ethyl benzene was investigated.

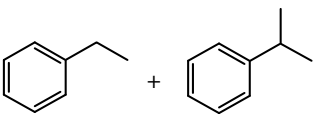
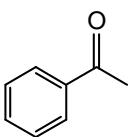
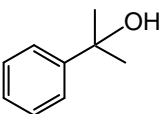
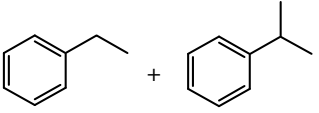
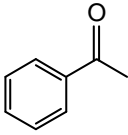
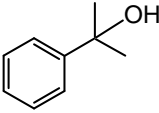
The reaction was performed at room temperature by using 0.2 mmol of cumene, 0.2 mmol of ethyl benzene, 0.22 mmol of  $\beta$ -CD and 0.2 mmol of 1,1,1-trifluoroacetone in 10 mL of water with eight additions of 0.5 mmol of Oxone and 1.55 mmol of  $\text{NaHCO}_3$  at 0 h, 1 h, 2 h, 3 h, 4 h, 5 h, 6 h and 7 h. Based on the GC analysis of the crude product mixture, acetophenone in 3% yield and cumyl alcohol in 23% yield were obtained with 59% ethyl benzene recovery and 50% cumene recovery (Table 4.3, entry 1). The reaction was then repeated in a mixture of water and acetonitrile in the absence of  $\beta$ -CD (Entry 2). Acetophenone in 4% yield and cumyl alcohol in 9% yield with 70% of ethyl benzene and 71% of cumene recovery were found.

This set of experiments shows that  $\beta$ -CD would exhibit molecular recognition of hydrocarbon mixtures in water. In the presence of  $\beta$ -CD, the oxidation of cumene was selectively enhanced in the mixture of cumene and ethyl benzene. According to literature,<sup>11</sup> the binding constant of cumene to  $\beta$ -CD ( $1.2 \times 10^3 \text{ M}^{-1}$ ) is about 4-fold higher than that of ethyl benzene ( $3.3 \times 10^2 \text{ M}^{-1}$ ).

This would lead to preferential binding cumene by  $\beta$ -CD. Based on

Curtius-Hammett principle, the product distribution is not necessarily controlled by the binding of cumene or ethyl benzene to  $\beta$ -CD, but from the C-H bond strength, and the fast equilibrium does not affect regioselectivity, but the reaction constant.<sup>12,13</sup> Indeed, the selectivity of oxidation of cumene-ethyl benzene mixture given by the reaction with  $\beta$ -CD (23 : 3) was 4-fold higher than that given by the reaction performed in H<sub>2</sub>O-CH<sub>3</sub>CN mixture (9 : 4). This reveals that, the selective enhancement of cumene oxidation is not only controlled by the C-H bond strength, but may also be affected by  $\beta$ -CD.

**Table 4.3** Effect of  $\beta$ -CD on Selective C-H Bond Oxidation of HydrocarbonMixtures <sup>a</sup>

Entry	Hydrocarbon mixture	Conditions	Product yield (substrate recovery) <sup>b</sup>	
1		H <sub>2</sub> O + $\beta$ -CD	 3 % (59%)	 23 % (50%)
2		H <sub>2</sub> O + CH <sub>3</sub> CN	 4 % (70%)	 9 % (71%)

<sup>a</sup> Unless otherwise indicated, reactions were conducted by stirring 0.2 mmol of each substrate, 0.2 mmol of 1,1,1-trifluoroacetone and 0.22 mmol of  $\beta$ -CD in 10 mL of water at room temperature with 8 additions of 0.5 mmol of Oxone and 1.55 mmol of NaHCO<sub>3</sub> at 0 h, 1 h, 2 h, 3 h, 4 h, 5 h, 6 h and 7 h. <sup>b</sup> The yield of the reaction was obtained by GC analysis of crude reaction mixture using authentic standards. <sup>c</sup> The reaction was performed in 4 mL of water and 6 mL of CH<sub>3</sub>CN without  $\beta$ -CD.

## 4.5 Conclusion

In summary, the oxidation reactions of cumene and ethyl benzene in the presence of  $\beta$ -CD were examined. In the presence of  $\beta$ -CD, cumene was oxidized to cumyl alcohol in 32% yield and ethyl benzene was oxidized to acetophenone in 15% yield by dioxiranes generated *in situ*. In the absence of  $\beta$ -CD in water, no reaction occurred and poor recovery of starting materials was obtained. In a mixture of water and  $\text{CH}_3\text{CN}$ , the dioxirane-based cumene oxidation and ethyl benzene oxidation gave poor conversions. This shows that  $\beta$ -CD could reduce the loss of cumene and ethyl benzene through evaporation, and give enhancement on the yield of oxidation of cumene and ethyl benzene in water.

Selective C-H bond oxidation of a mixture of cumene and ethyl benzene was achieved by supramolecular approach using  $\beta$ -CD. In the presence of  $\beta$ -CD, cumene was selectively oxidized in a mixture of cumene and ethyl benzene in water. This would be due to the preferential binding of cumene to  $\beta$ -CD as a result of its high binding constant.

## 4.6 Experimental Section

### 4.6.1 Experimental Procedures

#### (a) General Procedure for C-H Bond Oxidation of Hydrocarbon with $\beta$ -CD

To a mixture of 0.2 mmol of substrate and 0.22 mmol of  $\beta$ -CD, 10 mL of water was added, followed by adding 0.2 mmol of 1,1,1-trifluoroacetone. Then, the mixture was treated with 8 additions of 0.5 mmol of Oxone and 1.55 mmol of NaHCO<sub>3</sub> at 0 h, 2 h, 3 h, 4 h, 5 h, 6 h and 7 h. After stirring for 8 h, the resulting mixture was extracted by ethyl acetate (3 × 10 mL). The combined organic extract was dried over anhydrous Na<sub>2</sub>SO<sub>4</sub>. After that, 0.4 mL of the extract was mixed with a hexane solution of n-decane as internal standard, and made up to 0.9 mL solution by n-hexane in a 1.5 mL vial for GC analysis.

#### (b) Instrumentation of Gas Chromatographic Experiments

Gas chromatography experiments were carried out with HP 5890 gas chromatograph system equipped with a flame ionization detector operated at 280 °C. The injector temperature was set to be 250 °C. The column used was HP 5 column (30 m × 0.32 mm × 0.25 μm film thickness). The carrier gas was nitrogen at 12 psi. The running mode was splitless.

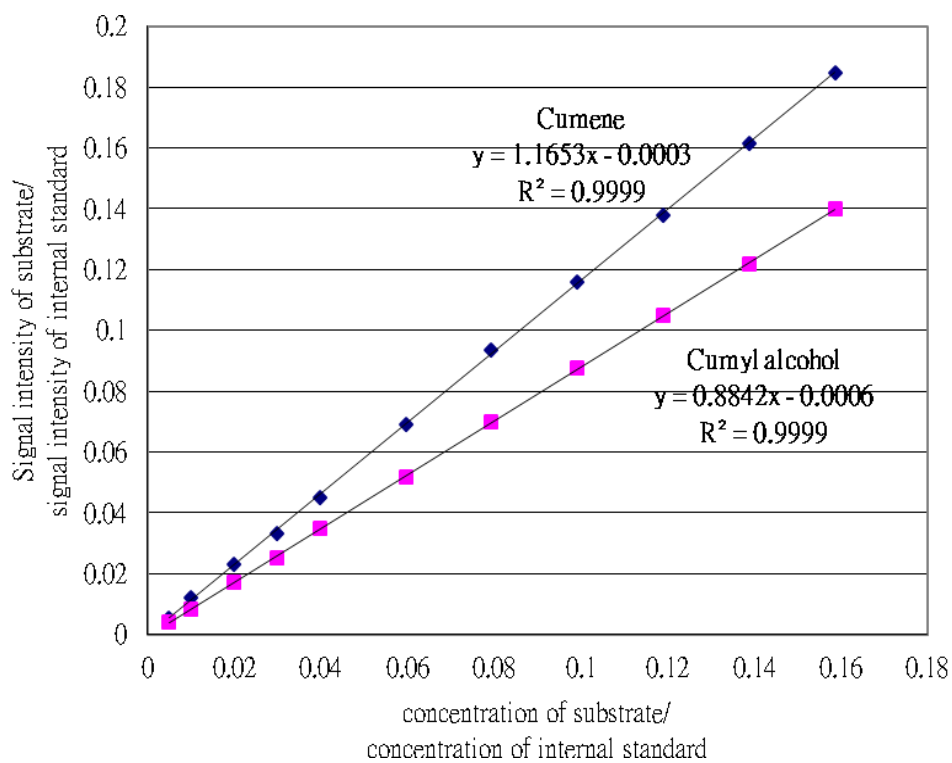


The sample injection was done by auto sampler. 1  $\mu\text{L}$  of solution was injected for each run.

#### 4.6.2 Calibration Curve of GC Analysis

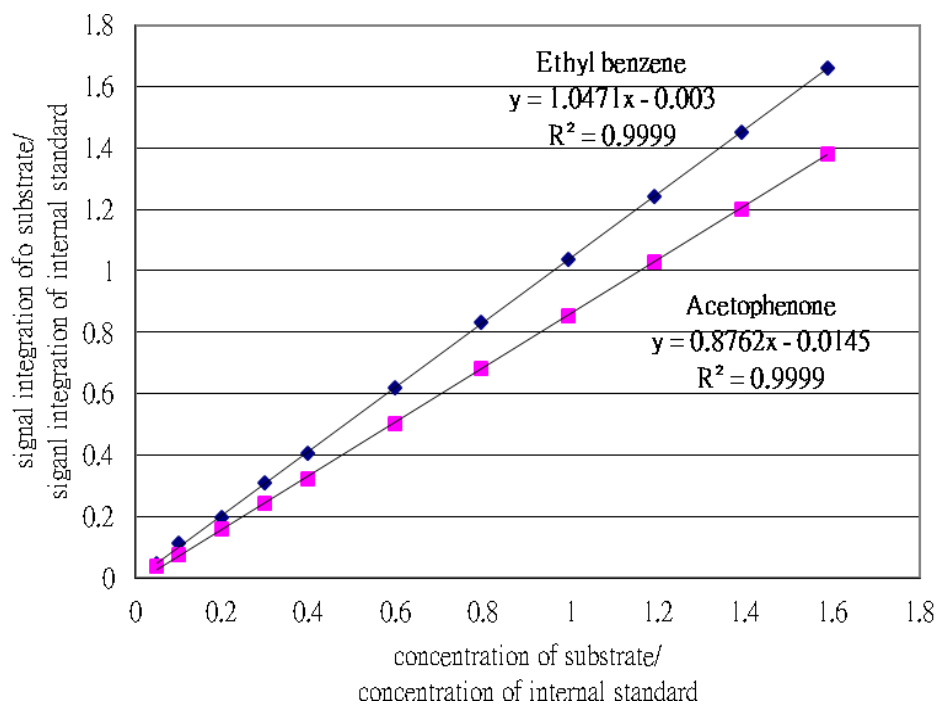
(a) Cumene and cumyl alcohol (25 ppm – 800 ppm), internal standard:

n-decane (5040 ppm)



(b) Ethyl benzene and acetophenone (25 ppm – 975 ppm), internal standard:

n-decane (504 ppm)

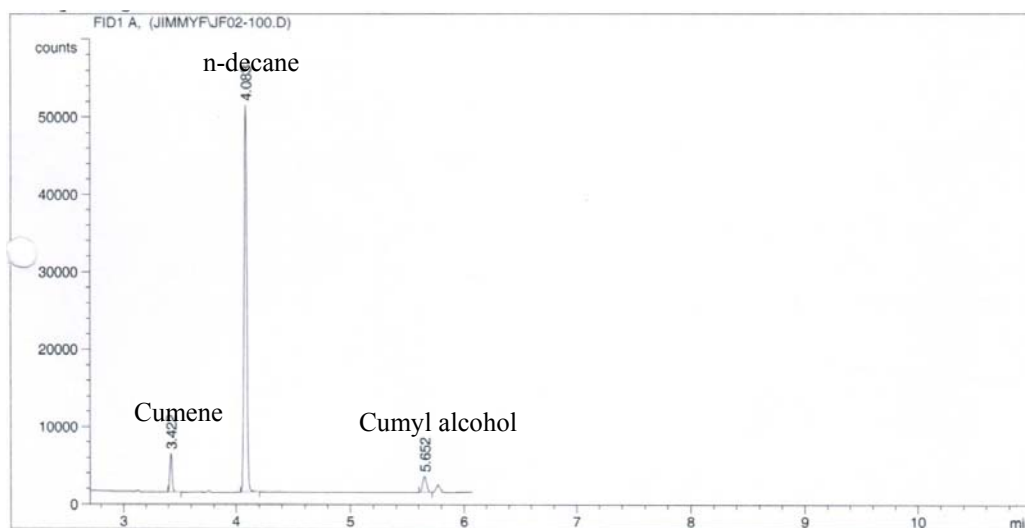


### 4.6.3 Chromatogram of C-H bond Oxidation of Aromatic Substrates

#### (a) Cumene oxidation in water with $\beta$ -CD

Temperature program: The temperature initially stayed at 105 °C for 3 min, then rose to 110 °C at the rate of 70 °C per min, and finally stayed at 110 °C for 3 min.

Concentration of internal standard: 3111 ppm



```
=====  
Area Percent Report  
=====
```

Reported By : Signal  
Multiplier : 1.0000  
Dilution : 1.0000

Signal 1: FID1 A,

Peak #	RetTime [min]	Type	Width [min]	Area counts*s	Height [counts]	Area %
1	3.422	BB	0.0220	6805.32422	4972.39062	7.14136
2	4.083	BB	0.0265	8.35267e4	4.99685e4	87.65111
3	5.652	BV	0.0362	4962.49072	2050.17944	5.20753

Totals : 9.52945e4 5.69911e4

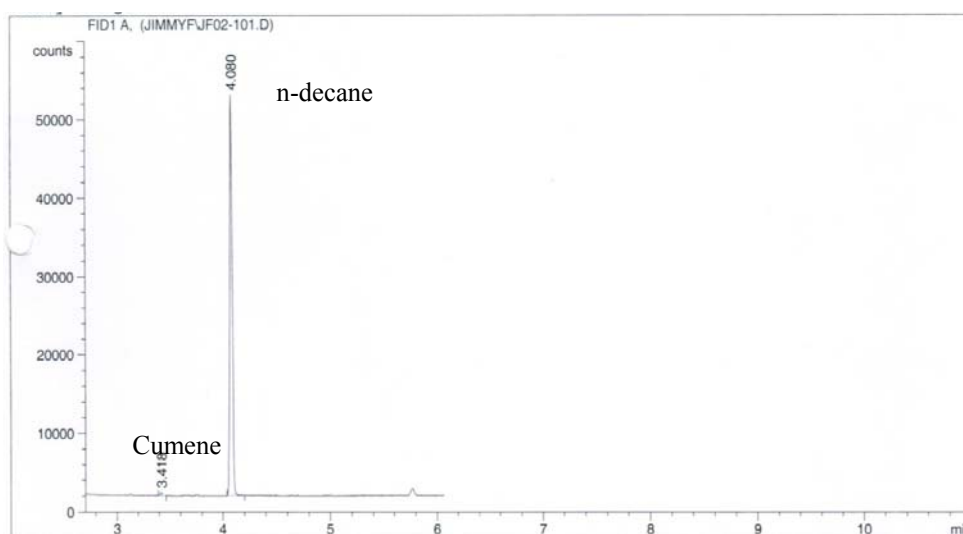
Results obtained with enhanced integrator!

```
=====  
*** End of Report ***
```

**(b) Cumene oxidation in water**

Temperature program: The temperature initially stayed at 105 °C for 3 min, then rose to 110 °C at the rate of 70 °C per min, and finally stayed at 110 °C for 3 min.

Concentration of internal standard: 3111 ppm



```
=====  
                          Area Percent Report  
=====
```

Sorted By	:	Signal
Multiplier	:	1.0000
Dilution	:	1.0000

Signal 1: FID1 A,

Peak #	RetTime [min]	Type	Width [min]	Area counts*s	Height [counts]	Area %
1	3.418	PB	0.0211	553.42493	426.21051	0.65376
2	4.080	BB	0.0262	8.40989e4	5.11577e4	99.34624

Totals :                    8.46523e4  5.15840e4

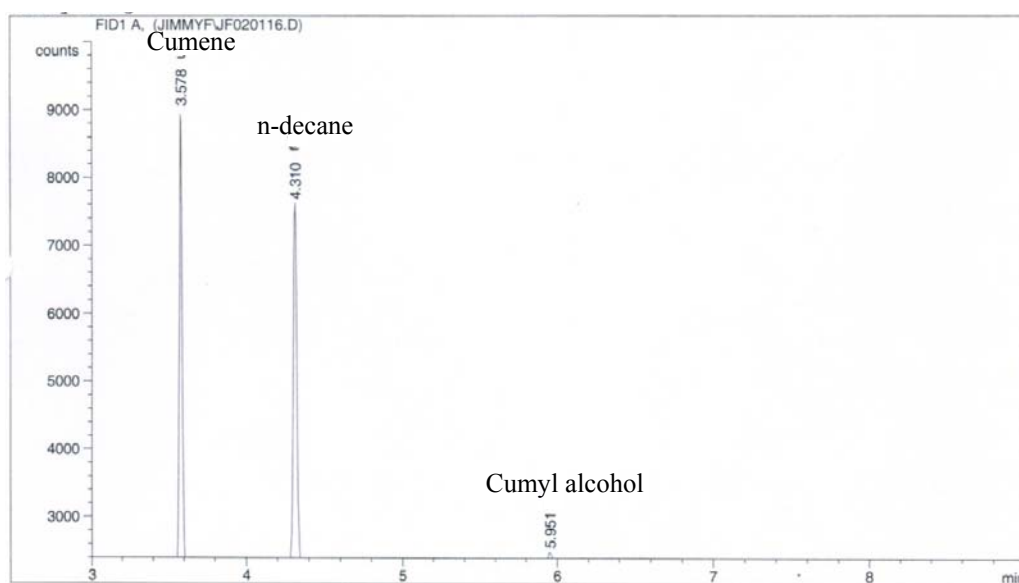
Results obtained with enhanced integrator!

```
=====  
*** End of Report ***
```

**(c) Cumene oxidation in a mixture of water and CH<sub>3</sub>CN without β-CD**

Temperature program: The temperature initially stayed at 100 °C for 3 min, then rose to 110 °C at the rate of 70 °C per min, and finally stayed at 110 °C for 3 min.

Concentration of internal standard: 311 ppm



```
=====  
Area Percent Report  
=====
```

Sorted By : Signal  
Multiplier : 1.0000  
Dilution : 1.0000

Signal 1: FID1 A,

Peak #	RetTime [min]	Type	Width [min]	Area counts*s	Height [counts]	Area %
1	3.578	BV	0.0198	8487.38379	6696.82227	47.50764
2	4.310	VB	0.0262	8798.01367	5352.95313	49.24637
3	5.951	BP	0.0315	579.90680	246.19954	3.24599

Totals : 1.78653e4 1.22960e4

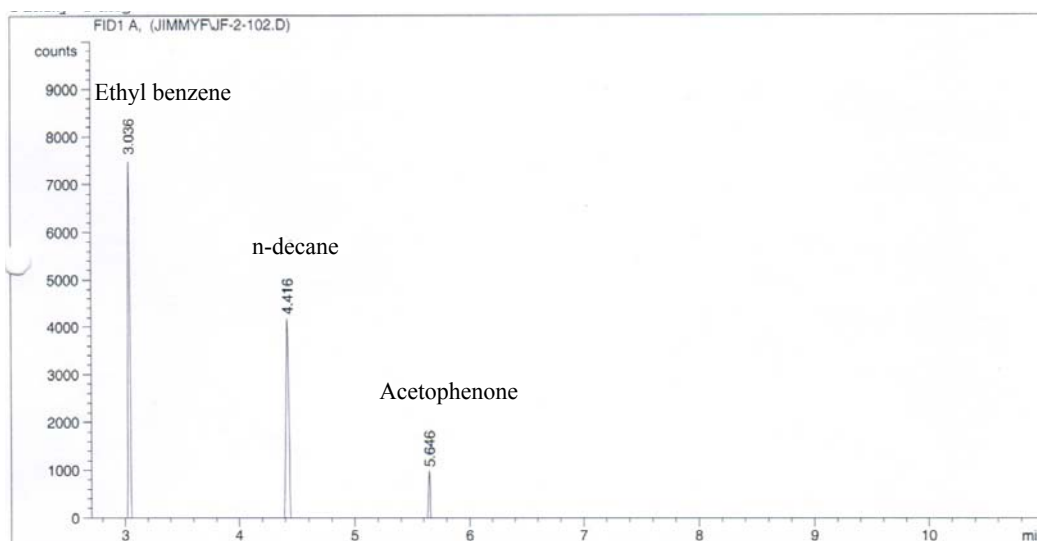
Results obtained with enhanced integrator!

```
=====  
*** End of Report ***
```

**(d) Ethyl benzene oxidation in water with  $\beta$ -CD**

Temperature program: The temperature initially stayed at 100 °C for 3 min, then rose to 180 °C at the rate of 70 °C per min, and finally stayed at 180 °C for 3 min.

Concentration of internal standard: 311 ppm



=====  
Area Percent Report  
=====

Reported By : Signal  
Multiplier : 1.0000  
Dilution : 1.0000  
Sample Amount : 1.00000 [ng/ul] (not used in calc.)

Signal 1: FID1 A,

Peak #	RetTime [min]	Type	Width [min]	Area counts*s	Height [counts]	Area %
1	3.036	PB	0.0191	9496.75781	7858.29980	46.45183
2	4.416	VB	0.0305	8946.07324	4647.00146	43.75825
3	5.646	BP	0.0211	2001.48279	1447.86682	9.78992

← eb  
← is  
← ebo

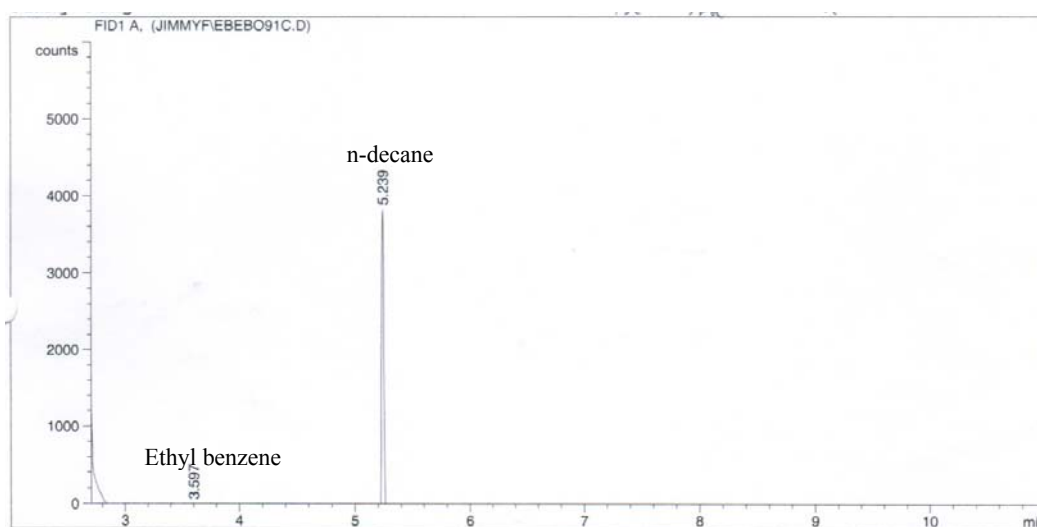
Totals : 2.04443e4 1.39532e4

Results obtained with enhanced integrator!  
=====

**(e) Ethyl benzene oxidation in water**

Temperature program: The temperature initially stayed at 100 °C for 5 min, then rose to 180 °C at the rate of 70 °C per min, and finally stayed at 180 °C for 2 min.

Concentration of internal standard: 311 ppm



```
=====  
Area Percent Report  
=====
```

Sorted By	:	Signal				
Multiplier	:	1.0000				
Dilution	:	1.0000				
Sample Amount	:	1.00000	[ng/ul]	(not used in calc.)		

Signal 1: FID1 A,

Peak #	RetTime [min]	Type	Width [min]	Area counts*s	Height [counts]	Area %
1	3.597	BP	0.0217	3354.67297	248.26387	4.74011
2	5.239	BV	0.0247	7127.70703	4452.40576	95.25989

Totals : 7482.38000 4700.66963

Results obtained with enhanced integrator!

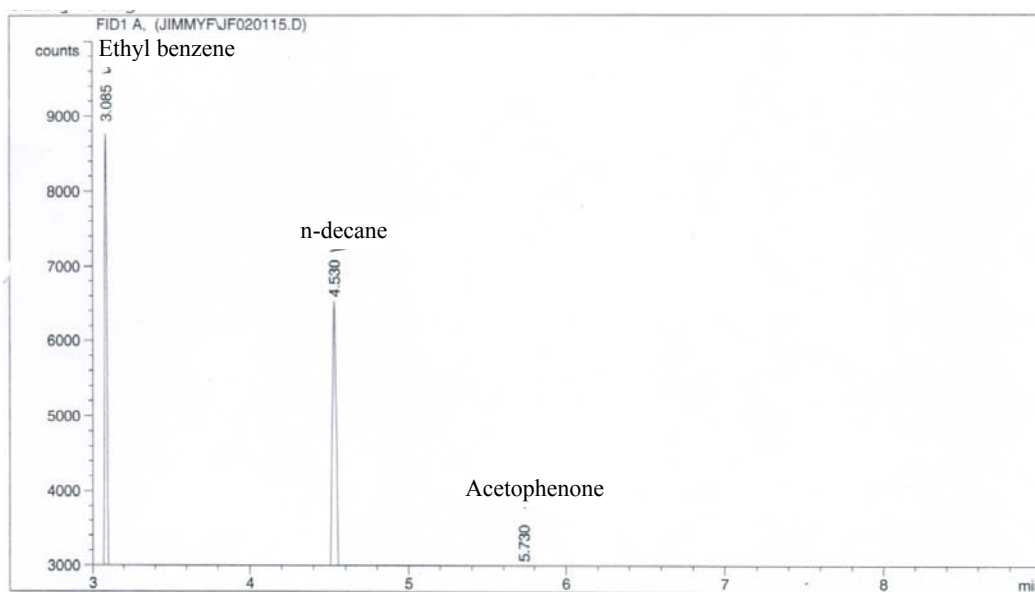
```
=====  
*** End of Report ***
```



**(f) Ethyl benzene oxidation in a mixture of water and CH<sub>3</sub>CN without β-CD**

Temperature program: The temperature initially stayed at 100 °C for 3 min, then rose to 180 °C at the rate of 70 °C per min, and finally stayed at 180 °C for 3 min.

Concentration of internal standard: 311 ppm



```
=====  
Area Percent Report  
=====
```

Sorted By : Signal  
Multiplier : 1.0000  
Dilution : 1.0000

Signal 1: FID1 A,

Peak #	RetTime [min]	Type	Width [min]	Area counts*s	Height [counts]	Area %
1	3.085	BP	0.0172	7318.51367	6479.84033	46.57081
2	4.530	PB	0.0296	8169.40381	4209.70801	51.98538
3	5.730	BV	0.0219	226.89276	148.01051	1.44381

Totals : 1.57148e4 1.08376e4

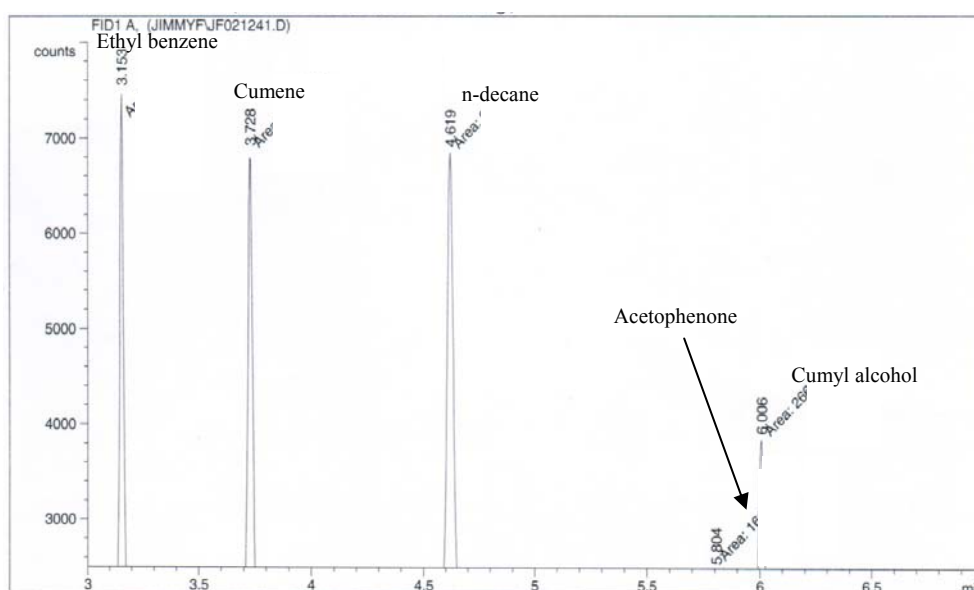
Results obtained with enhanced integrator!

```
=====  
*** End of Report ***
```

**(g) Oxidation of cumene-ethyl benzene mixture in water with  $\beta$ -CD**

Temperature program: The temperature initially stayed at 100 °C for 3 min, then rose to 180 °C at the rate of 70 °C per min, and finally stayed at 180 °C for 2 min.

Concentration of internal standard: 311 ppm



=====  
Area Percent Report  
=====

Sorted By : Signal  
Multiplier : 1.0000  
Dilution : 1.0000

Signal 1: FID1 A,

Peak #	RetTime [min]	Type	Width [min]	Area counts*s	Height [counts]	Area %
1	3.153	MM	0.0191	6220.30762	5415.76953	24.50126
2	3.728	MM	0.0241	6983.68750	4834.27930	27.50815
3	4.619	MM	0.0323	9355.64746	4820.53369	36.85110
4	5.804	MM	0.0236	161.70407	114.41843	0.63694
5	6.006	MM	0.0249	2666.35620	1786.06433	10.50255

Totals : 2.53877e4 1.69711e4

Results obtained with enhanced integrator!

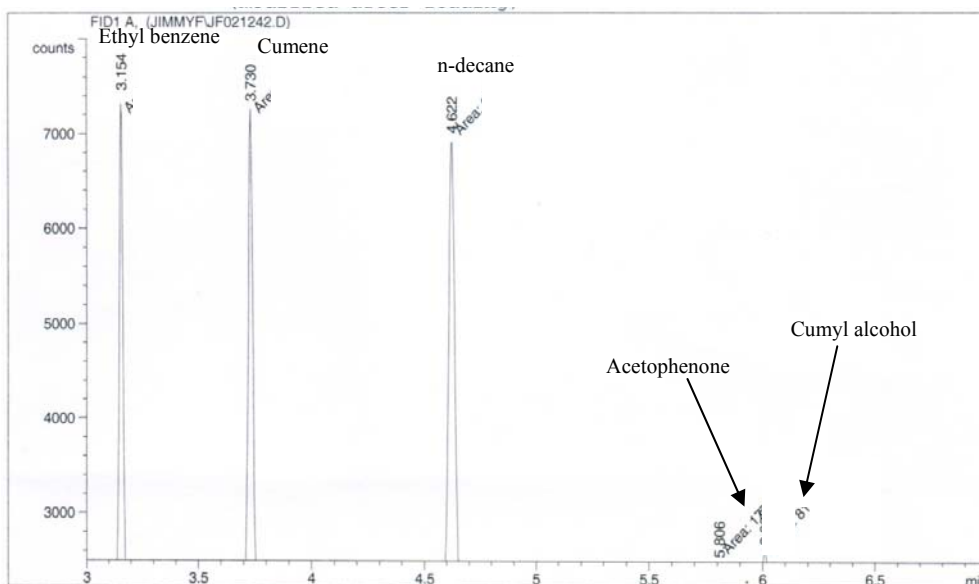
=====  
\*\*\* End of Report \*\*\*

**(h) Oxidation of cumene-ethyl benzene mixture in a mixture of water and**

**CH<sub>3</sub>CN without β-CD**

Temperature profile: The temperature initially stayed at 100 °C for 3 min, then rose to 180 °C at the rate of 70 °C per min, and finally stayed at 180 °C for 2 min.

Concentration of internal standard: 311 ppm



=====  
Area Percent Report  
=====

Sorted By : Signal  
Multiplier : 1.0000  
Dilution : 1.0000

Signal 1: FID1 A,

Peak #	RetTime [min]	Type	Width [min]	Area counts*s	Height [counts]	Area %
1	3.154	MM	0.0189	5984.56348	5269.64111	24.83551
2	3.730	MM	0.0238	7451.79248	5213.46387	30.92440
3	4.622	MM	0.0329	9665.46289	4899.29199	40.11098
4	5.806	MM	0.0211	177.60823	140.13611	0.73706
5	6.008	MM	0.0260	817.37604	523.15692	3.39205

Totals : 2.40968e4 1.60457e4

Results obtained with enhanced integrator!

## 4.7 References

- (1) For the examples of  $\beta$ -CD as reaction vessel for oxidation, see: (a) Surendra, K.; Krishnaveni, N. S.; Reddy, M. A.; Nageswar, Y. V. D.; Rao, K. R. *J. Org. Chem.* **2003**, *68*, 2058–2059. (b) Surendra, K., Krishnaveni, N. S.; Reddy, M. A.; Nageswar, Y. V. D.; Rao, K. R. *J. Org. Chem.* **2003**, *68*, 9119–9121. (c) Reddy, M. S.; Narender, M.; Rao, K. R. *Tetrahedron Lett.* **2005**, *46*, 1299–1301. (d) Ji, H. B.; Shi, D. P.; Shao, M.; Li, Z.; Wang, L. F. *Tetrahedron Lett.* **2005**, *46*, 2517–2520. (e) Surendra, K.; Krishnaveni, N. S.; Kumar, V. P.; Sridhar, R.; Rao, K. R. *Tetrahedron Lett.* **2005**, *46*, 4581–4583. (f) Narender, M.; Reddy, M. S.; Kumar, V. P.; Nageswar, Y. V. D.; Rao, L. R. *Tetrahedron Lett.* **2005**, *46*, 1971–1973. (g) Reddy, M. A.; Bhanumathi, N.; Rao, K. R. *Tetrahedron Lett.* **2002**, *43*, 3237–3238.
- (2) Franck, H. G.; Stadelhofer, J. W. *Industrial Aromatic Chemistry: raw materials, processes, products*; Berlin: Springer-Verlag, 1988.
- (3) Tsuji, J.; Ishino, M. *PCT Int. Appl.* **2004**, WO 2004058668 A1 20040715
- (4) Minematsu, H.; Matsumoto, K.; Saeki, T.; Kishi, A., *US Patent* **1981**, 4294946.
- (5) Marques, H. M. C. *Flavour Fragr. J.* **2010**, *25*, 313–326.
- (6) Siegel, H.; Eggersdorfer, M. “Ketones” in *Ullmann’s Encyclopedia of*

- Industrial Chemistry*, Wiley-VCH, Weinheim (2002).
- (7) Rhone-Poulenc, BE 815 578, 1973.
- (8) (a) Stoye, D.; Freitag, W.; Günter Beuschel *Resins for coatings: chemistry, properties, and applications* Hanser Gardner, 1996
- (9) (a) Gadamasetti, K. and Braish, T. *Process chemistry in the pharmaceutical industry* New York ; Basel : Marcel Dekker, 2007; Vol. 2. (b) Sittig, M. *Pharmaceutical manufacturing encyclopedia* Park Ridge, N. J.: Noyes Publications, 1988
- (10) Burdock, G. A. *Fenaroli's handbook of flavor ingredients* Boca Raton, Fla.: CRC Press, 2005.
- (11) Sanemasa, I.; Akamine, Y. *Bull. Chem. Soc. Jpn.* **1987**, 60, 2059-2066.
- (12) Carey, Francis A.; Sundberg, Richard J.; (1984). *Advanced Organic Chemistry Part A Structure and Mechanisms (2nd ed.)*. New York N.Y.: Plenum Press.
- (13) IUPAC, *Compendium of Chemical Terminology*, 2nd ed. (the "Gold Book") (1997).